(4)

N-1790
November 1988

NCEL
Technical Note

By J. Cox

Sponsored by Naval Facilities
Engineering Command

COUPLING OF THE FINITE AND BOUNDARY ELEMENT METHODS IN ELASTOSTATICS

ABSTRACT This study investigates the coupling of the finite and boundary element methods in elastostatics where each method is used to model a different portion of the domain. The principal interest is in applying a boundary element method (BEM) to model the infinite domain (assumed to be isotropic linear elastic) while using the finite element method (FEM) to model regions with more complex constitutive relations. The approach taken in this study, referred to as a FEM-hosted coupling, treats each BEM subdomain as a single finite element. Two derivations for an IBEM stiffness matrix are given; the first is a physically intuitive direct derivation while the second is the corresponding variational derivation. Though the emphasis is on the IBEM, the DBEM is also addressed. The inherent incompatibility between the BEM and FEM methods is discussed and explained in terms of the "shape function fallacy."

NAVAL CIVIL ENGINEERING LABORATORY PORT HUENEME, CALIFORNIA 93043

METRIC CONVERSION FACTORS

Approximate Conversions to Metric Measures

Symbol	When You Know	Multiply by	To Find	Symbol
		LENGTH		
in	inches	*2.5	centimeters	cm
ft	feet	30	centimeters	cm
yd	yards	0.9	meters	m
mi	miles	1.6	kilometers	km
		AREA		
in^2	square inches	6.5	square centimeters	cm^2
ft^2	square feet	0.09	square meters	m^2
yd^2	square yards	0.8	square meters	m^2
mi^2	square miles	2.6	square kilometers	km^2
	acres	0.4	hectares	ha
		MASS (weight)		
oz	ounces	28	grams	g
lb	pounds	0.45	kilograms	kg
	short tons (2,000 lb)	0.9	tonnes	t
		VOLUME		
tsp	teaspoons	5	milliliters	ml
Tbsp	tablespoons	15	milliliters	ml
fl oz	fluid ounces	30	milliliters	ml
c	cups	0.24	liters	l
pt	pints	0.47	liters	l
qt	quarts	0.95	liters	l
gal	gallons	3.8	liters	l
ft^3	cubic feet	0.03	cubic meters	m^3
yd^3	cubic yards	0.76	cubic meters	m^3
		TEMPERATURE (exact)		
°F	Fahrenheit temperature	5/9 (after subtracting 32)	Celsius temperature	°C

*1 in = 2.54 (exactly). For other exact conversions and more detailed tables, see NBS Misc. Publ. 286, Units of Weights and Measures, Price $2.25, SD Catalog No. C13.10:286.

Approximate Conversions from Metric Measures

Symbol	When You Know	Multiply by	To Find	Symbol
		LENGTH		
mm	millimeters	0.04	inches	in
cm	centimeters	0.4	inches	in
m	meters	3.3	feet	ft
m	meters	1.1	yards	yd
km	kilometers	0.6	miles	mi
		AREA		
cm^2	square centimeters	0.16	square inches	in^2
m^2	square meters	1.2	square yards	yd^2
km^2	square kilometers	0.4	square miles	mi^2
ha	hectares (10,000 m^2)	2.5	acres	
		MASS (weight)		
g	grams	0.035	ounces	oz
kg	kilograms	2.2	pounds	lb
t	tonnes (1,000 kg)	1.1	short tons	
		VOLUME		
ml	milliliters	0.03	fluid ounces	fl oz
l	liters	2.1	pints	pt
l	liters	1.06	quarts	qt
l	liters	0.26	gallons	gal
m^3	cubic meters	35	cubic feet	ft^3
m^3	cubic meters	1.3	cubic yards	yd^3
		TEMPERATURE (exact)		
°C	Celsius temperature	9/5 (then add 32)	Fahrenheit temperature	°F

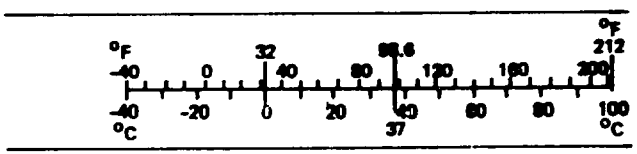

Unclassified

SECURITY CLASSIFICATION OF THIS PAGE (When Data Entered)

REPORT DOCUMENTATION PAGE		READ INSTRUCTIONS BEFORE COMPLETING FORM
1. REPORT NUMBER TN-1790	2. GOVT ACCESSION NO. DN665087	3. RECIPIENT'S CATALOG NUMBER
4. TITLE (and Subtitle) COUPLING OF THE FINITE AND BOUNDARY ELEMENT METHODS IN ELASTOSTATICS		5. TYPE OF REPORT & PERIOD COVERED Final; Oct 1985 - Sep 1987 6. PERFORMING ORG. REPORT NUMBER
7. AUTHOR(s) James V. Cox		8. CONTRACT OR GRANT NUMBER(s)
9. PERFORMING ORGANIZATION NAME AND ADDRESS NAVAL CIVIL ENGINEERING LABORATORY Port Hueneme, California 93043-5003		10. PROGRAM ELEMENT, PROJECT, TASK AREA & WORK UNIT NUMBERS 61153N; YR023.03.01.006
11. CONTROLLING OFFICE NAME AND ADDRESS Naval Facilities Engineering Command Alexandria, Virginia 22332		12. REPORT DATE November 1988 13. NUMBER OF PAGES 111
14. MONITORING AGENCY NAME & ADDRESS(if different from Controlling Office)		15. SECURITY CLASS. (of this report) Unclassified 15a. DECLASSIFICATION/DOWNGRADING SCHEDULE

16. DISTRIBUTION STATEMENT (of this Report)

Approved for public release; distribution is unlimited.

17. DISTRIBUTION STATEMENT (of the abstract entered in Block 20, if different from Report)

18. SUPPLEMENTARY NOTES

19. KEY WORDS (Continue on reverse side if necessary and identify by block number)

Boundary element, finite element, coupled methods, elastostatics

20. ABSTRACT (Continue on reverse side if necessary and identify by block number)

This study investigates the coupling of the finite and boundary element methods in elastostatics where each method is used to model a different portion of the domain. The principal interest is in applying a boundary element method (BEM) to model the infinite domain (assumed to be isotropic linear elastic) while using the finite element method (FEM) to model regions with more complex constitutive relations. The approach taken in this study, referred to as a FEM-hosted coupling, treats each BEM subdomain as a single finite

Continued

DD FORM 1 JAN 73 1473 EDITION OF 1 NOV 65 IS OBSOLETE

Unclassified

SECURITY CLASSIFICATION OF THIS PAGE (When Data Entered)

20. Continued

element. Two derivations for an IBEM stiffness matrix are given; the first is a physically intuitive direct derivation while the second is the corresponding variational derivation. Though the emphasis is on the IBEM, the DBEM is also addressed. The inherent incompatibility between the BEM and FEM methods is discussed and explained in terms of the "shape function fallacy."

Library Card

Naval Civil Engineering Laboratory
COUPLING OF THE FINITE AND BOUNDARY ELEMENT METHODS IN ELASTOSTATICS (Final), by James V. Cox
TN-1790 111 pp illus Nov 1988 Unclassified

1. Boundary element 2. Finite element I. YR023.03.01.006

This study investigates the coupling of the finite and boundary element methods in elastostatics where each method is used to model a different portion of the domain. The principal interest is in applying a boundary element method (BEM) to model the infinite domain (assumed to be isotropic linear elastic) while using the finite element method (FEM) to model regions with more complex constitutive relations. The approach taken in this study, referred to as a FEM-hosted coupling, treats each BEM subdomain as a single finite element. Two derivations for an IBEM stiffness matrix are given; the first is a physically intuitive direct derivation while the second is the corresponding variational derivation. Though the emphasis is on the IBEM, the DBEM is also addressed. The inherent incompatibility between the BEM and FEM methods is discussed and explained in terms of the "shape function fallacy."

Contents

INTRODUCTION

There are many classes of boundary value problems which are not effectively solved using a single numerical method. These problems might be more effectively solved by combining different methods, applying each method to portions of the domain where it is best suited. In this study we consider the coupling of the boundary element method (BEM) with the finite element method (FEM) to solve problems in elastostatics.

Boundary element methods have become an accepted alternative to domain-based methods, such as finite element and finite difference methods, for many classes of boundary value problems (Refs 1 and 2). The direct boundary element method (DBEM) and indirect boundary element method (IBEM) are two well established formulations that are used to solve a variety of boundary value problems in engineering. The key to these formulations is the existence of a fundamental singular solution (i.e., the solution for a point source or point load in an infinite domain -- a free-space Green's function).

The fundamental solution is jointly the blessing and curse of the methods. Since it is a solution of the governing differential equations, problems defined by a self-adjoint differential operator can be expressed by integral equations. With the governing equations satisfied only the boundary conditions remain to be satisfied. Numerically this means that for many classes of problems BEMs require only the boundary to be discretized. The dimensionality of these problems is reduced by one. The methods thus lend themselves to modeling problems with infinite domains since only the surface of cavities, not the domain, must be discretized. This decrease in dimensionality reduces the number of degrees of freedom (dof) in the approximation; however, the resulting equations are unsymmetric and fully-populated in contrast to the symmetric sparse systems characteristic of domain-based methods. The singular nature of the fundamental solution is suited to solving problems having high stress gradients. Yet this same singular nature complicates the numerical integrations inherent to the methods when higher order elements are employed. Fundamental

singular solutions exist for many classes of boundary value problems with homogeneous domains. However, for an arbitrary-inhomogeneous domain the fundamental solution is not known, and additional numerical effort is required (Ref 3). Since the methods are relatively new, they have not been as extensively developed as domain-based methods for nonlinear applications. They also lack the generality, in terms of extensive continuum and structural element libraries, that commercial finite element computer programs possess.

The finite element method (FEM) has been the most highly developed approximate solution technique for many classes of boundary value problems (Ref 4). The most general derivation follows from a weighted residual approximation of the boundary value problem. The error introduced by an assumed approximate solution form is orthogonalized with respect to a set of weighting functions to obtain the "best" approximate solution. For the Galerkin weighted residual statement the weighting functions correspond to the basis functions in which the approximate solution is expanded. For problems with a self-adjoint operator, the weak form of the Galerkin statement is equivalent to an alternative variational statement of the problem.

Basis functions in the FEM usually are locally based polynomials for which numerical integrations are relatively simple. The local nature of these functions leads to a sparse system of equations, but this same attribute hinders its ability to model infinite domains. To compensate for this limitation, Ungless (Ref 5, 1973) and Bettess (Ref 6, 1977) developed special elements (infinite elements) to model infinite domains which include shape functions "based on" the form of analytical solutions (i.e. they should decay radially outward towards infinity and integrations over the domain should remain finite). The generality of the Galerkin and variational statements allows nonlinearities and domain inhomogeneities to be accommodated. For most structural applications the resulting system of equations is also symmetric.

The boundary and finite element methods are related. In seeking to model problems having infinite domains, Zienkiewicz, Kelly and Bettes (Ref 7, 1977) interpreted the IBEM as a generalized finite

element methodology where the "shape functions"* were obtained directly in terms of the fundamental solution. The DBEM can be interpreted in the same manner but the unknown coefficients are nodal boundary tractions and displacements instead of artificial boundary tractions. (The physical identification of the coefficients made here is only valid for "continuous elements" using collocation.) This contrasts with Brebbia's work (Ref 8, 1978) relating the analytical basis of the methods (FEM, DBEM, and finite difference method) where he derives Somigliana's first identity by employing the fundamental singular solution as the weighting function in the weak statement of the boundary value problem.

Considering the individual strengths of boundary-based and domain-based methods, some classes of problems may be more effectively solved by combining the methods. Nonlinear soil-structure interaction and fracture mechanics are two classes of problems where a combined solution approach can potentially be more effective. For nonlinear soil-structure interaction problems, the FEM could be used to model the structure and a region of the soil which is expected to exhibit nonlinear behavior, and the BEM could be used to approximate the infinite domain. For brittle fracture mechanics problems, the FEM could be used to model all of the problem except a region local to the crack tip where the BEM could provide a crack tip "element" capable of representing very high stress gradients. (While BEMs have been formulated for modeling inelastic material behavior, the coupling approach of this study assumes the BEM region is linear elastic. Ductile fracture could be solved by a coupled approach but maybe with no gain in effectiveness.) For both

---

* The term "shape function" has been used in various ways by researchers working with coupled solution approaches. Many uses of the term in referring to the BEM are a bit of a misnomer. In the initial part of the work by Zienkiewicz *et al.* (Ref 7) "shape function" is defined as a function which spans the BEM region (a "super element"), but unlike typical FEM shape functions it is in general nonzero at all nodes. In this context the shape functions provide a basis for the displacement field however the variation of the shape function along a given portion of the boundary is not known *a priori* to be, for example, linear or quadratic. For the BEM, "shape function" is usually used to refer to a boundary interpolant used along a so called "boundary element" in performing the numerical integrations. These "shape functions" are nonzero at a single node; however they do not form a basis for the boundary response, only for the boundary distribution assumed for the integrations. This is discussed in more detail in a later section. This later definition will be used in this study.

of these problems one aspect of the problem is infinite: for the soil problem the domain, for the crack problem the stresses. While one might argue that both of these are mathematical fictions, they do effectively characterize the behavior of the respective problems.

Objective

The objectives of this thesis are to: (1) formulate stiffness matrices for both the indirect and direct boundary element methods that would allow them to be coupled to the finite element method, (2) develop a coupling algorithm which requires a minimum of modification to existing separate FEM and BEM software systems, (3) implement one of the stiffness matrix formulations, and (4) study the basic behavior of the coupled solutions including accuracy and the incompatibility along the FEM-BEM interface. The ultimate objective of this research is to determine whether a combination of boundary element and finite element solution methods could more effectively solve nonlinear structural/geotechnical problems.

Scope

In this study, I am investigating different approaches to obtaining a FEM-hosted coupling. The emphasis is on: (1) conceptually unifying some of the different coupling techniques, (2) providing an algorithm to facilitate implementation, and (3) studying the numerical behavior of a coupled system. A physically intuitive development of an IBEM stiffness matrix is included. This direct derivation of a stiffness matrix is followed by the corresponding variational derivation. Though the emphasis is on the IBEM, the DBEM is also addressed The numerical study is limited to two classical problems which illustrate the behavior of the coupled system. Overviews of both the DBEM and IBEM are given in following sections to establish nomenclature and to present the necessary equations for background.

Background on Coupled Solution Approaches

The idea of coupling the FEM and BEM is attributed to Wexler (Ref 9, 1972), who used integral equation solutions to constrain FEM solutions for infinite domain field problems in the early 1970s. Other early examples of using a combined solution approach dealt with wave phenomena, Chen and Mei (Ref 10, 1974) and Shaw (Ref 11, 1974). Zienkiewicz *et al.* (Ref 7, 1977) proposed a combined solution approach for statics problems followed by Osias, Wilson and Seitelman's (Ref 12, 1977) use of a coupled solution to solve elastostatic problems.

There are numerous approaches to coupling the methods (Ref 13). In this study the main classification is based upon "which method hosts the coupling." For a BEM-hosted coupling the FEM subdomain is treated as a BEM region; equilibrium and compatibility are approximately enforced continuously along the interface, analogous to the BEM approach to modeling piece-wise homogeneous problems. The resulting equations are unsymmetric and thus this approach only lends itself to problems numerically dominated by the BEM subdomain (Refs 13, 14, 15, 16 and 17). For a FEM hosted coupling the BEM subdomain is treated as one or many finite elements. In this "super-element" approach the resulting BEM equations reflect the "equivalent" stiffness of the subdomain and can be directly assembled by a FEM program. The term "super-element" reflects the high degree of connectivity which will typically be present for a BEM region. A coupled solution approach does not seem to necessitate a displacement based FEM; however due to its commercial success, it appears all the studies of coupled solutions have been based on this formulation.

In addition to the BEM-hosted and FEM-hosted coupling approaches, there have been a number of approaches where in a sense neither method hosts (as defined above) the coupling. This open-ended category mainly includes approaches where one method serves as a boundary condition for the other. Shaw's study (Ref 11, 1974) of time harmonic scattering is an early example of such an approach.

Shaw and Falby (Ref 18, 1977) devised another approach in which the boundary integral equation was incorporated into a variational formulation for the FEM region as a natural boundary condition (also see Ref 19).

The treatment of the BEM as a boundary condition to the FEM region has also been accomplished iteratively (Ref 20). The BEM regions are initially treated as if they are rigid and the FEM problem is solved. The reaction forces along the interfaces of the regions are applied to the BEM regions and the corresponding boundary value problems for the BEM regions are solved. The displacements, obtained by the BEM analyses, along the FEM-BEM interface are applied to the FEM region and the problem is re-solved. After a few iterations the interfaces converge to their equilibrium position.

Kamat and Brown (Ref 21, 1985) proposed yet another iterative approach. Instead of using a BEM, an "ancestor" to the IBEM is used where the unknowns are the positions and strengths of a finite number of point sources (for the potential problem). Their approach is "scalar" in nature in the sense that it does not require the explicit formulation of a stiffness matrix. The potential energy functional for the FEM region is augmented, via a penalty number, by a compatibility condition along the FEM-BEM interface. This compatibility condition requires a discrete least squares satisfaction (i.e., at three times as many points along the interface as there are point sources). The augmented functional is then minimized using a preconditioned conjugate gradient technique.

Within FEM-hosted couplings the first level of classification is the procedure used to obtain the stiffness relationship. The two approaches are: (1) a variational approach where a boundary variational principle is the basis of the relationship, and (2) a direct approach where the BEM equations are manipulated into a stiffness form. A key step to both approaches, using either BEM formulation, is establishing a relationship between the nodal tractions and the nodal displacements; an exception to this is a variational approach with the IBEM which retains the artificial tractions as unknowns in the system of equations (Refs 7, 13 and 14).

Chen and Mei (Ref 10, 1974) were apparently the first to formulate a coupled solution based on a variational principle. In their study of the action of sea waves on a harbor their "BEM" region was expressed as a finite series of Bessel functions. They used a modified functional for the FEM region to enforce continuity of the dependent variables and their derivatives across the FEM-BEM interface as a natural boundary condition. The outer "BEM" region was referred to as a "super element." Other early efforts using a variational approach include: Jeng and Wexler (Ref 22, 1977); Zienkiewicz, Kelly, and Bettess (Ref 7, 1977); and Kelly, Mustoe, and Zienkiewicz (Ref 13, 1979).

Approximation of the variational principle necessarily produces a symmetric system, and thus these approaches are sometimes grouped with some direct approaches as "symmetric couplings." In the variational approach considered in this study, a variational statement of the problem is written in a boundary form with the absence of body sources or forces (Refs 7 and 23). For elastostatics the functional corresponds to a boundary form of the potential energy functional. There have been many modifications of this functional for various purposes including (1) to relax essential boundary conditions or interface compatibility and (2) to enforce equilibrium (Refs 23 and 24).

In approximating the variational statement, relationships between boundary values obtained from the integral equations are substituted into the functional, reducing the number of unknowns. For a displacement-based FEM, the nodal tractions are usually expressed in terms of the nodal displacements, which requires the inversion of a fully-populated coefficient matrix. The previously mentioned exception to this approach (using the IBEM), writes the boundary displacements and tractions in terms of the artificial tractions. In this case stationarity is taken with respect to both the nodal displacements (of the adjacent "framing" region) and the nodal artificial

boundary tractions instead of nodal displacements alone. The lack of a matrix inversion is paid for by an increase in the number of unknowns* and a double integration process.

In contrast to the variational formulations, Brebbia (see e.g., Ref 2, 8, 15 or 25) directly manipulated the BEM equations into a stiffness form. In general direct formulations do not produce a symmetric stiffness matrix. Brebbia symmetrized the system by averaging the off-diagonal terms based on an error minimization argument using the method of least squares. The resulting stiffness matrix was of the same form as obtained by variational methods using the potential energy functional (Ref 7).

Despite the apparent agreement between the two approaches, agreement between proponents of the approaches was scarce. Kelly *et al.* (Ref 13) stated that the modification to obtain symmetry "apparently has no valid foundation except that the energy approach led to a similar form." Brebbia *et al.* (Ref 2) later concluded that there was no reason for the stiffness matrix to be symmetric other than for reasons of computational convenience and efficiency. In addition, he questioned the combination of variational principles and integral equations used in the variational approach. Initial efforts indicated that the symmetric matrix provided better results; however, more recent comparisons (Ref 24, 1982) using quadratic elements and providing for geometric discontinuities indicate the contrary. Fortunately for cases which have a relatively fine boundary descretization, Roudolphi (Ref 26) has found the degree of asymmetry to be insignificant. This is likely to be the case for geotechnical applications.

Hartman (Ref 27) gives a somewhat humorous overview of the problem as:

> "This boundary element method, as it is called, leads to nonsymmetric and fully-populated matrices and it is not easy to convince engineers, that anything good can come out of such strange matrices. Imagine these same engineers when they

---

* Zienkiewicz *et al.* (Ref 7) eliminate the coefficients corresponding to the artificial boundary traction distribution at the element level. Zienkiewicz (Refs 4 and 13) also points out the direct analogy that exist between this particular formulation and that of hybrid finite elements.

> discover that the stiffness matrices which they derive from these linear systems turn out to be nonsymmetric... . God knows there is not much engineers believe in, but they certainly believe that stiffness matrices have to be symmetric and they are therefore deeply irritated, finding themselves in a situation where two fundamental beliefs clash (Mathematics and Mechanics) and either one is equally convincing."

Another problem which is common to both approaches is failure of the stiffness matrix to satisfy equilibrium. Equilibrium requires the terms in each column corresponding to a given global direction to sum to zero. Boissenot, Lachat, and Watson (Ref 28, 1974) augmented the system of equations for the DBEM with two additional equations which cause the approximate traction distribution to identically satisfy equilibrium (in English see e.g. Refs 13 and 23). By this approach the equilibrium problem is addressed while establishing the nodal traction-displacement relationship instead of after the stiffness matrix is formed. Hartman (Ref 27) gives a theoretical discussion on the symmetry and equilibrium problems and provides advice on how to correct them. Tullberg and Bolteus (Ref 24) compare the accuracy and convergence characteristics of seven stiffness formulations for two simple two-dimensional problems -- uniaxial tension and bending. The seven stiffness matrices were obtained using the DBEM and included all the variations mentioned above. In their study the direct formulation, in it's unsymmetric form, gave the best accuracy and rates of convergence.

In addition to the differences used here to classify formulations, there have been numerous other variations. Some researchers (Ref 23) have used element condensation to reduce the unknowns for the BEM super-element to those located on the interface between the two representations. This could be useful in fracture mechanics applications where numerous boundary elements might be used near the crack tip. As previously mentioned, modified functionals have been used to relax compatibility requirements (e.g., when interfacing subdomains with different "shape functions"). As will be shown in this thesis, even when the "shape functions" between methods match the interfaces are inherently incompatible.

Variations in the BEM formulations themselves introduce additional classification parameters. Though not addressed in this study, for some applications traction discontinuity is an important

consideration. Many ways of treating this problem have been reported (Refs 24 and 29-31). A simple though less rigorous approach is to position the collocation points at the interior of the element. When all of the collocation points associated with an element are internally positioned, the elements are referred to as "discontinuous" or "nonconforming" elements (Ref 32). Though the "discontinuous" elements add some flexibility to the method in terms of mesh refinement, it is at the expense of increasing the number of equations by up to 100 percent. Discontinuous elements would appear to complicate a coupling algorithm since the collocation points do not correspond to node points.

Relationship to Previous Work by the Author

The study this thesis is based on was funded by the Naval Civil Engineering Laboratory (NCEL). This section gives an overview of the work which led to the current study. In our research at NCEL, the primary role of the BEM has been to compliment FEM analysis capabilities (i.e., coupled solution techniques). The BEM is in general a more analytically complicated technique, and thus the fundamentals of the method required investigation. As a result of these efforts the potential of the method as a separate analysis tool has also been observed. Thus our coupling efforts have emphasized a modular approach where it is assumed that both analysis methods can serve as an individual or a coupled tool.

In our first study (Ref 33) we investigated the IBEM formulation in one- and two-dimensional elastostatics and compared numerical results with the DBEM and analytical solutions. We used a crude element (constant distribution) but the potential of the method was evident. This study indicated the need for higher order elements and integration techniques to improve results in the near boundary region.

In our next study (Ref 17) we investigated a coupling of the BEM and FEM. We formulated a BEM-hosted coupling, approximating compatibility and equilibrium on the interfaces.

Qualitatively the coupling was a success, but the simple constant elements used for both methods prevented substantial quantitative evaluation. For nonlinear soil-structure applications where the FEM is used to model the nonlinear region, the FEM should host the coupling. Two areas required further study: (1) accuracy of the BEM formulations, and (2) a FEM-hosted coupling approach.

In our third study (Refs 34 and 35) we investigated higher order isoparametric boundary elements and their associated integration techniques. Lachat and Watson (Ref 36) adapted the isoparametric element formulation directly from FEM technology. However, for the BEM the integrands in the coefficient calculations are singular and thus their integration requires special attention. Though much effort had been devoted to dealing with the integration over the singularity an effective numerical approach to performing the integrations in the near boundary region appeared to be lacking. We developed a recursive algorithm which adaptively subdivides the element to maintain consistent accuracy independent of the response point location. The new element formulation has effectively eliminated near boundary error resulting from coarse numerical integration and has provided valuable insight to other errors inherent to the boundary element methods. This technique* is the key to allowing a numerical demonstration of the incompatibility which occurs in the coupling (see the numerical results section).

The initial effort in this study was presented in a preliminary report (Ref 38). This thesis completely supersedes the previous report.

---

* This technique serves as a "shell" to standard numerical integration techniques like Gauss quadrature. A dramatic increase in efficiency is attainable by improving the quadrature rule directly. A "shell" might still be necessary but it would be resorted to less frequently. For a recent paper on improved integration methods see reference 37.

Nomenclature

This is a list of principal symbols used within the thesis. Additional variables which have a limited scope of use are defined within the text. Modifications (such as the addition of a subscript) are also defined in the text unless given below. Instead of the matrix notation defined below, indicial notation will sometimes be used to clarify equations. Indices will always be lower case while identifying subscripts or superscripts will be upper case.

The most general form of a variable (i.e., with the least amount of supplementary symbols) is defined. For example, u_i represents a displacement vector but depending on the notation it may be continuous or discrete, known or unknown. There are some non-unique uses of Latin symbols. For these cases supplementary symbols are included as necessary. Indicial notation is only used in the definitions below for tensor quantities; the index range in this case is two. In the following definitions "V" represents a generic variable.

Mathematical Symbols

$V(\underline{x})$	Explicitly defines the quantity as continuous as opposed to discrete.
$\mathbf{V}$	A rectangular or square matrix of functions (e.g., $\mathbf{M}(\underline{x})$) or constants (e.g., $\mathbf{K}$).
$\underline{V}$	A column vector.
$\hat{V}$	A known value(s); for example, $\hat{\underline{u}}$ is a vector of known nodal displacements.
$\bar{V}$	An unknown value(s); for example, $\bar{\underline{t}}$ is a vector of unknown nodal tractions.
$\mathbf{V}^T$	Transpose of a matrix or vector. $\underline{V}^T$ is a row vector.
$\mathbf{V}^{-1}$	Inverse of a matrix.

Latin Symbols

A_{ik}	A constant tensor which provides a zero displacement for the fundamental singular sclution at a reference distance r_o. $A_{ik} = -\delta_{ik}C_1[C_2\ln(r_o) - 1]$.
C	Square, sparse matrix which contains boundary integrations of traction and displacement "shape function" products.
C_1, C_2, C_3, C_4	Constants used in defining the fundamental solution. Functions of the material constants (see text).
$e_k(\underline{\xi})$	A unit concentrated force used in the definition of the fundamental solution.
E	Young's modulus.
E	Square matrix relating nodal tractions to nodal displacements, $\underline{\bar{t}} = \mathbf{E}\,\underline{\bar{u}}$.
$E_{ijk}(\underline{x},\underline{\xi})$	Kernel function in Somigliana's 2nd identity relating boundary displacements to the stress field.
$\underline{f}$	Column vector of generalized nodal forces.
$F_{ij}(\underline{x},\underline{\xi})$	Kelvin solution for traction.
F	A matrix of element integrations involving the Kelvin solution for traction. Both the direct and indirect formulations consist of **F** matrices. The two **F** matrices differ due to the switch in roles of the field and source point and the indices.
$G_{ij}(\underline{x},\underline{\xi})$	Fundamental singular solution, Kelvin solution for displacement.
G	A matrix of element integrations invclving the fundamental solution. Due to the symmetries in the fundamental solution the **G** matrices for the direct and indirect formulations are equivalent.
$H_{ijk}(\underline{x},\underline{\xi})$	Kernel function in Somigliana's 2nd identity relating boundary tractions and body forces to the stress field.
$M(\underline{x})$	Traction "shape functions" used with nodal traction values to approximate a piecewise continuous traction distribution.
$N(\underline{x})$	Displacement "shape functions" used with nodal displacement values to approximate a continuous displacement distribution.
n	Order of the system of equations.

$\bar{P}_i$	Artificial boundary traction vector, analogous to simple-layer source or source density of potential problems.
r	Distance from the field to the source point, $r^2 = y_i y_i$.
t_i	Actual boundary traction vector.
$T_{ijk}(x,\xi)$	Kelvin solution for stress.
u_i	Displacement vector.
x_i	Position vector to a point on the boundary or within the domain of the problem depending upon the context.
y_i	Vector from the source to the field point, $y_i = x_i - \xi_i$.
z_i	Position vector for a point in the domain used in the integration of body forces.

Greek Symbols

Γ	Complete, finite boundary of the problem.
δ_{ij}	Kronecker delta symbol.
ϵ_{ij}	Cartesian strain tensor.
λ	A Lamé constant.
μ	A Lamé constant, the shear modulus.
ν	Poisson's ratio.
ξ_i	Position vector to a point on the boundary or within the domain of the problem depending upon the context.
σ_{ij}	Cartesian stress tensor.
Ω	Domain of the problem.
ψ_i	Vector of body forces per unit volume.

THEORY

This study focuses on the development of a stiffness matrix for a coupled solution approach. Each method of analysis is applied to portions of the domain where it is best suited. For illustration the domain Ω (Figure 1) is divided into two subdomains Ω^F, the FEM subdomain, and Ω^B, the BEM subdomain. The equations of equilibrium are given by

$$\sigma_{ji,j} + \psi_i = 0 \tag{1a}$$

$$\sigma_{ij} = \sigma_{ji} \tag{1b}$$

and the strain-displacement relations are given by

$$\varepsilon_{ij} = \frac{1}{2}(u_{i,j} + u_{j,i}) \tag{2}$$

The BEM subdomain is assumed to be a linear isotopic homogeneous elastic material. Thus the governing constitutive relations, generalized Hooke's law, are given as

$$\sigma_{ij} = 2\mu\varepsilon_{ij} + \lambda\varepsilon_{kk}\delta_{ij} \tag{3}$$

where λ and μ are the Lamé constants expressed in terms of Young's modulus (E) and Poisson's ratio (ν) as

$$\lambda = \frac{E\nu}{(1+\nu)(1-2\nu)}, \qquad \mu = \frac{E}{2(1+\nu)} \tag{4}$$

Alternatively the equilibrium (1), strain-displacement (2), and constitutive (3) relations can be combined to give a single set of equations in terms of displacement written as

$$\mu u_{i,jj} + (\lambda + \mu)u_{j,ji} + \psi_i = 0 \tag{5}$$

the Navier equations. The boundary conditions are given by

$$u_i(\underline{x}) = \hat{u}_i(\underline{x}) \qquad \underline{x} \in \Gamma_U \tag{6a}$$

$$t_i(\underline{x}) = \hat{t}_i(\underline{x}) \qquad \underline{x} \in \Gamma_T \tag{6b}$$

where $\hat{u}_i(\underline{x})$ and $\hat{t}_i(\underline{x})$ are prescribed distributions of boundary displacements and tractions, respectively. The simple notation does not imply that the boundary conditions are mutually exclusive; the fully-mixed boundary value problem is addressed.

The key solution to equation (5) for the more popular BEMs is the fundamental singular solution -- obtained for elasticity by Kelvin. This is the solution due to a concentrated load in an infinite space which has the same dimension as the problem to be solved. For plane strain conditions the Kelvin solution gives the responses due to a unit force $e_k(\xi)$ in an infinite plane. The indices i, j, and k assume values of 1 or 2, and repeated indices imply summation. The Kelvin solution gives the displacement field as

$$u_i(\underline{x}) = G_{ik}(\underline{x},\xi)\, e_k(\xi) \tag{7a}$$

where

$$G_{ik}(\underline{x},\xi) = C_1\left(C_2\delta_{ik}\ln r - \frac{y_i y_k}{r^2}\right) + A_{ik} \tag{7b}$$

$$C_1 = -\frac{1}{8\pi\mu(1-\nu)}$$

$$C_2 = 3 - 4\nu$$

A_{ik} = arbitrary constant tensor based on zero displacement reference distance

$$y_i = x_i - \xi_i$$

$$r^2 = y_i y_i$$

By incorporating equations (2) and (3), the stress field $\sigma_{ij}(\underline{x})$ is given as

$$\sigma_{ij}(\underline{x}) = T_{ijk}(\underline{x},\underline{\xi})\, e_k(\underline{\xi}) \tag{8a}$$

where

$$T_{ijk}(\underline{x},\underline{\xi}) = \frac{C_3}{r^2}\left[C_4\left(\delta_{ik}y_j + \delta_{jk}y_i - \delta_{ij}y_k\right) + \frac{2y_i y_j y_k}{r^2}\right] \tag{8b}$$

$$C_3 = -\frac{1}{4\pi(1-\nu)}$$

$$C_4 = 1 - 2\nu$$

Equilibrium conditions applied at a boundary point, with a unit outward normal $n_i(\underline{x})$, and equation (8a) combine to give the surface tractions $t_i(\underline{x})$ as

$$t_i(\underline{x}) = F_{ik}(\underline{x},\underline{\xi})\, e_k(\underline{\xi}) \tag{9a}$$

where

$$F_{ik}(\underline{x},\underline{\xi}) = \frac{C_3}{r^2}\left[C_4\left(n_k y_i - n_i y_k\right) + \left(C_4\delta_{ik} + \frac{2y_i y_k}{r^2}\right) y_j n_j \right] \tag{9b}$$

Figures 2 and 3 illustrate the singular behavior of the Kelvin solution components G_{11} and T_{111} respectively, for a point load applied at the origin of the Cartesian system. The singularity of G is order ln(r), while the singularity of T, obtained from derivatives of G, is order 1/r. The plane strain solution can be converted to the plane stress solution by specifying an effective Poisson ratio $\bar{\nu} = \nu/(1+\nu)$

The fundamental solution is a key ingredient in formulating integral equations for the indirect and direct BEMs. Integral equations are an equivalent statement of a boundary value problem. Finite difference solutions approximate the differential equations; finite element solutions approximate a variational principle or weak statement of the boundary value problem; and BEMs approximate the integral equations.

The following subsections provide an overview of both the direct and indirect BEMs and their associated integral equations. These overviews are followed by derivations, both direct and variational, of an IBEM stiffness matrix. The last subsection discusses the discontinuous nature of coupled solution techniques -- an inherent trait of integral equation methods.

Overview of Direct Boundary Element Method

The direct boundary element method is the most highly developed of all the integral equation methods. It was first applied to elastostatics by Rizzo (Ref 39). Cruse and Rizzo (Ref 40) followed with a solution of the general transient elastodynamic problem. Since these early applications, it has matured numerically and the scope of application has significantly broadened.

The integral equations on which the DBEM is based are known as the Somigliana identities. The first identity has been obtained by two different derivations. In both cases the fundamental solution plays a key role. The first derivation uses Betti's reciprocal work theorem in which one system is the actual boundary value problem and the second system corresponds to the fundamental solution (Ref 39). The second derivation, due to Brebbia (Ref 8, 1978), starts with the weak statement of the boundary value problem and incorporates the fundamental solution as the test or weighting function. Betti (1872-73) and Somigliana (1885-86) were the first to apply potential methods to elasticity (Ref 23); thus it is not surprising that Betti's theorem and Somigliana's first identity are the Navier equation counterparts to Green's second and third formula from potential theory.

Somigliana's first identity is given by

$$u_j(\xi) = \int_\Gamma \left[G_{ij}(x,\xi)\, t_i(x) - F_{ij}(x,\xi)\, u_i(x) \right] d\Gamma_x + \int_\Omega G_{ij}(z,\xi)\, \hat{\psi}_i(z)\, d\Omega_z \qquad (10a)$$

$$(x \in \Gamma \wedge z \in \Omega)$$

in which the displacement field is written in terms of the boundary tractions, boundary displacements, and body forces. The second identity is obtained by combining equation (10a) with the strain-displacement (2) and constitutive (3) relations giving the stress tensor as

$$\sigma_{jk}(\xi) = \int_\Gamma \left[H_{ijk}(x,\xi)\, \hat{t}_i(x) - E_{ijk}(x,\xi)\, \hat{u}_i(x) \right] d\Gamma_x + \int_\Omega H_{ijk}(z,\xi)\, \hat{\psi}_i(z)\, d\Omega_z \qquad (10b)$$

in which the stress field is now expressed in terms of boundary tractions, boundary displacements, and body forces. Since the strain-displacement relations (2) involve derivatives of displacement, the kernel functions H and E have singularities of orders $1/r$ and $1/r^2$, respectively.

The DBEM is formulated by the numerical approximation of equations (10). Equation (10a) is used to obtain the unknown boundary values, and then both equations allow the calculation of internal responses. The two approximations made to obtain the unknown boundary values are: (1) integrating in a piecewise manner and (2) solving the equation in a boundary collocation sense. That is, the integration is subdivided over boundary elements and domain cells; and the integral equations are applied to a discrete number of points on the boundary.

The early applications of the method used analytical integrations over elements which could model constant or linear distributions of boundary and domain values. More recent applications apply isoparametric element concepts common to the finite element method (Ref 36). However, unlike the FEM all quantities are interpolated at the same order (i.e., linear boundary elements interpolate

geometry, displacements, and tractions linearly). The boundary distribution of any field variable γ on a single element is written as

$$\gamma_i(\eta) = \sum_{\alpha=1}^{N_{EN}} N_\alpha(\eta)\, \gamma_{i\alpha} \tag{11}$$

where α is the node index; N_{EN} is the number of element nodes; η is the normalized local curvilinear coordinate; $\gamma_{i\alpha}$ are nodal values of the field variable; and $N_\alpha(\eta)$ are the appropriate polynomial "shape functions" for the element. A typical quadratic element ($N_{EN} = 3$) is shown in Figure 4. The "shape functions" for this element are given by

$$N_1(\eta) = \frac{1}{2}(\eta^2 - \eta) \tag{12a}$$

$$N_2(\eta) = (1 - \eta^2) \tag{12b}$$

$$N_3(\eta) = \frac{1}{2}(\eta^2 + \eta) \tag{12c}$$

The kernel functions in the integral equations are singular and require special treatment when considering the response at points on (Ref 1) or near (Ref 34) the boundary. The corresponding numerical details are omitted here for brevity. While the use of the fundamental solution ensures the satisfaction of the governing differential equations, the boundary collocation ensures violation of the boundary conditions. This point is discussed in a later section with respect to a coupled solution approach.

The piecewise integration and boundary collocation allow equation (10a) to be approximated by a system of linear equations in terms of the nodal boundary values and body forces as

$$\mathbf{G}\,\underline{t} - \mathbf{F}\,\underline{u} + \mathbf{G}'\,\underline{\hat{\psi}} = \underline{0} \tag{13}$$

(for details see Ref 1 or 2). The body forces are specified and thus the product with G' gives a known vector. For a mixed boundary value problem the vectors of nodal tractions and displacements contain known and unknown values. To solve for the unknown nodal values we partition the system as

$$\left[G_1 \; G_2\right]\left\{\begin{matrix}\underline{t} \\ \hat{\underline{t}}\end{matrix}\right\} - \left[F_1 \; F_2\right]\left\{\begin{matrix}\hat{\underline{u}} \\ \underline{u}\end{matrix}\right\} + G'\hat{\underline{\psi}} = \underline{0} \tag{14}$$

and then collect the unknown nodal values to give

$$\left[G_1 \; -F_2\right]\left\{\begin{matrix}\underline{t} \\ \underline{u}\end{matrix}\right\} = \left[F_1 \; -G_2\right]\left\{\begin{matrix}\hat{\underline{u}} \\ \hat{\underline{t}}\end{matrix}\right\} - G'\hat{\underline{\psi}} \tag{15}$$

The unknown nodal values are obtained by solving the above system. Then Somigliana's identities can be used to obtain the desired internal responses.

Overview of Indirect Boundary Element Method

The indirect boundary element method is probably the second most common integral equation method. Like the direct method it also has its origins in classical potential theory (Refs 41, 42 and 43). Single- and double layer potentials were used in the theory of classical electrodynamics to express boundary value problems as integral equations. The most advanced implementation of the method appears to remain in its application to electromagnetic field problems (Refs 11, 23 and 44). The indirect method appears to have first been applied to elastostatics by Massonnet (Ref 45, 1965). The numerical development of IBEM, for elasticity problems, paralleled that of the DBEM until the mid 1970s. In recent years it has not been developed as extensively as the direct method; however, its physically meaningful formulation provides insight to b thods (Ref 35).

The integral equation on which the IBEM is based can be derived from Somigliana's first identity by considering two displacement boundary value problems associated with the domain, Ω, and its compliment space (i.e. the interior and exterior problems with respect to Γ). Banerjee and Butterfield (Ref 1) present the analogous development for steady state and transient potential flow based on an idea originally due to Lamb (Ref 46). Eringen and Suhubi (Ref 47) derive the integral equations for elastodynamics by the same argument. The brief presentation of the IBEM which follows is based on a physically intuitive argument.

The integral equations on which the IBEM is based are a single-layer potential statement of the boundary value problem. The domain Ω is embedded in an infinite plane as shown in Figure 5. For elasticity applications the single-layer source corresponds to a vector of artificial tractions, $P_k(\xi)$ with $\xi \in \Gamma$. In this formulation we seek the boundary distribution of artificial tractions which satisfy the prescribed boundary conditions. These tractions are artificial in the sense that they only exist because the domain, Ω, has been embedded in an infinite plane. They represent an intermediate step in the formulation and do not correspond to the actual boundary tractions. Artificial tractions and body forces can be expressed as a "continuous" distribution of $e_k(\xi)$. Thus the displacement, stress and traction fields are given by integrating equations (7a), (8a) and (9a) respectively as

$$u_i(\underline{x}) = \int_\Gamma G_{ik}(\underline{x},\xi)\, P_k(\xi)\, d\xi + \int_\Omega G_{ik}(\underline{x},\underline{z})\, \hat{\psi}_k(\underline{z})\, d\underline{z} \tag{16}$$

$$\sigma_{ij}(\underline{x}) = \int_\Gamma T_{ijk}(\underline{x},\xi)\, P_k(\xi)\, d\xi + \int_\Omega T_{ijk}(\underline{x},\underline{z})\, \hat{\psi}_k(\underline{z})\, d\underline{z} \tag{17}$$

$$t_i(\underline{x}) = \int_\Gamma F_{ik}(\underline{x},\xi)\, P_k(\xi)\, d\xi + \int_\Omega F_{ik}(\underline{x},\underline{z})\, \hat{\psi}_k(\underline{z})\, d\underline{z} \tag{18}$$

Since the solution is expressed as a superposition of the fundamental solution, the governing differential equations are satisfied over the entire plane (excluding Γ).

To determine the distribution of the artificial tractions we bring the field point $\underline{x}$ to the boundary Γ and enforce the boundary conditions (6). The resulting integral expressions are given as

$$\hat{u}_i(\underline{x}) = \int_\Gamma G_{ik}(\underline{x},\underline{\xi})\, \bar{P}_k(\underline{\xi})\, d\underline{\xi} + \int_\Omega G_{ik}(\underline{x},\underline{z})\, \hat{\psi}_k(\underline{z})\, d\underline{z} \qquad \underline{x} \in \Gamma_U \tag{19}$$

$$\hat{t}_i(\underline{x}) = \int_\Gamma F_{ik}(\underline{x},\underline{\xi})\, \bar{P}_k(\underline{\xi})\, d\underline{\xi} + \int_\Omega F_{ik}(\underline{x},\underline{z})\, \hat{\psi}_k(\underline{z})\, d\underline{z} \qquad \underline{x} \in \Gamma_T \tag{20}$$

Equation (19) is regular upon integration while equation (20) must be interpreted in a Cauchy principal value sense and is thus written as

$$\hat{t}_i(\underline{x}) = \pm\tfrac{1}{2}\delta_{ik}\bar{P}_k(\underline{x}) + \int_\Gamma F_{ik}(\underline{x},\underline{\xi})\, \bar{P}_k(\underline{\xi})\, d\underline{\xi} + \int_\Omega F_{ik}(\underline{x},\underline{z})\, \hat{\psi}_k(\underline{z})\, d\underline{z} \qquad \underline{x} \in \Gamma_T \tag{21}$$

The first term represents the singularity contribution assuming a tangent line through $\underline{x}$; the sign depends on the orientation of the element with respect to Ω. The boundary integral must be interpreted as a Cauchy principal value integral.

The IBEM is formulated by the numerical approximation of equations (16) through (21). Equations (19) and (21) are used to determine the unknown artificial tractions, and then equations (16) through (18) allow the calculation of internal responses. As with the DBEM, the two approximations made to obtain the unknowns are: (1) integrating in a piecewise manner and (2) solving the integral equations in a weighted residual sense (on the boundary). The integration is subdivided over boundary elements and domain cells. Normally the integral equations are satisfied in a collocation sense; however, Lean *et al.* (Ref 44) report improved accuracy by a Galerkin

approximation.* This study is limited to a collocation approximation of the equations. Equations (19) and (21) are then approximated as

$$\hat{\underline{u}} = \mathbf{G}\dot{\underline{P}} + \mathbf{G}'\hat{\underline{\Psi}} \tag{22a}$$

$$\hat{\underline{t}} = \mathbf{F}\dot{\underline{P}} + \mathbf{F}'\hat{\underline{\Psi}} \tag{22b}$$

where $\hat{\underline{u}}$ and $\hat{\underline{t}}$ are values of boundary displacements and tractions at collocation points. For "continuous elements" the collocation points correspond to element node points. The coefficient matrices **G**, **G'**, **F**, and **F'** are obtained by integrations of (19) and (21) with respect to the appropriate "shape functions." $\dot{\underline{P}}$ is the vector of unknown nodal artificial traction values, and the last term provides the effect of the body forces at each collocation point. For details see reference 1, 2, 35 or 54.

For a mixed boundary value problem† equations (22a) and (22b) are applied to Γ_U and Γ_T respectively giving

$$\begin{Bmatrix} \hat{\underline{u}} \\ \hat{\underline{t}} \end{Bmatrix} = \begin{bmatrix} \mathbf{G} \\ \mathbf{F} \end{bmatrix} \dot{\underline{P}} + \begin{bmatrix} \mathbf{G}' \\ \mathbf{F}' \end{bmatrix} \hat{\underline{\Psi}} \tag{23}$$

The nodal artificial tractions are obtained by solving the above system. Then equations (16) through (18) can be used to obtain the desired internal responses. As when developing the system of equations, boundary values are obtained by letting $\underline{x}$ go to the boundary (as (19) and (21)).

---

* For additional information on the application of the Galerkin and related approximations to integral equations see Refs 7, 48, 49, 50, 51 and 52. Over-collocation has also been applied in the approximation of integral equations (Ref 53).

† Improved IBEM formulations have been developed to address the mixed boundary value problem (Ref 55) which incorporate dislocation doublets as well as artificial tractions as unknowns.

Consider a few of the differences between the two BEMs. Let N_{CP} be the number of boundary collocation points. Ignoring the integrations associated with body forces, the DBEM (15) and IBEM (23) require the calculation of $2(2N_{CP})^2$ and $(2N_{CP})^2$ coefficients, respectively. However, in solving the system of equations, the DBEM yields the unknown boundary values directly while the IBEM yields the artificial traction distribution. To calculate all the unknown boundary values the IBEM requires an additional $(2N_{CP})^2$ coefficient calculations. Though the total number of coefficients, and thus integrations, required to obtain the unknown boundary values are equal -- the computational effort is not. The coefficient matrices of the DBEM are calculated "simultaneously" and thus the "overhead calculations" (e.g., calculation of the Jacobian) associated with the numerical integrations are done once. Since these "overhead calculations" are performed twice by the IBEM, it requires more effort. However, this comparison has assumed the analyst needs all the boundary values. They are required by the DBEM to calculate internal responses by the Somigliana identities; they are not needed by the IBEM for internal response calculation and thus the analyst can be selective.

The calculation of internal responses also differs between the methods. The DBEM obtains internal responses by the Somigliana identities (10) which integrate the effects of both the boundary tractions and displacements. The IBEM only integrates the effects of artificial tractions, (16) through (18). As in developing the system of equations, though the effort is not doubled for the DBEM, it is considerably more. Another important difference in the internal response calculations is the order of singularity of the kernel functions. For two dimensional problems the methods have the following orders of singularity:

	Displacement	Strain, Stress, Traction
DBEM	o(ln r) and o(1/r)	o(1/r) and o($1/r^2$)
IBEM	o(ln r)	o(1/r)

Thus the DBEM must deal with stronger singularities and correspondingly more difficult integrations. This problem is most severe in the near boundary region (Refs 34 and 35). In fairness, the indirect method is not without its problems in calculating internal responses. Though the integration effort is reduced in the IBEM, often the accuracy is too. A problem that is inherent to the IBEM is associated with loading and geometric discontinuities. In these areas, the artificial tractions experience very high gradients even though boundary conditions may be very well behaved. Thus unless these areas receive special treatment in the numerical formulation or modeling, accuracy is locally very poor.

For coupled solution approaches, particularly for infinite domain problems, it is not easy to determine which BEM would be the most effective. Both methods must calculate two coefficient matrices which involve the same orders of singularity. In addition, discontinuities can often be avoided, eliminating them as a factor. In the following section the IBEM is used to illustrate a direct derivation of a stiffness matrix. The ideas can be applied to the DBEM but are explained with the IBEM due to its conceptual simplicity.

A Direct Derivation of an IBEM Stiffness Matrix

This section presents a physically intuitive derivation of an IBEM stiffness matrix. The relation between nodal displacements and tractions is identical to the relation obtained directly by Kelly *et al.* (Ref 13). The physical approach provides additional insight to the stiffness formulation.

A stiffness matrix relates nodal displacements to generalized nodal forces in the form

$$\mathbf{K}\,\underline{\bar{u}} = \underline{\hat{f}} \tag{24}$$

where $\mathbf{K}$, $\underline{\bar{u}}$ and $\underline{\hat{f}}$ are the stiffness matrix, displacement vector, and generalized force vector, respectively. This basic definition and a numerical solution provided by the IBEM allow a stiffness matrix to be calculated for a BEM region. Consider the displacement boundary value

problem shown in Figure 6. The boundary, Γ, is subdivided into N_E boundary elements. The elements are shown as isoparametric quadratic elements for illustration. All displacements are zero except the j^{th} dof which has a unit displacement. We can now use the IBEM to solve the displacement boundary value problem. As given by equation (22a) with body forces omitted, the unknown nodal artificial boundary tractions are related to the known nodal displacements by

$$\hat{\underline{u}} = \mathbf{G}\,\hat{\underline{P}} \tag{25}$$

This system of equations can be solved for the nodal artificial traction values which can then be used to obtain the unknown real boundary tractions by an approximation of equation (18). The nodal tractions can be expressed in matrix form as

$$\hat{\underline{t}} = \mathbf{F}\,\hat{\underline{P}} \tag{26}$$

The distribution of the traction along the boundary is then approximated in terms of the locally based "shape functions"* as

$$\underline{t}(\underline{x}) = \mathbf{M}(\underline{x})\,\hat{\underline{t}} \tag{27}$$

which by incorporating equation (26) becomes

$$\underline{t}(\underline{x}) = \mathbf{M}(\underline{x})\,\mathbf{F}\,\hat{\underline{P}} \tag{28}$$

With the distribution of boundary tractions, generalized nodal forces (on the boundary) can now be obtained. The nodal forces are determined by "measuring" the work done by the tractions due to a series of virtual displacements -- displacement "shape functions." The generalized forces are given by

---

* In this context the "shape functions" are locally based but defined globally. That is, they are nonzero on one or two elements but defined on all Γ.

$$\hat{f} = \int_{\Gamma} N^T(\underline{x})\, t(\underline{x})\, d\underline{x} \tag{29}$$

For the prescribed displacements $\hat{u}$ the generalized forces are the j^{th} column of a stiffness matrix for the domain Ω. To completely calculate the stiffness matrix we must individually subject each remaining nodal dof to a unit perturbation, solve the corresponding displacement boundary value problem, and then determine the generalized forces by equation (29) to obtain each column of **K**.

We now seek to express the above procedure in equation form. Using indicial notation, the nodal displacement vector for the J^{th} perturbation is given by

$$\bar{u}_i^J = \begin{cases} 1, & i = J \\ 0, & i \neq J \end{cases} \tag{30}$$

where i ranges from 1 to the number of dof (n). Each $\bar{u}^J$ is the J^{th} coordinate vector in the n dimensional space. Combining all of the vectors into a single matrix (i.e., the superscript J becomes an index j) allows equation (25) to be rewritten as

$$\bar{u}_{ij} = G_{ik}\hat{P}_{kj} \tag{31}$$

By equation (30), $\bar{u}_{ij}$ is simply the identity matrix. Thus we can easily solve for the artificial tractions as

$$\hat{P}_{ij} = G_{ij}^{-1} \tag{32}$$

This formulation provides insight to the character of $\mathbf{G}^{-1}$; each column of $\mathbf{G}^{-1}$ is the vector of artificial tractions resulting from a unit perturbation of the corresponding dof. **G** is of full column rank and thus invertible if the collocation point positions are unique. Inserting this result into equations (28) and (29) yields the stiffness matrix as

$$K_{ij} = \int_{\Gamma} N_{ki}(\underline{x})\, M_{kl}(\underline{x})\, d\underline{x}\; F_{lm} G^{-1}_{mj} \tag{33}$$

or in matrix notation

$$\mathbf{K} = \int_{\Gamma} \mathbf{N}^{T}(\underline{x})\, \mathbf{M}(\underline{x})\, d\underline{x}\; \mathbf{F}\,\mathbf{G}^{-1} \tag{34}$$

Kelly *et al.* (Ref 13) obtained the same form of solution for the potential problem by eliminating the source density. For the elastostatics problem this is equivalent to eliminating $\overline{\underline{P}}$ from equations (25) and (26). With their approach we see that the product of **F** and $\mathbf{G}^{-1}$ provides the relation between nodal tractions and displacements. We can write equation (34) in an abbreviated form as

$$\mathbf{K} = \mathbf{C}\,\mathbf{E} \tag{35}$$

where

$$\mathbf{C} = \int_{\Gamma} \mathbf{N}^{T}(\underline{x})\, \mathbf{M}(\underline{x})\, d\underline{x} \tag{36}$$

and

$$\mathbf{E} = \mathbf{F}\,\mathbf{G}^{-1} \tag{37}$$

Brebbia's direct approach (Ref 25) to obtaining a stiffness matrix for the DBEM also has the same form. For the DBEM however, **E** is given by

$$\mathbf{E} = \mathbf{G}^{-1}\,\mathbf{F} \tag{38}$$

where **F** is not the same as obtained for the IBEM. The DBEM uses the same fundamental solution; however the roles of the source and field points and the roles of the indices are reversed in obtaining the Somigliana identities.

As previously mentioned, direct formulations of stiffness matrices in general do not initially yield a symmetric matrix. The following variational derivation of an IBEM stiffness matrix somewhat justifies taking the symmetric component of the above **K**.

A Variational Derivation of an IBEM Stiffness Matrix

This section presents a variational derivation of an IBEM stiffness matrix. The boundary variational statement on which this derivation is based was presented by Zienkiewicz *et al.* (Ref 7).

As an alternative to the previously given strong statement of the boundary value problem an equivalent variational statement can be used. The solution to the boundary value problem is the displacement field which satisfies the essential boundary conditions (6a) and minimizes the potential energy functional given by

$$\Pi(u_i) = \int_{\Omega}\left(\frac{1}{2}\sigma_{ij}\varepsilon_{ij} - \hat{\psi}_i u_i\right) d\underline{z} - \int_{\Gamma_T}\hat{t}_i u_i \, d\underline{x} \qquad (\underline{z} \in \Omega \wedge \underline{x} \in \Gamma_T) \qquad (39)$$

The essential boundary conditions can be explicitly included in the functional via the use of Lagrange multipliers; the functional quantity

$$\int_{\Gamma_U}\lambda_i(u_i - \hat{u}_i) \, d\underline{x}$$

can be subtracted from (39) to give a modified functional, Π^*. It can be shown by variational calculus that the Lagrange multiplier is equal to the boundary traction and thus the modified functional can be written as

$$\Pi^*(u_i) = \int_{\Omega}\left(\frac{1}{2}\sigma_{ij}\varepsilon_{ij} - \hat{\psi}_i u_i\right) d\underline{z} - \int_{\Gamma_T}\hat{t}_i u_i \, d\underline{x} - \int_{\Gamma_U} t_i(u_i - \hat{u}_i) \, d\underline{x} \qquad (40)$$

Note that this variational principle corresponds to the Hu-Washizu principle for the case where the compatibility constraint over the domain is satisfied. This functional does not have an obvious physical interpretation; however, within the context of its numerical approximation the last term might be thought of as the work done by tractions on Γ_U due to the violation of essential boundary conditions.

Our objective is to express both functionals in terms of boundary values. To attain this objective we must eliminate the domain integration. The strain energy term can be rewritten as

$$\begin{aligned}\sigma_{ij}\varepsilon_{ij} &= \sigma_{ij}u_{i,j} \\ &= (\sigma_{ij}u_i)_{,j} - \sigma_{ij,j}u_i \\ &= (\sigma_{ij}u_i)_{,j} + \hat{\psi}_i u_i \end{aligned} \tag{41}$$

Substituting (41) into (39) and applying the divergence theorem to the first term gives

$$\Pi(u_i) = \frac{1}{2}\int_{\Gamma} t_i u_i \, d\underline{x} - \frac{1}{2}\int_{\Omega} \hat{\psi}_i u_i \, d\underline{z} - \int_{\Gamma_T} \hat{t}_i u_i \, d\underline{x} \tag{42}$$

The only approach found for eliminating the body force term is simply assuming an absence of body forces (granted not a satisfying assumption). With this assumption the functional reduces to

$$\Pi(u_i) = \frac{1}{2}\int_{\Gamma} t_i u_i \, d\underline{x} - \int_{\Gamma_T} \hat{t}_i u_i \, d\underline{x} \tag{43}$$

Similarly the modified functional can be expressed in terms of boundary values as

$$\Pi^*(u_i) = \int_{\Gamma_T}\left(\frac{1}{2}t_i - \hat{t}_i\right)u_i \, d\underline{x} - \int_{\Gamma_U}\left(\frac{1}{2}u_i - \hat{u}_i\right)t_i \, d\underline{x} \tag{44}$$

Many researchers (see e.g. Refs 4, 7, 13, 23 and 24) have used the functional of equation (43) to obtain stiffness formulations of the DBEM. Mustoe (Ref 14), apparently based on the work of Zienkiewicz *et al.* (Ref 7), used the modified functional (44) to obtain a stiffness formulation to the IBEM which included the artificial tractions in the vector of unknowns. The modified functional has also been used with the DBEM when the interface was "obviously incompatible" (e.g., when different "shape functions" were used for the two methods). Tullberg and Bolteus (Ref 24, 1982) considered yet another modified functional which constrained the boundary tractions to satisfy over-all equilibrium.

The following derivation uses the boundary form of the potential energy functional (43) to obtain a stiffness matrix for the IBEM. I have not seen this particular derivation in the literature, but literature searches are inherently incomplete. It actually differs very little with the DBEM derivations; we simply obtain our nodal displacement-traction relation from the approximation of a different set of integral equations. The use of equation (43) to develop a stiffness matrix usually implies the existence of continuity at the element boundaries. As will be discussed later, we actually violate inter-element continuity in the following derivation but do so in good company.

The analogous derivation for the DBEM has been expressed in a more general form (see e.g. Ref 23). In the following derivation we neither: (1) consider the essential boundary conditions nor (2) perform condensation at the element level. The key relation for the BEM expresses the nodal tractions in terms of the nodal displacements. As mentioned in the previous section (assuming no body forces), this relationship has been obtained for the IBEM by eliminating the artificial traction vector from equations (22) giving

$$\underline{t} = \mathbf{E}\,\underline{u} \tag{45}$$

where $\mathbf{E} = \mathbf{F}\mathbf{G}^{-1}$ as equation (37).

Using the above relationship and expressing the boundary distribution of traction and displacement in terms of the so called "shape functions," we approximate the functional of equation (43) as

$$\Pi(\underline{u}) = \frac{1}{2}\underline{u}^T \int_{\Gamma} \mathbf{N}^T(\underline{x})\, \mathbf{M}(\underline{x})\, d\underline{x}\, \mathbf{E}\, \underline{u} - \underline{u}^T \int_{\Gamma_T} \mathbf{N}^T(\underline{x})\, \hat{\underline{t}}(\underline{x})\, d\underline{x} \tag{46}$$

Stationarity with respect to each nodal displacement then gives

$$\mathbf{K}\,\underline{u} - \hat{\underline{f}} = 0 \tag{47}$$

where

$$\mathbf{K} = \frac{1}{2}\left(\mathbf{CE} + (\mathbf{CE})^T\right) \tag{48}$$

and

$$\hat{\underline{f}} = \int_{\Gamma_T} \mathbf{N}^T(\underline{x})\, \hat{\underline{t}}(\underline{x})\, d\underline{x} \tag{49}$$

An analogous functional and stiffness matrix derivation exist for potential problems where the vector-valued tractions and displacements are replaced by scalar-valued sources and potentials, respectively.

Note that the matrix in the quadratic term of the above functional is the **K** of the previous section; however, its skew symmetric component contributes nothing to the value of the functional and stationarity gives its symmetric component. The symmetric component of the stiffness matrix is exactly what Brebbia retained, based on heuristic reasoning, from his direct derivation of a DBEM stiffness matrix.

As indicated in the introduction, the symmetry issue has received significant debate. The Maxwell-Betti reciprocal theorem seems to imply that a stiffness matrix should be symmetric for a linear elastic domain; however, this implication assumes that concentrated nodal forces are weighted

identically in obtaining generalized nodal forces. Consider for example a FEM stiffness matrix obtained by a weighted residual formulation using polynomial shape functions and trigonometric weighting functions. In this case the nonsymmetry of the stiffness matrix does not imply that the reciprocal theorem is violated. For direct derivations of the BEM stiffness matrix, the weighting functions used in obtaining the generalized nodal forces (29) are such that nonsymmetry of the stiffness matrix does imply violation of the reciprocal theorem (for concentrated nodal forces).

One could argue that concentrated nodal forces on Γ_I have no meaning since the original BEM model is undefined when a field (collocation) point and source point (concentrated load) coincide. Georgiou (Ref 2 or 56) has apparently taken this view in arguing that the reciprocal theorem is not directly applicable to generalized nodal forces. For an arbitrary distributed traction symmetry only implies the reciprocal theorem is satisfied in some average sense and nonsymmetry does not necessarily imply the reciprocal theorem is violated. However the argument seems somewhat sterile if we think of a unit concentrated load as a uniformly distributed load (with a resultant of one) subject to the limit of the distribution area tending to zero.

From a practical stand-point, if one is coupling the BEM to an existing FEM program its likely that the architecture of the existing code is based on a symmetric stiffness matrix. Thus symmetry is a cherished property and will be treated as such in the remainder of this study.

In addition to lack of symmetry, both the direct and variational formulations can produce stiffness matrices which violate equilibrium and fail to allow rigid body motion. Hartman (Ref 27, 1981) attributed these problems to the approximations made in obtaining the nodal traction-displacement relationship (via **E** of equations (37) and (38) for the IBEM and DBEM, respectively). As previously mentioned, for the DBEM the equilibrium problem can be addressed when formulating **E**; equation (13) is augmented with two additional equations and corresponding Lagrange multipliers, which force the traction distribution to "identically" satisfy equilibrium (Ref 13). Most

approaches to these problems modify the stiffness matrix rather than address the traction-displacement relationship (Ref 24).

Hartman appears (I won't pretend to have fully digested his analysis) to have presented an excellent analysis of the numerical errors which occur in forming a stiffness matrix based upon the DBEM. The numerical solution of integral equations can produce a stiffness matrix with the above mentioned undesirable properties; in addition, the numerical approximations result in an inherent incompatibility along Γ_I, which is discussed in the next section.

Discontinuity of Boundary Element Methods

Regardless of the formulation there is a characteristic of BEM formulated stiffness matrices and BEM solutions in general which is often not realized; **BEMs* are inherently incompatible at the interface of homogeneous regions.**

Derivations of BEMs usually indicate that the governing differential equations are satisfied exactly in the domain while the boundary conditions are only satisfied in an average sense. Often this is interpreted as meaning the boundary element "shape functions" constrain the displacement field. Actually the meaning has greater depth. This interpretation is often a consequence of invalid analogies between BEMs and FEMs. The methods are theoretically related (Refs 8,7, and 13) and certainly the BEM has borrowed much technology from the FEM; however, the accepted use of the name "boundary element methods" for the numerical solution of boundary integral equation methods is misleading. This interpretation is usually not enlightened by numerical experience since many BEM programs can not accurately calculate responses in the near boundary region.

---

* This statement assumes the BEMs are using the fundamental singular solution as presented in previous sections.

The "shape functions" used for the so called "boundary elements" do not constrain the displacement field but merely offer an approximation of the boundary values to facilitate numerical integration. That is, these "shape functions" serve as a basis for the approximate distribution of boundary values in the integral equations -- not for the boundary response obtained by these approximated integral equations. Typically the integral equations are satisfied in a collocation sense (i.e., at discrete points along the boundary) and thus the boundary conditions are satisfied at the collocation points (which coincide with nodal points for "continuous" element formulations). In between these points, boundary conditions can be grossly violated. This is graphically illustrated in reference 35.

Since the term "shape function" and "boundary element" only apply to the discretization of the integral equations the terms "continuous element" and "discontinuous element"* have the same limitation. The integral equations used in the calculation of internal responses give a continuous response throughout the domain; however for "discontinuous elements," large response oscillations can occur near the boundary value discontinuities.† The response with both elements is continuous but their violation of the boundary conditions will differ.

Similar to the displacement-based FEMs' satisfaction of equilibrium equations in a nodal sense, the BEM (using nodal collocation and "continuous elements") only satisfies boundary conditions in a nodal sense. Many researchers indicate that compatibility between the BEM and FEM is easily satisfied by using the same "shape functions" (Refs 1, 7, 13, 15, 23, 25, 26 and 58); this is not

---

* "Continuous elements" are characterized by their C^0 continuity modeling of boundary values. "Discontinuous elements" are not collocated at extreme nodes and thus can represent a discontinuous boundary value distribution.

† If the discontinuities are prescribed boundary conditions then these oscillations reflect a limitation in our theory since: 1) we assume displacement continuity and 2) traction discontinuity implies a violation of equilibrium equation (1b) (neither the divergence theorem or mean value theorem are applicable). Otherwise the discontinuities and the associated near-boundary errors are simply a liability of this element formulation. The lack of C^1 continuity with "continuous elements" can also reduce the accuracy in the near-boundary region but usually to a much lesser extent. This was the motivation for Bilgen's (Ref 57, 1982) development of a cubic spline element.

true.* In general, continuity (for a stiffness modeled BEM region) can not be satisfied *a priori* simply by the selection of "shape functions." This is more obvious for the IBEM since the initial use of "shape functions" is for the approximation of the artificial traction distribution instead of the actual boundary values. Zienkiewicz *et al.* (Ref 7) and Mustoe (Ref 14) realized the incompatibility which existed in their variational derivation of an IBEM stiffness matrix based upon (44). However, it appears they attributed this incompatibility to the use of the modified functional since their other direct and variational derivations explicitly indicated that continuity was satisfied. The derivations of this study have ignored this inter-element continuity violation like most derivations in the literature. This incompatibility is numerically demonstrated for the IBEM in a following section.

Incompatibility does not necessarily imply poor results. On the contrary many incompatible finite elements exhibit improved performance, and many accurate BEM solutions have been reported. Recognition of this basic incompatible behavior could be of practical use. It affects the convergence properties of the method and can potentially explain other solution characteristics. One very useful application could be in mesh refinement. Whether the refinement is a manual or an adaptive process, the variation in computed responses between collocation points can provide a measure on which to base the refinement. For example, one could base the mesh refinement criteria on the relative error between "shape function" interpolated displacements and integral equation calculated displacements sampled at a few points between element nodes.

Margulies (Ref 62, 1981) showed that the use of a bounded Green's function instead of the free-space Green's function (as used in this study) allows the incompatibility to be eliminated. He

---

* When the preliminary report on this study (Ref 38) was written, I had not found any references recognizing this incompatibility. Among possibly others, Jirousek (Refs 59, 1978; 60; 61) and Margulies (Ref 62, 1981) had recognized the incompatibility which exists, but the compatibility fallacy continues to propagate throughout the literature.

indicated that since we have freedom in selecting the geometry of Γ_I, the appropriate Green's function can often be readily obtained.

NUMERICAL IMPLEMENTATION

This section discusses the numerical implementation of the IBEM stiffness matrix developed above. Algorithms, in the form of pseudo-code outlines, provide detail on key aspects of the implementation. These algorithms have been implemented in a research code. The scope of this discussion is limited to the calculation of the stiffness matrix; assembly of element stiffness matrices is well documented elsewhere (Ref 4). Both the IBEM and DBEM are addressed below since their stiffness matrices (35) can have the same form. Rudolphi (Ref 26) provides a general outline for the calculation of a stiffness matrix including the BEM coefficient matrix calculations. His paper deals principally with the potential problem using the DBEM. Though Rudolphi's work was not referenced while implementing the research code, the main steps in the calculations are independent of the application and the particular BEM.

Due to the complexity of BEM and FEM software systems emphasis must be placed on the modular design of the coupled software system. Figure 7 illustrates the extent of the software coupling used in this study. In the following discussion I assume BEM and FEM systems exist and require modification. The stiffness matrix calculation can be organized as three tasks:

(1) Calculation of the coefficient matrices (**G** and **F**) and **C**

(2) Preliminary **K** calculation, inverse and matrix product calculations as shown in equation (34)

(3) Optional adjustments in **K** to satisfy equilibrium and symmetry

The first task requires modification of the BEM program. The second and third tasks can be added to the BEM program, comprise a separate module, or be incorporated into an element routine of the FEM program. I prefer to "weakly couple" the software systems so that they can still serve as individual research and analysis tools. By this approach the first task is completely performed by the modified BEM program. The second and third tasks are performed by a separate program

module which except for the three component matrices of **K** (i.e., **C**, **F**, and **G**) requires no access to the BEM data. An element routine is then added to the FEM program which reads data defining the "super element" connectivity and assembles the BEM **K** into the global system at the time of assembly. Solution of the FEM system provides nodal displacements from which stresses can be calculated in both the FEM and BEM domains.

When boundary tractions or internal responses are required in the BEM region, the displacements associated with BEM nodes must be retained. For either BEM, boundary tractions can be obtained by the equation: $\bar{t} = \mathbf{E}\,\hat{u}$. For the DBEM the known boundary values in combination with Somigliana's identities (10) provide internal responses. For the IBEM the tractions or displacements could be used to solve a boundary value problem for the artificial tractions. Alternatively $\mathbf{G}^{-1}$ could be saved during the **K** calculations giving $\bar{P} = \mathbf{G}^{-1}\,\hat{u}$. The effect of the artificial tractions is then integrated to obtain internal responses according to (16) through (18). The remainder of this discussion concentrates on the calculation of the stiffness matrix.

For smaller problems the calculation of the matrices comprising **K** dominates the numerical effort. The coefficient matrices are inherently full and their formulation requires extensive numerical integration. The cost of their calculation would appear to increase with the square of the number of boundary elements. There is an element "overhead cost" which follows this trend; however for a program which uses a variable order integration scheme the cost of the average element integration decreases. This is due to the reduction in the order of integration with a decrease in the ratio of element length to collocation point distance (Refs 35 and 36).

Calculation of **E** requires an IBEM program to generate both **F** and **G** for a single homogeneous domain. These are the same equations required to combine homogeneous BEM regions by approximate satisfaction of equilibrium and continuity along their interface. Thus many existing BEM programs already have this capability. The calculation of two coefficient matrices does not

double the numerical effort because much of the overhead in the numerical integrations is common to both types of coefficients.

In the DBEM both **F** and **G** are always calculated. The only modification which might be required, depending on the program design, is the retention of all the coefficients. Some implementations immediately multiply known boundary values by corresponding coefficients and sum the terms into the known vector to form the system of equations (15).

Calculating the integration of the shape function product matrix, **C**, according to (36) is effectively performed at the element level. Because of the locally based nature of the "shape functions," **C** is very sparse. For quadratic elements, rows associated with a mid-node have three nonzero terms, and those associated with an extreme node have five nonzero terms. In this implementation tractions and displacements are interpolated at the same order (quadratic), and there are no provisions for traction discontinuities. As a result $\mathbf{M}(\underline{x}) = \mathbf{N}(\underline{x})$ and therefore **C** is symmetric. Not providing for traction discontinuities does place geometrical constraints on the BEM region. However for BEM regions comprised of several elements and few corners, Rudolphi (Ref 26) concludes that traction continuity has a negligible effect on the accuracy. For applications where the BEM region is used as an "infinite element" the analyst determines the shape of the FEM-BEM interface and thus geometric discontinuities pose no problem.

For a vector boundary value problem such as the elasticity problem, the two rows of **C** corresponding to a common node have identical terms but differ in their position, column. Except for the diagonal terms in **C** each term calculated at the element level is complete (i.e., no summation is required) and could be formally assembled into four positions of **C**. Only the diagonal terms of **C** which correspond to shape functions spanning two elements require the addition of a second term. Thus it is very efficient to both calculate **C** and perform its multiplication with **E** at an element level. There is a maximum of six unique terms for a single

element. Execution and storage requirements associated with **C** are trivial compared to **F** and **G** which are full coefficient matrices.

The algorithm below outlines the calculation of **C** at the element level. The research code is written in the Modula-2 language (Ref 63) which is a descendent of Pascal and Modula. Those familiar with Pascal will recognize the dialect below. I have attempted to remove enough syntactical idiosyncrasies from the code to permit communication. Calls to Modula-2 procedures (analogous to FORTRAN subroutines) are supplemented with short descriptions of their purpose. Comments which do not replace actual code are enclosed in (* *)'s. General file operations and variable definitions are omitted. Descriptive variable names supplemented by comments are used to define variables. Many modern languages provide for user defined data types. Nnode and Mnode are variables which can have the enumerated values of (a,c,b), the node indices listed by extreme nodes first. This corresponds to α of Figure 4 taking the values of (1,3,2) respectively. These variables, Nnode and Mnode, serve as nodal indices to arrays and promote internal documentation. More complicated data types such as records have been converted to arrays to simplify the description.

Algorithm 1. Shape function product matrix calculation.

```
PROCEDURE GenerateShapeProductMatrix
(ContNode,       (* array of continuous element node numbers
                    indexed as (element_number,node_index) *)
 numeltotal,     (* total number of continuous elements *)
 ShapeIntOrder)  (* numerical integration order *)

BEGIN (* the GenerateShapeProductMatrix procedure *)
FOR elnum = 1 TO numeltotal DO (* for each element *)
  (* determine shape function (N) & weight-Jacobian product values at each
     integration point *)
  FOR Nnode = a TO b DO (* an index on the node *)
    Write the equation number for node ContNode[elnum,Nnode] to the NMfile
  END (* the Nnode loop *)
  FOR intpt = 1 TO ShapeIntOrder DO (* each integration point *)
    position = GAUSSpt[ShapeIntOrder,intpt] (* obtain the position of the
      integration point *)
    SHAPEfunctions(position,Nvalues,intpt) (* calculate the shape function
      values at "position" and save in Nvalues
      indexed as [intpt,node_index] *)
    Calculate the Jacobian at "position"
    WGTdetJ[intpt] = GAUSSwgt[ShapeIntOrder,intpt]*J (* calculate the
      integration weight Jacobian product at each integration point *)
  END (* the integration point loop *)
  FOR Nnode = a TO b DO (* for each nonzero shape function *)
    FOR Mnode = Nnode TO b DO (* for each unique combination of
      shape function, i.e., N=M thus symmetry is considered *)
      integral = 0.0 (* initialize integration *)
      FOR intpt = 1 TO ShapeIntOrder DO (* each int. pt *)
        integral = integral + Nvalues[intpt,Nnode]*
          Nvalues[intpt,Mnode]*WGTdetJ[intpt]
      END (* the integration point loop *)
      Write the integral value to the NMfile
    END (* the Mnode, M shape function, loop *)
  END (* the Nnode, N shape function, loop *)
END (* the element loop *)
END (* the GenerateShapeProductMatrix procedure *)
```

The six integration results are written to the NMfile in the order: a-a, a-c, a-b, c-c, c-b, and b-b, where the letters indicate the node index of each "shape function" in the product.

With all of the component matrices for **K** calculated, the second task of calculating an initial unsymmetrical stiffness matrix can proceed. The third task of satisfying equilibrium and obtaining a symmetric form can be combined with the matrix operations of the second task. The details of integrating the two tasks are highly dependent on the method used to obtain symmetry and

equilibrium. For this research code, the tasks are independent, so different methods can be investigated. This also allows the symmetry of the original stiffness matrix to be examined.

The initial steps required in the calculation of **K** differ in the two BEMs. This difference results from the reversal of **F** and $\mathbf{G}^{-1}$ in the traction-displacement relations, (37) and (38). As a result of this difference the IBEM is burdened with n^3 additional multiplications and $(n-1)n^2$ additions if **E** is to be obtained in a column order. Additionally the DBEM has reduced memory requirements since **F** can be read from disk one column at a time. Each column of **E** can immediately be used to calculate the corresponding column of **K**.*

As the order of the system of equations increases, the "calculation of the inverse" in equation (37) or (38) becomes the most costly step. For Gauss elimination the cost increases as n^3. A common approach (Refs 26 and 58) to reducing the cost of "calculating the inverse" is to subdivide the single BEM region into several BEM regions, providing many small stiffness matrices instead of one large stiffness matrix. This subdivision introduces additional boundary elements, and thus more equations, but the equations corresponding to the complete BEM domain are now block banded. Mitsui *et al.* (Ref 58) suggests that with regard to efficiency there is an optimal degree of subdivision. Subdividing the BEM region may also require that traction discontinuities and the violation of equilibrium be treated more rigorously since the occurrence of geometric discontinuities and a relatively small number of elements would be more likely. Kagawa, Yamabuchi and Kitagami (Ref 64) take this approach to the limit; each boundary element on Γ_I belongs to a unique homogeneous BEM region. Thus each BEM region is bounded by three boundary elements -- one finite length element on Γ_I and two "infinite boundary elements"

---

* The approach presented here and used in the following algorithm breaks a cardinal rule of numerical analysis -- an inverse is calculated. An alternative exist via some linear algebra: $\mathbf{E} = \mathbf{F}\mathbf{G}^{-1} \Leftrightarrow \mathbf{E}\mathbf{G} = \mathbf{F} \Leftrightarrow \mathbf{G}^T\mathbf{E}^T = \mathbf{F}^T$. In contrast to the previous approach, solving this system of equations gives **E** by rows instead of by columns. **F** could be read from disk a row at a time, but **K** would have to be kept in-core even if the unsymmetric **K** was to be used.

extending away from Γ_I. The bandwidth is minimized but so is the accuracy. To improve the accuracy in the region of principle interest, Ω^F can be enlarged to further isolate Γ_I. Thus for comparable accuracy the bandwidth can be reduced at the cost of increasing the number of equations.

For both BEMs, a column of **E** is immediately used to calculate the corresponding column of **K**. The above algorithm calculates **C** at the element level and writes the values to NMfile. An algorithm to calculate an initial **K**, given the component matrices, is shown below. Values of **C** are read from NMfile, consistent with the previous algorithm. In this implementation the pseudo-code given below is a separate program (a Modula-2 program module).

Algorithm 2. Stiffness matrix calculation.

```
MODULE StiffnessMatrix
BEGIN (* the StiffnessMatrix module *)
ReadCmatrix(EqNum,C,numeltotal,order) (* read C: EqNum contains the
  equation numbers for each node indexed as [element_number,node_index]
  and C contains the integration of the shape function products indexed as
  [element_number,0..5] *)
ReadGmatrix (* read G *)
ReadFmatrix (* read F: For the Modula-2 implementation these two
  procedures cause G and F to be read by modules involved in the
  calculation of E.  This module does not have access to the data
  of G and F. *)

(* Calculate the stiffness matrix, K *)
Initialize K to zero
FOR col = 1 TO order DO (* for each column of K *)
  CalcEcol(col,Ecol) (* calculates a single column of E stored in Ecol *)
  FOR elnum = 1 TO numeltotal DO (* for each element *)
    Ccount = 0 (* initialize the index for the C array *)
    FOR node1 = a TO b DO (* node index for the first shape function *)
      roweq = EqNum[elnum,node1] (*first row equation for node1*)
      FOR node2 = node1 TO b DO (* for each new combination *)
        coleq = EqNum[elnum,node2] (* first column equation for node2 *)
        Cval = C[elnum,Ccount] (* extract the C term from the element
          array *)
        FOR eqincrement = 0 TO 1 DO (* for each nodal dof *)
          Crow = roweq+eqincrement
          Ccol = coleq+eqincrement
          (* calc. contributions in both symmetrical terms *)
          K[Crow,col] = K[Crow,col] + Ecol[Ccol]*Cval
          IF roweq#coleq THEN  (* not a diagonal term *)
            K[Ccol,col] = K[Ccol,col] + Ecol[Crow]*Cval
          END
        END (* the eqincrement loop *)
        increment Ccount
      END (* the node2 loop *)
    END (* the node1 loop *)
  END (* the elnum loop *)
END (* the col loop *)

Adjust K for equilibrium and symmetry
Write the upper triangular portion of K to disk
END (* the StiffnessMatrix module *)
```

As previously noted, due to symmetry and the vector nature of the elasticity problem each element C value (except diagonal terms) has four positions in the assembled C. The "eqincrement loop" above multiplies each element C value by four terms (two for diagonal terms) in the column of E

and assembles the products into the corresponding four **K** terms. By this approach the sparsity of **C** is exploited and the matrix is never assembled.

The last task in calculating a stiffness matrix is adjusting **K** to satisfy symmetry and equilibrium. The work of Tullberg and Bolteus (Ref 24) provides guidance, based on numerical studies, for both of these problems . As previously mentioned, numerical studies have shown the unsymmetric **K** obtained by the direct approach to be more accurate than the symmetrical form obtained by a variational approach. However when combining the matrix with an existing FEM system a symmetric form is usually preferable. An exception can occur if the FEM is used to model plasticity governed by nonassociative flow rule; in this case the resulting FEM system can be unsymmetric. In this study the stiffness matrix is symmetrized by averaging the off-diagonal terms.

In the initial implementation of the research code, equilibrium considerations have not been included. Our principal interest is in infinite domain problems where previously mentioned techniques are not applicable. For finite domain problems, one of the methods implemented by Tullberg and Bolteus (Ref 24) to solve the equilibrium problem might be improved upon. The equilibrium error for a given direction was corrected by adding the average error to each term. This approach did not consider the relative magnitude of each term. A better approximation might be obtained by basing the error distribution on the normalized magnitude of each term where the sum of absolute values of the stiffness terms is the normalizing factor.

The FEM program used in this study was a modified version of SAPIV (Ref 65). An isoparametric eight-node quad was added to the program as well as the BEM element routine for reading previously generated stiffness matrix (see Figure 7). Since the BEM region was not subdivided, local arrays in the element assembly routine had to be enlarged to allow assembly of the super element.

NUMERICAL RESULTS

This section includes the numerical results for two classical problems of elastostatics. Both consists of a cavity in an infinite media subjected to an internal pressure; the first is simple (a circular hole), the second is not (a crack). For both problems IBEM analyses were attempted using the standard formulation (i.e., using polynomial "shape functions" and collocation) and a stiffness formulation (the symmetric stiffness formulation presented in previous sections). For the circular hole problem the stiffness formulation gave acceptable results so a coupled solution was pursued.

Pressurized Circular Hole in an Infinite Media

The problem is depicted in Figure 8 which shows the two boundary element models used (a 6 and a 12 element model). Using Airy stress functions in polar coordinates the exact solution is found to be

$$u_r = P_o\left(\frac{1+\nu}{E}\right)\frac{a^2}{r} \qquad u_\theta = 0$$

$$\sigma_{rr} = -\sigma_{\theta\theta} = -P_o\left(\frac{a}{r}\right)^2 \qquad \sigma_{r\theta} = 0$$

where "a" is the radius of the cavity. In particular I considered the problem where: $P_o = 100$, $a = 3$, $E = 207{,}900$ and $\nu = 0.1$ (Refs 8 and 17). It is interesting to note that with this stress field all the strain energy is distortional, the plane strain and plane stress solutions coincide, and the associated plane-strain problem gives the exact solution to the plane problem. The same holds true for the problem of a circular cavity subjected to a uniform shear; thus these results hold for any uniform load (of constant direction with respect to the polar system). At the other extreme we can consider the original problem with a finite, circular, outer boundary. As the outer boundary approaches the inner boundary (the case of a thin walled shell for plane strain) all the strain energy becomes dilational.

The standard IBEM analysis was posed as both a traction and a displacement boundary value problem where the radial displacement was obtained from the a' ve analytical solution. Both problems were of interest because the stiffness formulation uses the coefficient matrices of both problems. The results for the six element model (model 1) are compared with the analytical solution in Figure 9. Overall the results of the displacement boundary value problem are the most accurate, however it also has its greatest error in the most critical region -- near the boundary. The results for the twelve element model (model 2) are compared with the analytical solution in Figure 10. The accuracy of both boundary value problems improved with the refined discretization. Note that unlike most domain-based methods the BEM calculates displacements and stresses to comparable accuracies.

The next models considered for this problem used the IBEM in the previously presented symmetric stiffness formulation. The IBEM was used to calculate a stiffness matrix which was then read into SAP IV to calculate the nodal displacements. With the nodal displacements, the IBEM solved the resulting displacement boundary value problem for the nodal artificial tractions and then any subsequent internal responses.

The results for the six (model 3) and twelve (model 4) element models are given in Figures 11 and 12, respectively. Note that the responses along radial lines thru element extreme and mid-side nodes differ.* This difference indicates the results oscillate about the solution with respect to change in the angle. For the domain as a whole there is significant improvement in the results with the model refinement. However, while the displacements improve on the boundary the stresses do not appear to do so. This behavior will be discussed when considering the coupled solution that follows.

---

* For Figure 11 response lines along the x-axis and y-axis correspond to lines thru the extreme and mid-side node respectively.

Prior to considering the response of the coupled solution let's examine the degree of asymmetry in the stiffness matrices of models 3 and 4. In Figure 13 a measure of asymmetry in each term of the stiffness matrix is indicated. A blank indicates the stiffness value was less than 10^{-7}. An integer n in the i-j position implies that $|(K_{ij} - (K_{ij}+K_{ji})/2)/K_{ii}| \leq n\%$ (i.e. the difference in the old and new stiffness terms relative to the magnitude of the diagonal stiffness term of the i^{th} row). This measure of asymmetry was used because it emphasizes the asymmetry in the significant terms (those of large magnitude) of the stiffness matrix. For example, an asymmetry of 50% relative to $(K_{ij}+K_{ji})/2$ is not very significant if the magnitude of K_{ij} is such that $1000K_{ij}<K_{ii}$. Due in part to this measure the asymmetries are "magnitude banded" around the diagonal. The nodes were simply numbered in a counter-clockwise manner; so the large relative asymmetries correspond to dof associated with nodes that are geometrically close. For both models the degree of asymmetry was on the order of 5%.

Figure 14 shows the results obtained using a simple 4 element FEM model (model 5) which exploited the axisymmetry of the problem. A 60 degree sector was modeled where the first element had a radial length of 3 and each successive element doubled in length. The outer boundary was at a radius of 48 and the nodes on this boundary were fixed against translation. The overall accuracy was very good. As expected, note the improved accuracy of σ_{rr} at the Gauss points compared to the center of the element. The numerical results do not provide a great deal of motivation for a coupled approach, but that is due to the simplicity of the problem. Without axisymmetry in loading and geometry, a large model would be required and the bandwidth would necessarily be quite large. The motivation increases in dynamics applications where artificial boundaries can produce reflections from waves that should continue to propagate outward.

The two coupled models are shown in Figures 15. For both models Γ_I is a circle with a radius of 6. Figures 16 and 17 give the numerical results for the coupled models. Again the results indicate a convergence tendency with model refinement. As with the models 3 and 4, the stresses along the boundary to the BEM region do not appear to improve, but the error does become more localized.

Even though the BEM region has its maximum error along Γ_I, it appears that this oscillation in the response does not cause the accuracy in the FEM region to be sacrificed.

Figures 18 and 19 summarize the behavior of the IBEM stiffness formulation along boundaries -- both by itself and coupled. As discussed in a previous section the "shape functions" do not serve as a basis for the boundary response for the BEM. This is graphically illustrated in both figures. In Figure 18, the response lines labeled as "BEM" are the values given by the integral equations rather than being simply interpolated between nodal values by the "shape functions." Due to the use of collocation the response estimates coincide at the collocation points (the nodal points in this formulation). The relative errors at the extreme and mid-side nodes for models 3 and 4 are

	Extreme Nodes	Mid-side Nodes
Model 3	-14.3%	7.73%
Model 4	-5.46%	3.64%

where a negative sign indicates an underestimate of the value. Similarly the errors for models 6 and 7 along Γ_I are

	Extreme Nodes	Mid-side Nodes
Model 6	-5.99%	1.80%
Model 7	-2.21%	1.21%

The smaller errors for the coupled problem are probably due to two factors: 1) Γ_I is in a region with a lower stress gradient and 2) the FEM region tends to resist the distortion of Γ_I.

For both the IBEM stiffness formulation and the coupled approach, the discrepancy between the two response curves for a given model gives a measure of the goodness of the discretization. The "shape function" curve gives the assumed distribution used in calculating the stiffness matrix, and the BEM curve gives the resulting response as calculated by the integral equation (for the IBEM equation [16]); so if the discrepancy is "significant" the assumed distribution was meaningless. For a BEM analysis (standard or stiffness formulation) the exact solution occurs when the integral

equation calculations exactly yield the boundary values. For a coupled analysis we can think of the discrepancy as an indication of the incompatibility between the two methods. In this particular case the two subdomains overlap rather than form a gap.

In considering the discrepancy between the assumed distribution of boundary values and the distribution given by the integral equations, it is instructive to consider a more basic problem. Consider the problem of the circular cavity (geometrically given by model 3) subjected to a radial load of 1000 at one node with the remainder of the nodes fixed. Figures 20 and 21 give the results to this problem along a portion of Γ for the cases of the load applied to both a mid-side and extreme node, respectively.

The integral equation results have a higher order of continuity than the "shape functions," and both the integral equation curves are of similar shape. For the IBEM, "shape functions" are used to interpolate the artificial tractions in the standard formulation but not the real boundary values. (This differs with the DBEM where the unknowns in the system of equations are nodal values of the real boundary values [15].) In forming the stiffness matrix the IBEM also uses the "shape functions" to interpolate the boundary values (see equations [27], [29] and [46]). This at least partially accounts for the significant reduction in accuracy when using the stiffness formulation.

Note that the "shape functions" predicted by the BEM are not locally based, as assumed, and are only zero at collocation points. It might be possible to use analyses such as this (in an automated manner) to adjust some element parameters that would slightly change the original "shape functions" used to interpolate boundary values. However it would probably be more effective to simply use the discrepancy to determine the need for mesh refinement. It is interesting to note that if the "shape functions" predicted by the integral equations were used to obtain generalized nodal forces (49), the mid-side node and extreme node generalized forces would decrease and increase, respectively -- exactly what appears to be needed (Figures 18 and 19).

Note the similarities here with an eigenfunction problem (especially for the DBEM). We seek a distribution of boundary values (both tractions and displacements) that when operated on by integral operators gives back the same distribution of boundary values. We use the difference in the distributions to evaluate the iteration and continue to iterate (refine the mesh) if necessary.

For both the IBEM stiffness formulation and the coupled solution the stresses along Γ_I do not improve with mesh refinement. This is consistent with the displacement results shown in Figures 18 and 19. The amplitude and period of the oscillation in the boundary values decrease with mesh refinement but in a manner that leaves the derivatives of the displacement (on the boundary) nearly unchanged relative to a given position on an element. At practical levels of discretization this oscillatory error in the near boundary region may always exist. The key point though is that this error had no apparent effect on the accuracy in the FEM region. This might not be the case for all problems.

From an energy point of view one might expect the average displacements in Figures 18 and 19 to under estimate the theoretical value. Since the predicted radial displacement is nonuniform, the model predicts the presence of dilational energy as well as the expected distortional energy. Since the stiffness associated with dilation is greater than that of distortion, the reduced average displacement is consistent with this apparent redistribution of strain energy.

For this simple problem the coupled solution performed reasonably well. The errors are small and are localized around Γ_I. This problem suggests that the coupled solution approach does have potential when the BEM is used to model the infinite domain. In this problem we considered the best possible shape for a cavity; in the next problem we consider the worst possible shape.

Pressurized Crack in an Infinite Media

This problem consists of a unit length pressurized crack in an infinite media as shown in Figure 22. The motivation for this problem is the idea of using the BEM to form a crack tip element for

coupled solutions. My particular IBEM stiffness formulation does not provide for rigid body motions, so it is not possible to limit the BEM region to the crack tip; instead the entire crack is modeled by the boundary element method.

The difficulty with this problem is that the stress has a singularity of $1/\sqrt{r}$ at the crack tip. For this problem I chose the strain energy density (SED) as a measure of the accuracy in the tensor stress field. Figure 23 shows the analytical solution (based on Westergaard's solution [Ref 66]) for the strain energy density near the crack tip and emphasizes the severity of the stress gradients.

Fracture mechanics problems are often solved using complex series (Ref 67). In the vicinity of the crack tip only the singular term in the series expansion is important. Thus to evaluate a numerical solution one should consider a region where the singular term dominates the problem. As shown in Figure 24, the singular solution is the major contributor to the strain energy density for the region to be considered in the subsequent analyses.

Figure 25 shows the various geometries of the IBEM crack models considered in this study. To apply the IBEM or the DBEM to a crack problem requires the introduction of a gap (a separation of the crack faces) into the model. The necessity of a gap is easiest to explain for the IBEM. Consider a horizontal crack subjected to mode I (i.e. opening mode) loading. By symmetry, on the opposing crack faces the vertical artificial tractions are expected to be of equal magnitude but opposite direction; the horizontal artificial tractions are expected to be equivalent. The use of the term "symmetry" suggests that the crack faces are on opposite sides of the crack axis. So one might consider the geometry of the crack as being defined as the limit of two crack faces approaching an axis. If this limiting process is not considered when applying the IBEM the numerical results will not be unique. Consider the integral equations which the IBEM approximates (19 and 21) for the case of coincident crack faces. Symmetry requires the vertical tractions on opposing crack faces to be equal in magnitude and opposite in direction. Since they are applied along the same line their effects in the integral equations cancel, thus their magnitude

can not be uniquely determined. Numerically this manifests itself as a singular matrix -- in the reality of finite precision, a very ill-conditioned matrix. Due to finite precision the method gives results but they are absolutely useless.

The introduction of a gap into the model can be thought of as our numerical approximation to the above mentioned limit. As shown in Figure 22, for each model the elements nearest the tips taper to close the cavity. (Model 4 used 2 elements on each face to taper toward a tip.) If the gap is too large the model fails to geometrically resemble a crack. If the gap is too small: 1) the method is prone to roundoff error, 2) the system of equations can be very poorly conditioned, and 3) the numerical integrations can be come very expensive. The first problem occurs with approximately equal magnitude vertical tractions separated by a small distance. At a response point relatively far from these tractions, the difference in their effects (via the integral equations) would be many digits into the real word -- thus producing roundoff error. The third problem is due to the close proximity of collocation points to neighboring elements. As the gap decreases the collocation points become closer to neighboring elements and thus the cost of numerical integrations increases. The crack problem can not even be practically attempted with a standard BEM code unless it can accurately calculate responses in the near boundary region.

The following figures (26, 27 and 28) summarize a parameter study that varied the boundary discretization (model) and the gap. The symbols used for a given gap were defined in Figure 25; in addition, the length of the dash for each curve indicates the relative gap sizes. The solid curve near the bottom of each plot gives the error in the strain energy density for the singular term of the analytical solution compared to the complete solution. A positive error indicates an under prediction of the strain energy density.

In the following results there are two compounding difficulties for the IBEM -- both associated with the geometric discontinuity. The most obvious is the infinite stresses at the crack tip. The second problem is the IBEM's difficulty in dealing with any geometric discontinuity; near

geometric discontinuities the artificial tractions appear to become unbounded. Both problems are addressed in concentrating elements near the crack tip.

In Figure 26 the error initially decreases away from the tip followed by a subsequent increase. Note that the accuracy is highest for the largest gap. At first glance it might appear that the increase in error is due to the previously mentioned roundoff error problem. However (though not shown) the error does decrease again. Apparently this increase in error with distance from the tip is a result of the IBEM's difficulty with geometric discontinuities. The initial increase in accuracy with gap size (i.e., as the geometric discontinuity decreases) reinforces this conclusion. For these results the elements adjacent to the tip are internally collocated (i.e., a so called "discontinuous" formulation) to prevent collocation at the crack tip where a traction discontinuity exist.

Figures 27 and 28 further enforce the above conclusion. In the region where I have attributed the error to the IBEM's problem with discontinuities, the analysis based on the largest gap performs the best. At a distance further from the tip the smaller gap analyses give the better results. Note that the smallest gap does not give the best results (see e.g. Figure 28). All of the previously mentioned problems which might occur with a small gap are suspect. There is another problem which occurs with the method that is apparent more from a physical perspective. Recall the initial derivation of the IBEM. There we considered our actual problem as embedded in an infinite domain, and the artificial tractions were determined on the boundary such that the boundary conditions were satisfied. For this problem embedding the problem in the infinite domain implies that material exist inside the crack. As the gap decreases, the stiffness (relative to crack opening) of this sliver of material in the crack increases; that is, it requires greater artificial tractions to open the crack. For this problem a gap in the range [0.0025,0.005] gave the best results.

Figure 29 illustrates the improvement of the results with mesh refinement. (In this case the smaller the dash the finer the mesh near the crack tip.) As the mesh is concentrated near the crack tip the

error resulting from the singularity and the IBEM's discontinuity problem (apparently the dominant problem) becomes progressively more localized.

Figure 30 addresses the effect of collocating at the element crack tip. This analysis was performed in preparation for an IBEM stiffness formulation. The specified boundary values were zero traction at the tip. I expected a reduction in accuracy when collocating at the crack tip; such was not the case. Collocating at the crack tip actually gave better results overall. For distances greater than 0.03 from the tip, model 3 gave relative errors of less than 5%.

For this problem, the need for a better discretization was evident by a comparison with the exact solution. In a real application there are two measures which could be considered in determining the goodness of a discretization based on a single analysis: 1) the difference between the "shape function" interpolated values and the integral equation values along the boundary (as previously discussed) or 2) an inspection of the artificial traction distribution. Figures 31 give the artificial traction distribution along the upper right face for model 4 (gap = 0.005 and "discontinuous elements" are used adjacent to the crack tip). As expected the artificial tractions are relatively uniform near the center of the crack and have high gradients near the crack tip. The gross slope discontinuities in the plot near the crack tip indicate further resources must be concentrated in this region to obtain accurate results near the boundary.

Figure 32 gives a more complete picture of model 4's accuracy (or lack thereof) near the crack tip. At a radius of approximately 0.05 from the tip, the error in the strain energy density is 15% or less. Considering that only twenty elements were used to model the entire crack and that the code was not modified to deal with the singularity, the results for this model are reasonably good.

As with the previous problem the stiffness formulation was less accurate than the standard IBEM formulation. Model 3 gave the "best of the bad results;" for a response line from the crack tip (perpendicular to the crack) the error in the strain energy density remained at approximately 70% for distances in the range [0.05,1.0]. The asymmetries in the stiffness matrix were as large as

40%. Both the factors in the stiffness matrix calculation (35) are of questionable accuracy. The nodal traction-displacement relationship (**E**) is only accurate if the artificial tractions are modeled accurately by the "shape functions." The "shape function" product matrix (**C**) is only accurate if the variation of the real boundary values between nodes is also accurately represented by the "shape functions". Near the crack tip it is doubtful that any of the boundary values, real or artificial, are accurately represented by the "shape functions."

The crack problem was investigated to evaluate the potential of the method in fracture mechanics. Considering the limitations of the current implementation familiarity rather than accuracy was the main objective. I have not investigated the developments in the application of the BEM to fracture mechanics. However, it is worth noting a few modifications that could be incorporated in the current implementation to improve the numerical results. (I'll omit the obvious ones like increasing the capacity of the code beyond 88 dof's.)

1) Provide for rigid body motion in the stiffness formulation so BEM crack tip elements could be developed. Then all the resources of the BEM could be concentrated near the crack tip. To maximize the accuracy geometric discontinuities should be accounted for. For a crack not subjected to crack face loading, many boundary elements could be concentrated near the tip with the corresponding degrees of freedom eliminated at the element level.

2) Incorporate singular "shape functions" at the crack tip for the artificial tractions.

3) Consider a more natural integral equation formulation for the crack problem. In particular, the displacement discontinuity method is based on the analytical solution to the problem of a constant discontinuity in displacement along a finite line in an infinite medium (Ref 54). The formulation follows the same development as the IBEM except the unknowns are displacement discontinuities instead of artificial tractions.

For the reader interested in a modern treatment of fracture mechanics by the BEM the recent survey of advances in the BEM by Cruse (Ref 68) is an excellent starting point. In addition Mukherjee (Ref 69) dedicates a few chapters in his text to the application of the BEM to fracture mechanics.

SUMMARY AND CONCLUSIONS

Fundamental differences in the finite element and boundary element methods result in corresponding strengths and weaknesses. Thus a combination of the methods using the strengths of each may allow some classes of problems to be solved more effectively. Applications with infinite or semi-infinite domains and applications in fracture mechanics are candidates for combined solution approaches.

The direct and indirect boundary element methods are the most common integral equation methods in use. They have their origins in classical potential theory and the fundamental singular solution is a key component of their derivations. For both methods the approximations common to most formulations are: (1) integrating in a piecewise manner, and (2) solving the integral equations in a collocation sense. The collocation approximation limits the satisfaction of boundary conditions to discrete points; as a result coupled solutions have inherent incompatibilities at interface boundaries. While the "shape functions" serve as a basis for the assumed boundary value distribution, they are not a basis for the boundary responses. Thus the prescription of identical shape functions in adjoining regions does not imply the existence of compatibility.

Coupling approaches can be categorized by several parameters. The primary classification in this study indicated which numerical method hosts the coupling. That is, is the final form of the equations "BEM like" or "FEM like"? This study addresses FEM-hosted or stiffness couplings. These can be further categorized by the derivation of the stiffness matrix. Either the stiffness matrix is obtained directly or by a variational statement of the problem. For many direct and variational formulations the key matrices are the fully-populated coefficient matrices generated by the BEMs and a sparse matrix obtained by the integration of "shape function" products. The BEM coefficient matrices are manipulated to establish a relationship between the boundary tractions and displacements; this relation is then used directly to obtain a stiffness matrix, or substituted into a boundary variational statement.

For FEM-hosted couplings in elastostatics, the methods can be combined without requiring major modifications to the existing FEM and BEM computer programs. This allows each program to serve as an independent analysis tool or as one component of a coupled approach.

The major problems with the BEM stiffness matrices are their lack of symmetry, violation of equilibrium, and inability to represent rigid body motions. A variational formulation inherently produces a symmetric system which is equivalent to taking the symmetric component of the corresponding directly-formulated stiffness matrix. Investigators have offered several alternatives for dealing with the equilibrium and rigid body problems. They range from the introduction of Lagrange multipliers which enforce equilibrium to *ad hoc* adjustments of the stiffness matrix.

In many cases, stiffness matrix calculations for both BEMs follow the same main steps. However, the direct BEM is slightly better suited to the coupled solution approaches considered in this study because of its simpler traction-displacement relationship. For smaller problems, the calculation of matrices comprising the stiffness matrix accounts for the most numerical effort. For larger problems the "inverse calculation" of a fully-populated matrix dominates the numerical effort. The only known method for reducing this cost is to subdivide the homogeneous boundary element region (Ω^B) into a number of smaller regions--trading the calculation of a large inverse for the calculation of several smaller ones. The subdivision of Ω^B also reduces the bandwidth of the final system of equations. However, to maintain comparable accuracy it appears the interface boundary (Γ_I) must be positioned at a greater distance from the region of interest (usually a localized region within the finite element region).

Alternative formulations where the BEM is incorporated by considering it as a boundary condition to the FEM region might be more economical than the FEM-hosted couplings considered in this study. These formulations were not considered in detail. I am not sure if the objective of "weak software coupling" would be met by these formulations.

The only matrix in the stiffness calculation not calculated by standard BEM programs is the "shape function" product matrix **C**. For continuous boundary elements **C** is symmetric. Additionally the locally based nature of the "shape functions" makes **C** very sparse. The calculation of **C** and its product with other matrices are effectively performed at the element level.

Many derivations of BEM stiffness matrices have unknowingly ignored the incompatibility along Γ_I. Both numerical examples in this study indicated that the standard IBEM is more accurate than the stiffness formulation considered. However, as shown by the circular cavity problem reasonably good results can still be obtained by the coupled solution except for a local region near Γ_I (i.e., the overall accuracy is not sacrificed). For this problem the BEM is used to model the infinite domain -- a role it is well suited for. I am unaware of any convergence proofs which address the coupled solution approach when the incompatibility has been ignored. Though numerous numerical studies suggest convergence will occur, there's nothing quite as comforting as a mathematical proof. When the incompatibility is recognized it can either be explicitly included in a variational statement (Refs 7, 59, 60, 61) or eliminated by using a different Green's function (Ref 62).

The discrepancy between the assumed boundary value distribution and that given by the integral equations is potentially very useful in mesh refinement. The difference in the values could be used in an automated setting to determine when to either subdivide critical elements or completely remesh the boundary.

The pressurized crack problem served as the ultimate test for both the standard and stiffness formulations of the IBEM. To address the problem, the geometrical approximation of a gap (i.e., an initial crack opening) had to be introduced. In addition an integration strategy which is accurate in the near boundary region was a necessity. While the accuracy was not beyond reproach, the results seemed reasonably good for a "stock program" with no modifications to confront the crack

problem. There are numerous approaches to improving the accuracy, including completely different boundary methods better suited to the crack problem.

The inaccuracies in both problems were interpreted in terms of the "shape function fallacy." The reduced accuracy in the stiffness formulation was interpreted as being due to the increased use of the "shape functions" to interpolate the distribution of boundary values. The effect was most pronounced when Γ_I intersected regions of high gradients; for it was this case that the "shape function" distribution had the greatest error. The only boundary values we know are those at the collocation points. This is brought out in the following analogy which summarizes the results for the crack problem.

When a camper sets up his tent he wants the bottom of the tent to remain on the ground. However, during a bad storm the only points remaining on the ground are those at the tent stakes. These are the collocation points for the camper (though most campers don't seem to use this terminology). When the "numerical winds" blow the BEM "hangs on" by its collocation points. The crack problem produces the tornado of "numerical winds." The tent "beat in the wind" using the BEM; it nearly pulled the stakes out when we tried to use the stiffness formulation of the IBEM.

RECOMMENDATIONS

The following recommendations are broken into two categories: 1) recommendations for future implementation and 2) recommendations for future theoretical investigations. Implementation suggestions focus on modifying the existing IBEM program for more effective coupled analyses, and the development of other boundary methods for parallel studies between the methods. Most of the theoretical basis for this work is available in the literature. Future implementation efforts might address:

- an extension of the code for semi-infinite domains to address soil-structure interaction
- symmetry considerations in formulating the BEM equations
- a further investigation of element integrations
  - -- special techniques for integrations over singularities (including the geometric discontinuity case)
  - -- special techniques for the near boundary region
  - -- order of integration calculations in variable order integration schemes
- Galerkin and related formulations of BEMs
- development of different boundary integral method codes to be used in parallel with the IBEM in future investigations
  - -- a DBEM code
  - -- a displacement discontinuity formulation for fracture problems
- the addition of infinite boundary elements allowing BEM subdomains to be subdivided for coupled solutions
- modification of the IBEM stiffness formulation to represent rigid body motions for modeling finite domains
- the addition of special features to more effectively address fracture mechanics problems

Within the contexts of elastostatics the following areas are worthy of additional theoretical investigation:

- methods where the BEM serves as a boundary condition to the FEM subdomain
- the work of Jirousek (Refs 59, 60, and 61) and the relationship between BEM stiffness formulations and hybrid finite elements
- the work of Margulies (Ref 62) and alternative Green's functions which might be advantageous for the coupled problems
- the application of the modified functional (40) with the DBEM
- the use of the interface incompatibility in an adaptive mesh refinement scheme

This last recommendation suggests using the discrepancy between the "shape function" interpolated boundary values and those predicted by the integral equations as a measure of the goodness of a mesh. It is equally applicable to BEM and coupled solutions -- "continuous" and "discontinuous" elements. Thus it could serve as the needed feed-back for an adaptive mesh refinement algorithm for BEMs.

Towards our long term objective we must investigate the application of the boundary element method in elastodynamics and how it can be coupled with the finite element method in this context. Then the potential of applying coupled solutions to soil-structure interaction problems can be evaluated.

ACKNOWLEDGEMENTS

I would like to thank professors J.R. Hutchinson, L.R. Herrmann, and K.D. Mish for serving on my thesis committee -- a capacity which requires an abnormal amount of wisdom and patience. I especially appreciate professors Hutchinson's and Herrmann's gentle encouragement to "get this behind me." I finally admitted that this study would never be complete or perfect; it's simply over with. There will always be one more paper to read, one more problem to do, and one more page to rewrite.

I would also like to thank the Naval Civil Engineering Laboratory for their support of this work. In particular, Dr. Ted Shugar for his review and support of this study and our division director Bill Armstrong for his support and encouragement.

I would like to thank my family and friends for their patient support. My wife Donna (who must be the only non-engineer who enjoyed reading this document) was supportive in every possible way. My daughter Breanna sacrificed many bed-time stories and hugs, which I now hope to repay. Most of all I thank God (II Corinthians 12:9-10).

REFERENCES

1. P.K. Banerjee and R. Butterfield. Boundary element methods in engineering science. McGraw-Hill, New York, NY, 1981.

2. C.A. Brebbia, J.C.F. Telles, and L.C. Wrobel. Boundary element techniques--theory and application in engineering. Springer-Verlag, Berlin, Germany,1984.

3. R. Butterfield. "An application of the boundary element method to potential flow problems in generally inhomogeneous bodies," Recent Advances in Boundary Element Methods, C.A. Brebbia, editor, Pentech Press., London, England, 1978, pp 123-135.

4. O.C. Zienkiewicz. The finite element method. 3rd edition, McGraw-Hill, London, England, 1977.

5. R.F. Ungless. An infinite finite element, M. Sc. Thesis, Department of Civil Engineering, University of British Columbia, 1973.

6. P. Bettess. "Infinite elements," *International Journal of Numerical Methods in Engineering*, vol 11, 1977, pp 53-64.

7. O.C. Zienkiewicz, D.W. Kelly, and P. Bettes. "The coupling of finite element and boundary solution procedures," *International Journal of Numerical Methods in Engineering*, vol 11, 1977, pp 355-375.

8. C.A. Brebbia. The boundary element method for engineers. Pentech Press, London, England, 1978.

9. B.H. McDonald and A. Wexler. "Finite element solution of unbounded field problems," *IEEE Transactions on Microwave Theory and Techniques*, vol MTT-20, no. 12, December 1972, pp 841-847.

10. H.S. Chen and C.C. Mei. "Oscillations and wave forces in a man-made harbor in open sea," Proceedings of 10th Naval Hydrodynamics Symposium, Department of Civil Engineering, Massachusetts Institute of Technology, Cambridge, Mass, June 1974, pp 573-596.

11. R.P. Shaw. "Time harmonic scattering by obstacles surrounded by an inhomogeneous medium," *Journal of the Acoustics Society of America*, vol 56, no. 5, 1974, pp 1437-1443.

12. J.R. Osias, R.B. Wilson, and L.A.Seitelman, "Combined boundary integral equation finite element analysis of solids," Proceedings of the International Symposium on Innovative Numerical Analysis in Applied Engineering Science, Versailles, France, CETIM, 23-27 May 1977, pp 103-106.

13. D.W. Kelly, G. Mustoe and O.C. Zienkiewicz. "Coupling boundary element methods with other numerical methods," Developments in Boundary Element Methods--1, P. K. Banerjee and R. Butterfield, editors, Applied Science Publishers, London, England, 1979, pp 251-285.

14. G. Mustoe. Coupling of boundary solution procedures and finite elements for continuum problems, Ph.D. thesis, University of Wales, University College, Swansea, 1979.

15. C.A. Brebbia and P. Georgiou. "Combination of boundary and finite elements in elastostatics," *Applied Math Modelling*, vol 3, Jun 1979, pp 212-220.

16. L. Bolteus and O. Tullberg. "BEMSTAT - a new type of boundary element program for two-dimensional elasticity problems," Boundary Element Methods, Proceedings of the 3rd International Seminar, Irvine, CA, C.A. Brebbia, editor, Springer-Verlag, Berlin, Germany, July 1981, pp 518-537.

17. T.A. Shugar and J.V. Cox. "A study of coupling the boundary and finite element methods in two-dimensional elastostatics," Technical Note N-1710, Naval Civil Engineering Laboratory, Port Hueneme, CA., Oct 1984.

18. R.P. Shaw and W. Falby. "FEBIE -- A Combined Finite Element-Boundary Integral Equation Method," Proceedings of the International Symposium on Innovative Numerical Analysis in Applied Engineering Science, Versailles, France, CETIM, 23-27 May 1977, pp 97-101.

19. R.P. Shaw. "Coupling the boundary integral equation methods to other numerical techniques," Recent advances in boundary element techniques, C.A. Brebbia, editor, Pentech Press, London, England, 1978, pp 137-147.

20. B. Loret. "Topics in singular and regular integral equations," Department of Civil Engineering Syminar," University of California, Davis, February, 1987, (Dr. Loret works for Laboratoire de Mécanique des Solides Ecole Polytechnique, Paris, France).

21. M.P. Kamat and S.A. Brown. "Coupling of finite and boundary element solutions using a direct minimization approach," Boundary Elements VII, Proceedings of the 7th International Conference, Villa Olmo, Lake Como, Italy, Springer-Verlag, Berlin, Germany, September 1985, pp 11.23-11.27.

22. G. Jeng and A. Wexler. "Finite-element solution of boundary integral equations," Proceedings of the International Symposium on Large Engineering Systems, A. Wexler, editor, Pergamon Press, Oxford, England, 1977, pp 112-121.

23. S.N. Atluri and J.J. Grannell. "Boundary element methods (BEM) and combination of BEM-FEM," Report no. GIT-ESM-SA-78-16, Center for the Advancement of Computational Mechanics, School of Civil Engineering, Georgia Institute of Technology, Atlanta, Georgia, Nov 1978.

24. O. Tullberg and L. Bolteus. "A critical study of different boundary element stiffness matrices," Proceedings of the 4th International Conference on Boundary Element Methods, C.A. Brebbia, editor, Springer-Verlag, Berlin, Germany, 1982, pp 621-635.

25. C.A. Brebbia and S. Walker. Boundary element techniques in engineering. Newnes-Butterworths, London, England, 1980.

26. T.J. Rudolphi. "Nonhomogeneous potential and elasticity problems by combined boundary and finite elements," Advanced Topics in Boundary Element Analysis, T.A. Cruse, A.B. Pifko, and H. Armen, editors, American Society of Mechanical Engineers, AMD-vol 72, November 1985, pp 113-131.

27. F. Hartmann. "The derivation of stiffness matrices from integral equations," Boundary Element Methods, Proceedings of the 3rd International Seminar, Irvine, CA, C.A. Brebbia, editor, Springer-Verlag, Berlin, Germany, July 1981, pp 552-566.

28. J.M. Boissenot, J.C. Lachat, and J. Watson. "Etude par equations integrales d'une eprouvette C.T.15," *Revue Physique Appliquee*, vol 9, Dept. D.T.E.--CETIM, Senlis, France, July 1974, pp 611-615.

29. M. Chaudonneret. "On the discontinuity of the stress vector in the boundary integral equation method for elastic analysis," International Symposium on Recent Advances in the BEM, Southampton, England, Pentech Press, London, England, July 1978, pp 185-194.

30. E. Alarcon, A. Martin, and F. Paris. "Boundary elements in potential and elasticity theory," *Computers and Structures*, vol 10, 1979, pp 351-362.

31. G. Mustoe and F. Volait. "A symmetric direct boundary integral equation method for two-dimensional elastostatics," 2nd International Seminar on Boundary Element Methods, Southampton, England, 1980.

32. C. Patterson and M.A. Sheikh. "Non-conforming boundary elements for stress analysis," Boundary Element Methods, Proceedings of the 3rd International Seminar, Irvine, CA, C.A. Brebbia, editor, Springer-Verlag, Berlin, Germany, July 1981, pp 137-152.

33. T.A. Shugar and J.V. Cox. "An investigation of the indirect boundary element method in one- and two-dimensional elastostatics," Technical Note 1664, Navy Civil Engineering Laboratory, Port Hueneme, CA, May 1983.

34. J.V. Cox and T.A. Shugar. "A recursive integration technique for boundary element methods in elastostatics," Advanced Topics in Boundary Element Analysis, T.A. Cruse, A.B. Pifko, and H. Armen, editors, American Society of Mechanical Engineers, AMD-vol 72, November 1985, pp 133-153.

35. J.V. Cox and T.A. Shugar. "A recursive boundary element with initial error investigation," Technical Note 1730, Navy Civil Engineering Laboratory, Port Hueneme, CA, December 1985.

36. J.C. Lachat and J.O. Watson. "A second generation boundary integral equation program for three dimensional elastic analysis," Boundary Integral Equation Method: Computational Applications in Applied Mechanics, T.A. Cruse and F.J. Rizzo, editors, American Society of Mechanical Engineers, AMD-vol 11, 1975, pp 85-100.

37. J.C.F. Telles. "A self-adaptive co-ordinate transformation for effective numerical evaluation of general boundary element integrals," *International Journal for Numerical Methods in Engineering*, vol 24, 1987, pp 959-973.

38. J.V. Cox. "A preliminary study on finite element-hosted couplings with the boundary element method," Technical Note 1783, Navy Civil Engineering Laboratory, Port Hueneme, CA, April 1988.

39. F.J. Rizzo. "An integral equation approach to boundary value problems of classical elastostatics", *Quart. Appl. Math*, vol 25, 1967, pp 83-95.

40. T.A. Cruse and F.J. Rizzo. "A direct formulation and numerical solution of the general transient elasto-dynamic problem," *Journal of Mathematical Analysis and Applications*, vol 22, 1968, pp 244-259.

41. M.A. Jaswon, "Integral equation methods in potential theory; I," *Proc. Roy. Soc.*, Series A, vol 275, 1963, pp 23-33.

42. M.A. Jaswon and A.R. Ponter, "An integral equation solution of the torsion problem," *Proc. Roy. Soc.*, Series A, vol 273, 1963, pp 237-246.

43. M.H. Lean, M. Friedman, and A. Wexler. "Application of the boundary element method in electrical engineering problems," Developments in Boundary Element Methods--1, P.K. Banerjee and R. Butterfield, editors, Applied Science Publishers, London, England, 1979, pp 207-250.

44. M.A. Jaswon and G.T. Symm. Integral equation methods in potential theory and elastostatics. Academic Press Inc., London, England, 1977.

45. C.E. Massonnet. "Numerical use of integral procedures," Stress Analysis, O.C. Zienkiewicz and G.S. Holister, editors, John Wiley and Sons, London, England, 1965, chapter 10.

46. A.E.H. Love, A treatise on the mathematical theory of elasticity, 4^{th} edition, Dover Publications, New York, NY, 1944.

47. A.C. Eringen and E.S. Suhubi. elastodynamics, volume 2 -- linear theory. Academic Press, New York, NY, 1975.

48. D.N. Arnold and W.L. Wendland. "Collocation vs. Galerkin procedures for boundary integral methods," Boundary Element Methods in Engineering, Springer-Verlag, Berlin, Germany, 1982, pp 18-33.

49. W.L. Wenland. "Asymptotic accuracy and convergence," Chapter 9 of Progress in Boundary Element Methods, vol 1, C.A. Brebbia, editor, Pentech Press, London, England, 1981, pp 289-313.

50. W.L. Wenland. "On the asymptotic convergence of boundary integral methods," Boundary Element Methods, Proceedings of the 3rd International Syminar, Irvine, CA, Springer-Verlag, Berlin, Germany, 1981, pp 413-430.

51. C. Polizzotto. "A BEM approach to bounding techniques," Boundary Elements VII, Proceedings of the 7th International Syminar, Villa Olmo, Lake Como, Italy, Springer-Verlag, Berlin, Germany, 1985, pp 13.103-114.

52. G. Mustoe. "A symmetric direct boundary integral equation method for two-dimensional elastostatics," Proceedings of the 2nd International Symposium on Boundary Element Methods, Southampton University, March 1980.

53. J.R. Hutchinson. "An alternative BEM formulation applied to membrane vibrations," Boundary Elements VII, Proceedings of the 7th International Syminar, Villa Olmo, Lake Como, Italy, Springer-Verlag, Berlin, Germany, 1985, pp 6.13-6.25.

54. S.L. Crouch and A.M. Starfield. Boundary Element Methods in Solid Mechanics (with applications in rock mechanics and geotechnical engineering). George Allen & Urwin Inc., Winchester, MA, 1983.

55. N.J. Altiero and S.D. Gauazza. "An effective boundary-integral approach for the mixed boundary-value problems of linear elastostatics," *Applied Math Modeling*, vol 3, no. 2, April 1979, pp 99-104.

56. P. Georgiou. The Coupling of the direct boundary element method with the finite element displacement technique in elastostatics, Ph.D. thesis, Southampton University, 1981.

57. S. Bilgen. Cubic Spline Elements for Boundary Integral Equations, Ph.D. thesis, University of Manitoba, Dept. of Electrical Engineering, report no. TR82-5, Manitoba, Canada, 1982.

58. Y. Mitsui, Y. Ichikawa, Y. Obara, and T. Kawamoto. "A coupling scheme for boundary and finite elements using a joint element," *International Journal for Numerical and Analytical Methods in Geomechanics*, vol 9, 1985, pp 161-172.

59. J. Jirousek. "Basis for Development of Large Finite Elements Locally Satisfying all Field Equations," *Computer Methods in Applied Mechanics and Engineering*, vol 14, 1978, pp 65-92.

60. J. Jirousek. "Large Finite Elements Method for the Solution of Problems in the Theory of Elasticity," *Computers & Structures*, vol 15, no. 5, 1982, pp 575-587.

61. J. Jirousek and L. Guex. "The Hybrid-Trefftz Finite Element Model and its Application to Plate Bending," *International Journal for Numerical Methods in Engineering*, vol 23, 1986, pp 651-693.

62. M. Margulies. "Combination of the boundary element and finite element methods," chapter 8 of Progress in Boundary Element Methods, vol 1, C.A. Brebbia, editor, Pentech Press, London, England, 1981, pp 258-288.

63. N. Wirth. Programming in Modula-2, 3rd edition, Springer-Verlag, Berlin, Germany, 1985.

64. Y. Kagawa, T. Yamabuchi, and S. Kitagami..."Infinite boundary element and its application to a combined finite-boundary element technique for unbounded field problems," Boundary Element Methods, Proceedings of the 5th International Syminar, C.A. Brebbia, editor, Springer-Verlag, Berlin, Germany, 1983, pp 1017-1027.

65. K. Bathe, E.L. Wilson, and F.E. Peterson. "SAP IV -- a structural analysis program for static and dynamic response of linear systems," Earthquake Engineering Research Center, University of California, Berkeley, report no. EERC 73-11, June 1973.

66. H.M. Westergaard. "Bearing pressures and cracks," *Journal of Applied Mechanics*, Transactions of the American Society of Mechanical Engineers, vol 61, 1939.

67. N.I. Muskhelishvili. Some problems of mathematical theory of elasticity, (published in Russian in 1933), English translation, P. Noordhoff and Co., 1953.

68. T.A. Cruse. "Recent Advances in Boundary Element Analysis Methods," *Computer Methods in Applied Mechanics and Engineering*, vol 62, 1987, pp 227-244.

69. S. Mukherjee. Boundary Element Methods in Creep and Fracture. Applied Science Publishers, New York, NY, 1982.

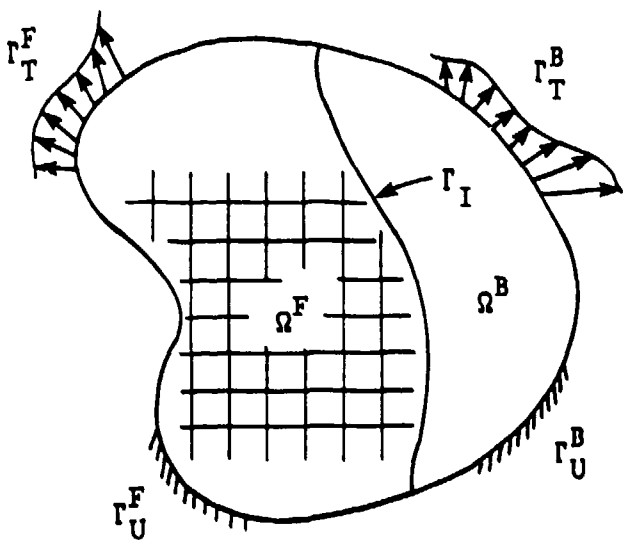

$$\Omega = \Omega^F \cup \Omega^B$$

$$\Gamma^F = \Gamma_T^F \cup \Gamma_U^F \cup \Gamma_I$$

$$\Gamma^B = \Gamma_T^B \cup \Gamma_U^B \cup \Gamma_I$$

$$\Gamma_U = \Gamma_U^F \cup \Gamma_U^B$$

$$\Gamma_T = \Gamma_T^F \cup \Gamma_T^B$$

Figure 1. Two-dimensional elastostatics problem using coupled solution approach.

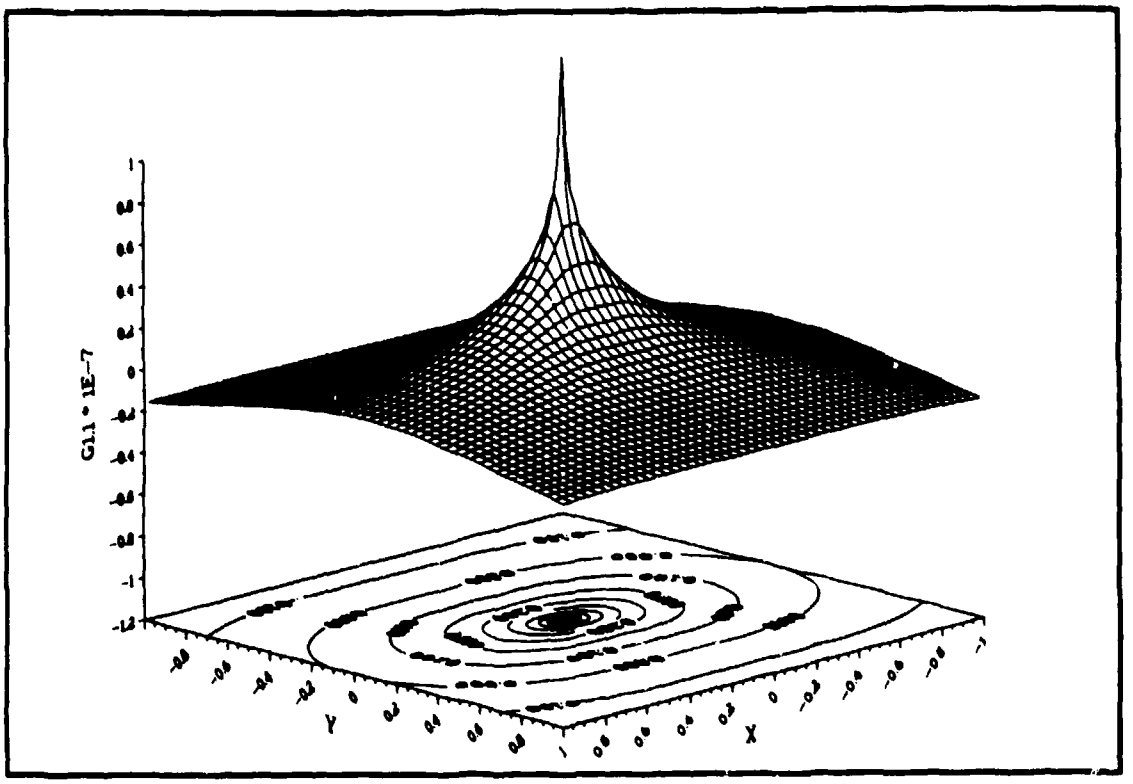

Figure 2. Kelvin solution for displacement, G_{11} component.

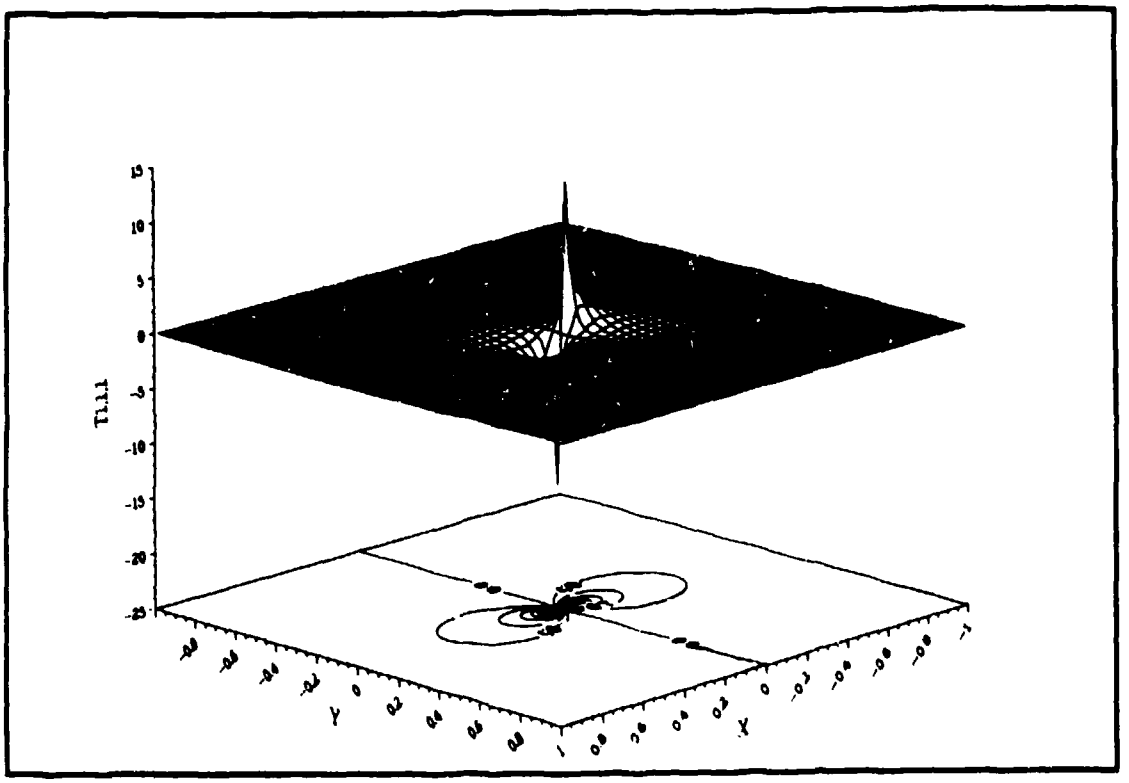

Figure 3. Kelvin solution for stress, T_{111} component.

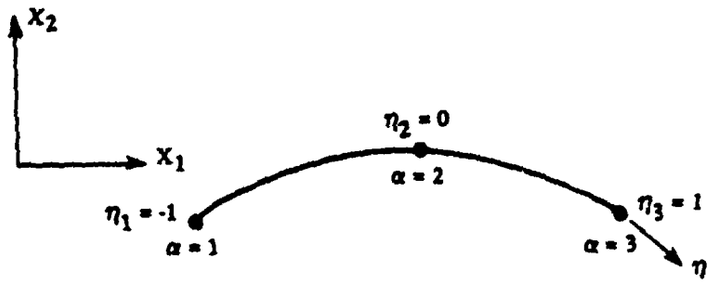

Figure 4. Quadratic isoparametric boundary element.

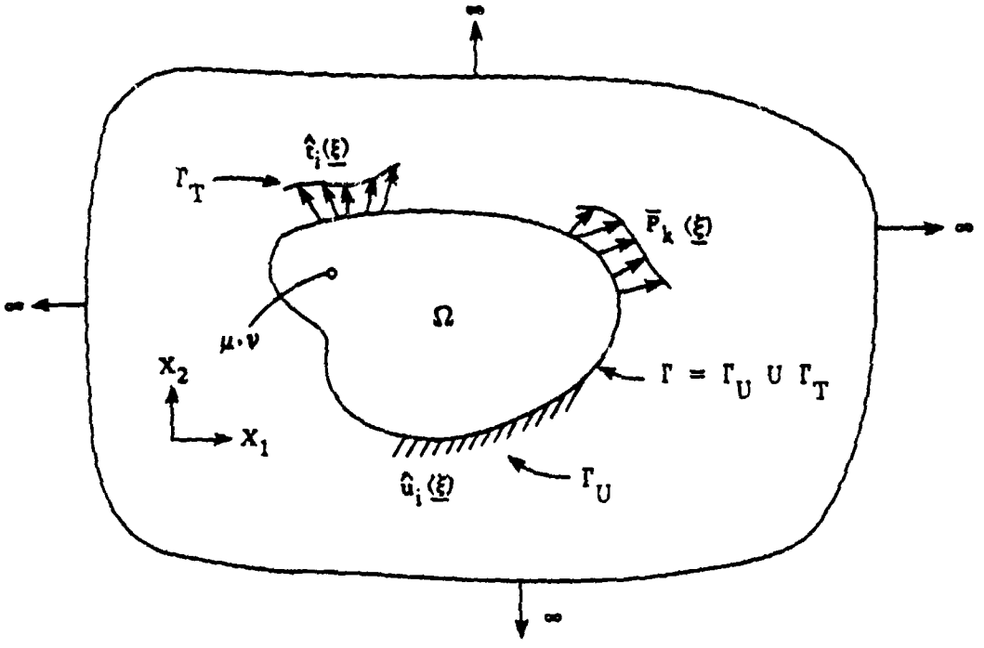

Figure 5. Two-dimensional elastostatics problem embedded in an infinite plane.

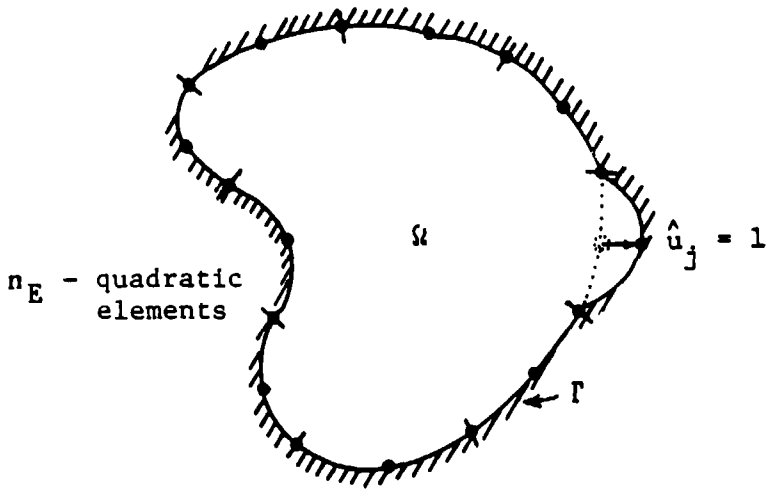

Figure 6. Unit perturbation of a BEM region's j^{th} degree of freedom.

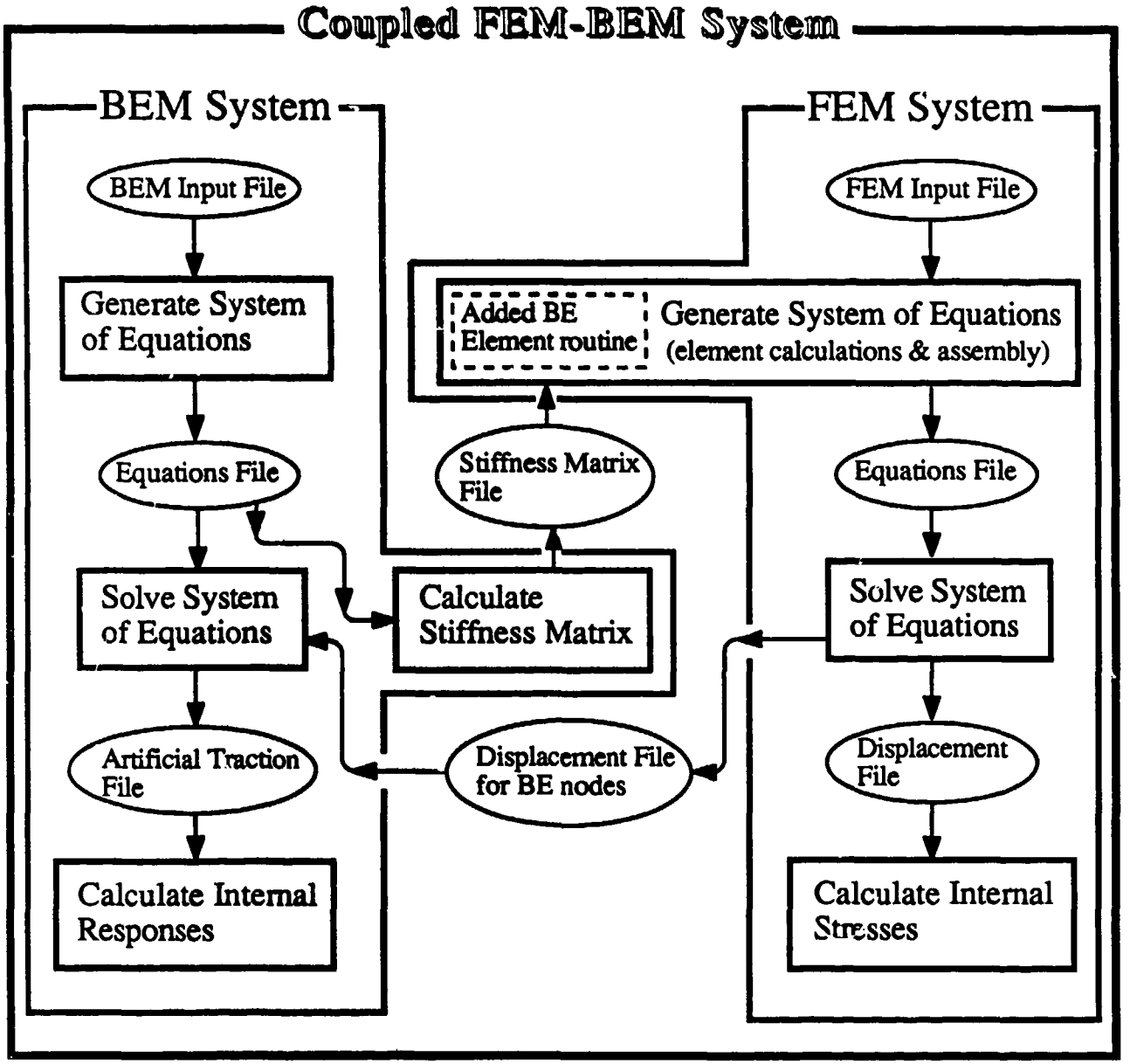

Figure 7. Interaction of BEM and FEM software systems for the FEM-hosted coupling.

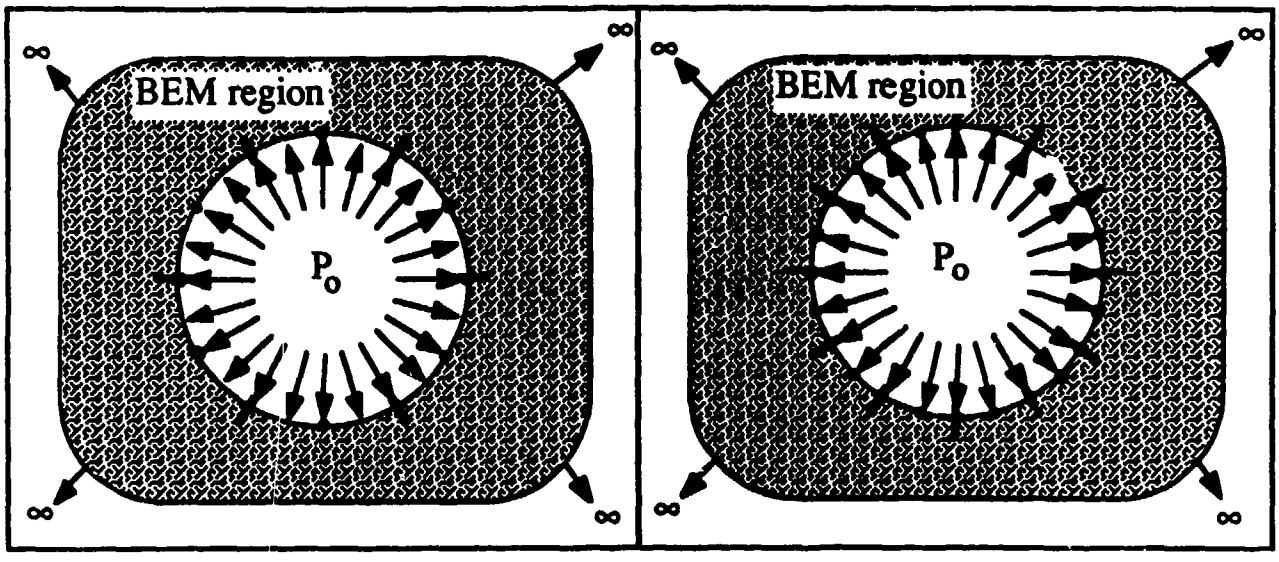

Figure 8. Six element (models 1 and 3) and twelve element (models 2 and 4) IBEM models of circular cavity problem.

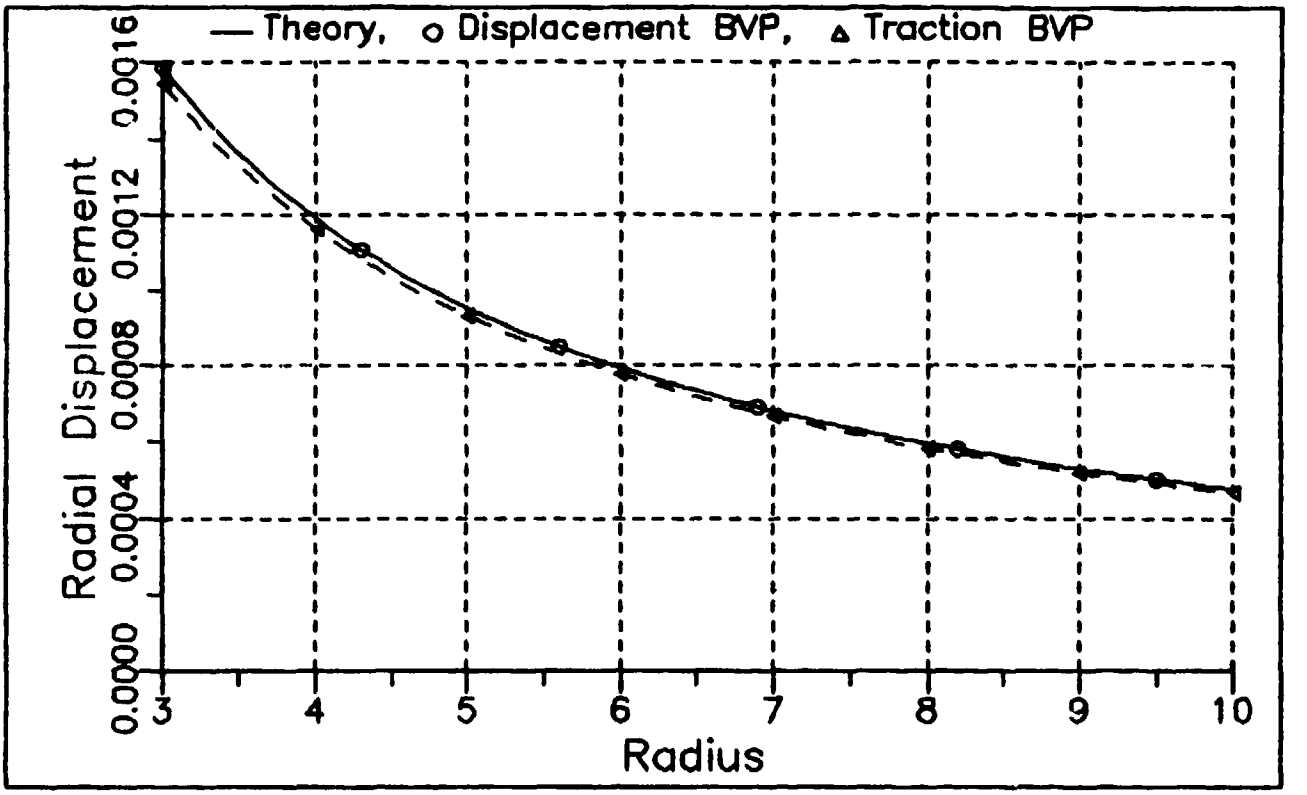

Figure 9a. Model 1: numerical prediction of u_r versus theory.

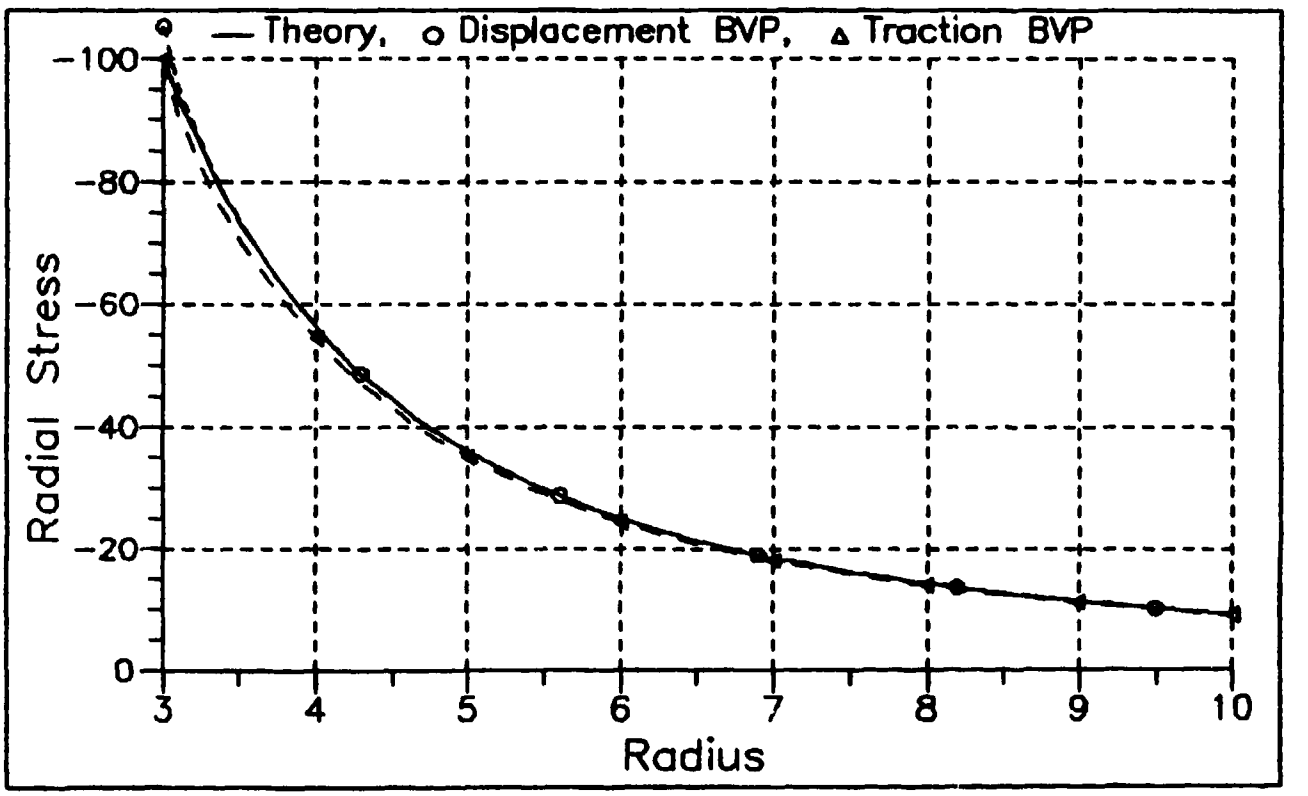

Figure 9b. Model 1: numerical prediction of σ_{rr} versus theory.

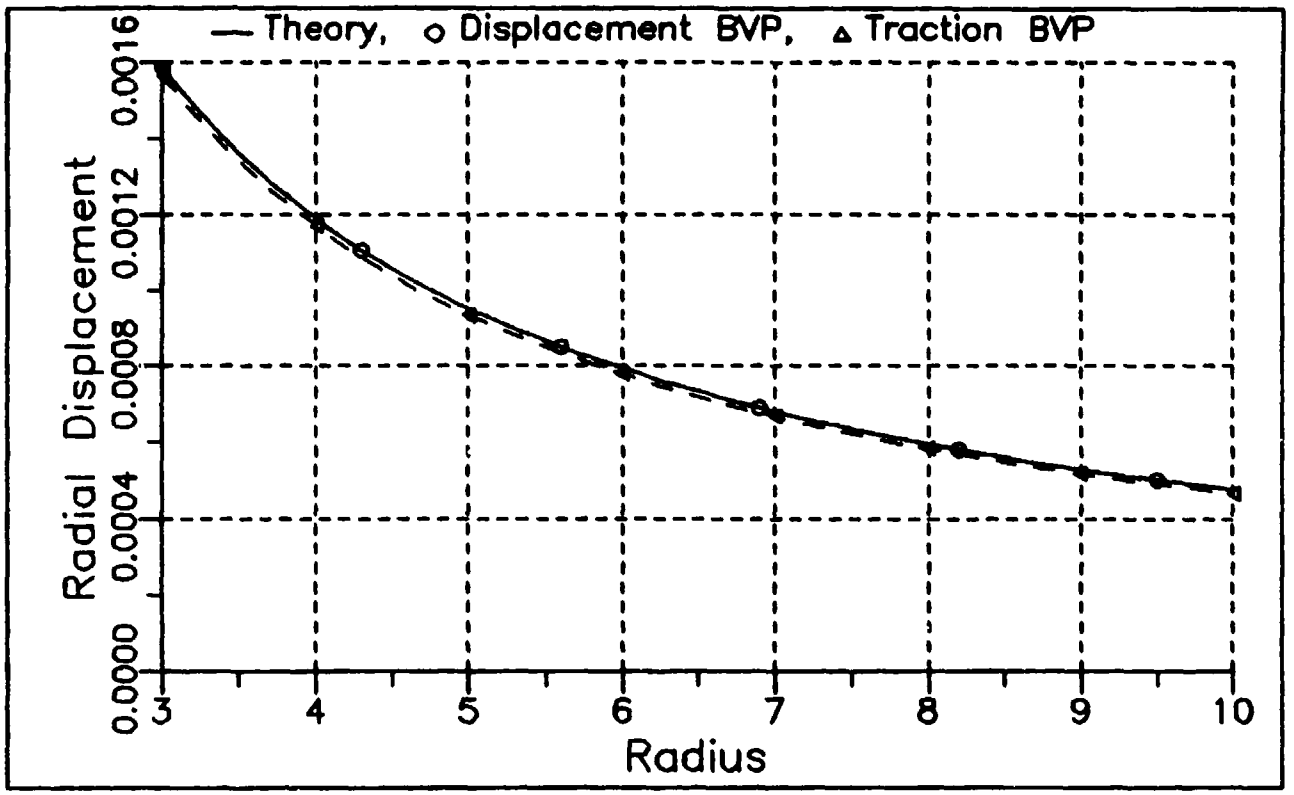

Figure 10a. Model 2: numerical prediction of u_r versus theory.

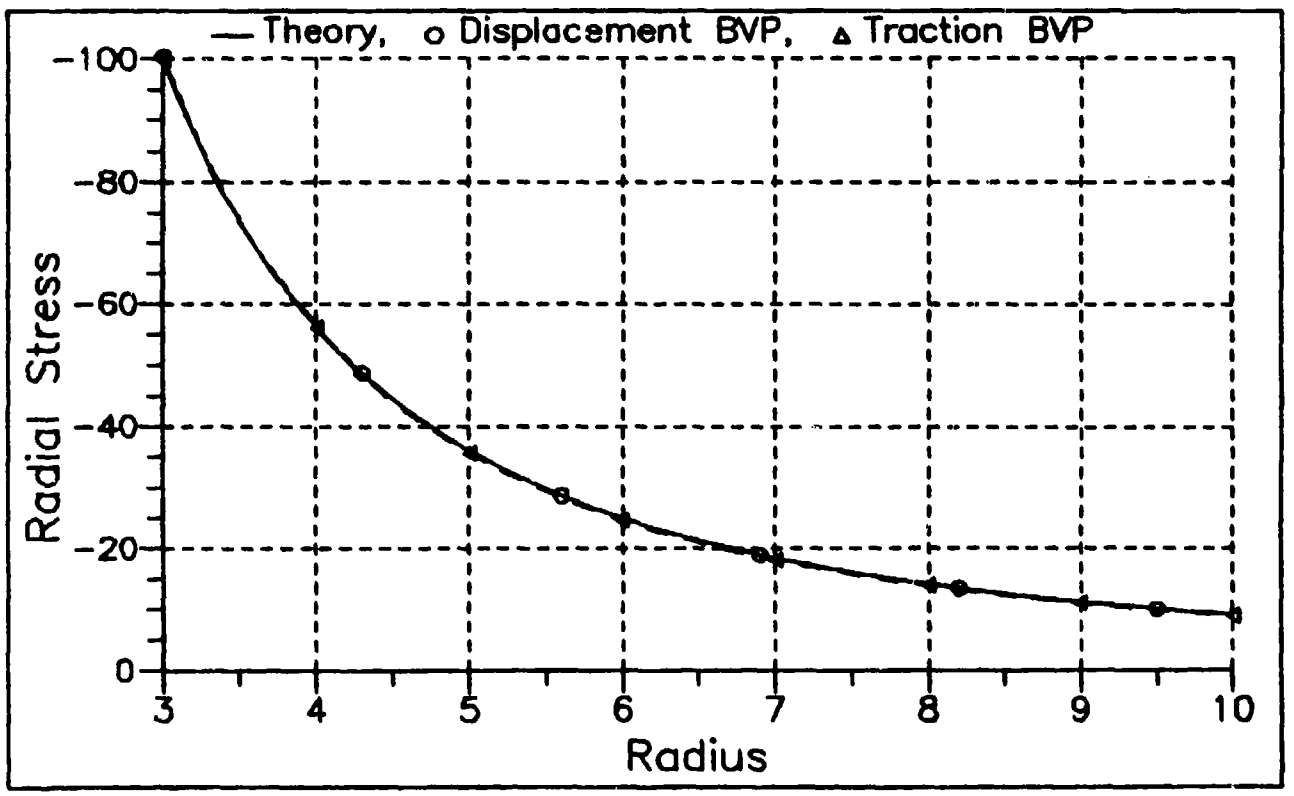

Figure 10b. Model 2: numerical prediction of σ_{rr} versus theory.

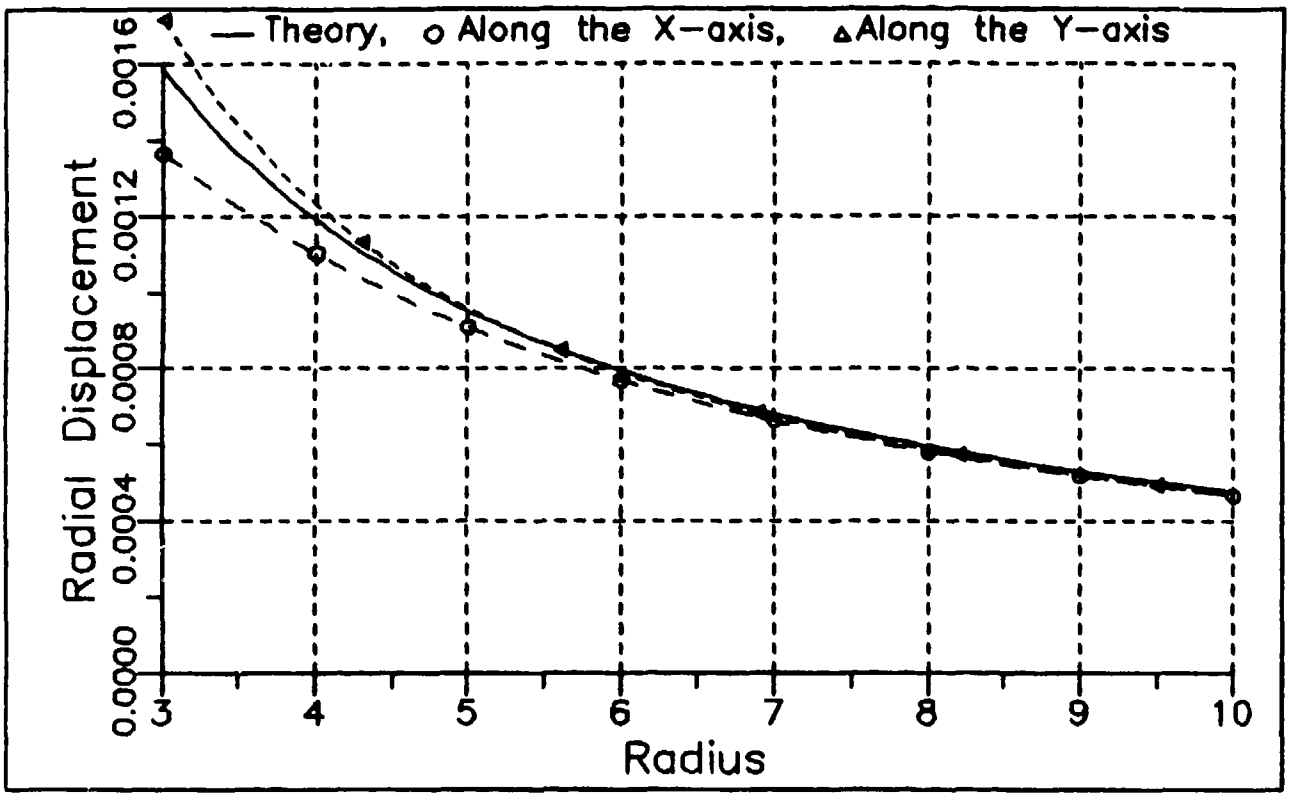

Figure 11a. Model 3: numerical prediction of u_r versus theory.

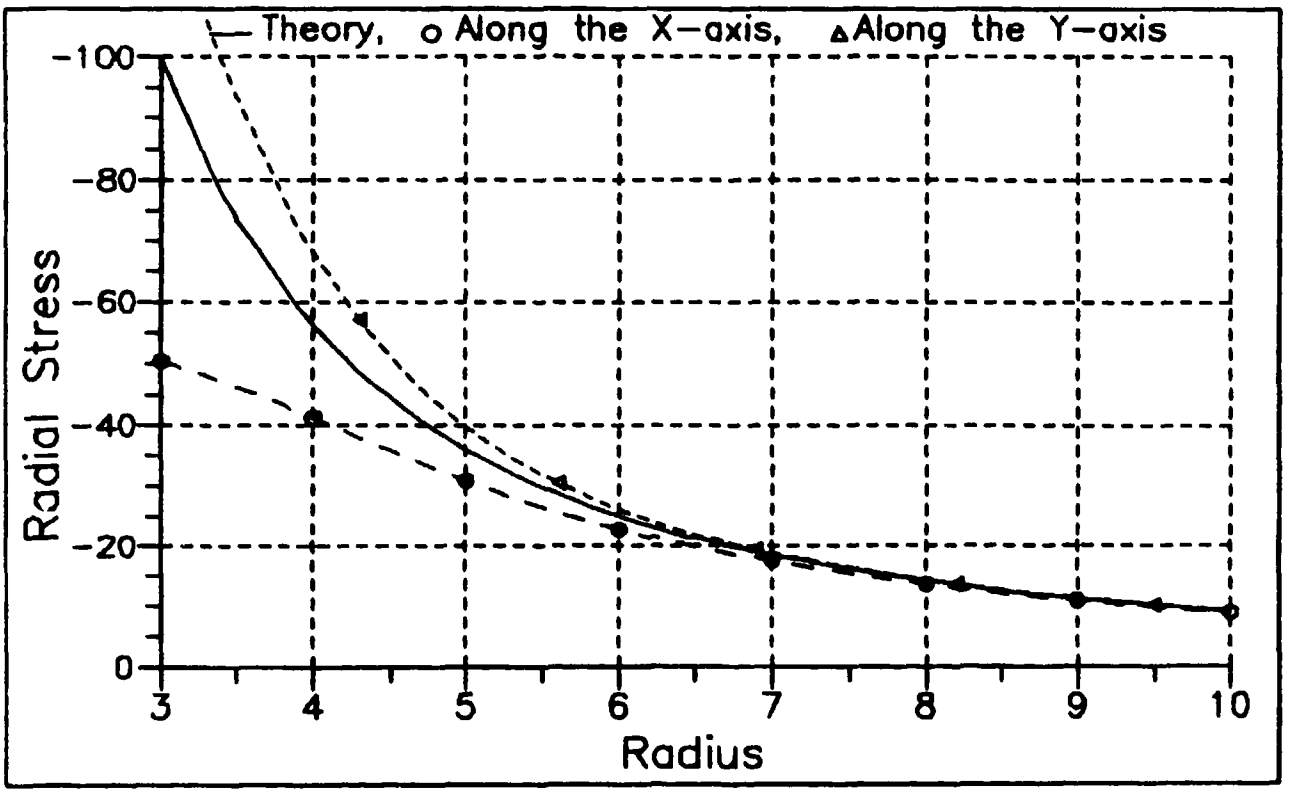

Figure 11b. Model 3: numerical prediction of σ_{rr} versus theory.

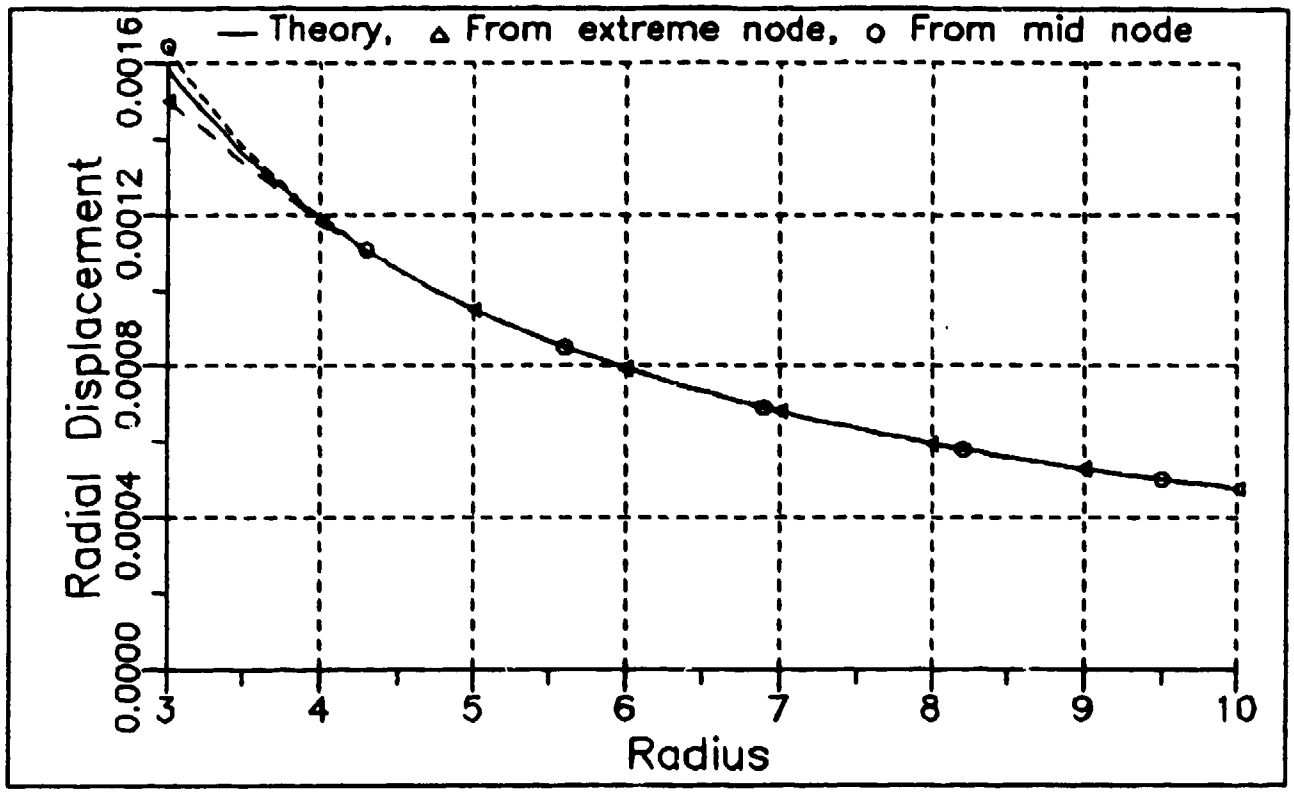

Figure 12a. Model 4: numerical prediction of u_r versus theory.

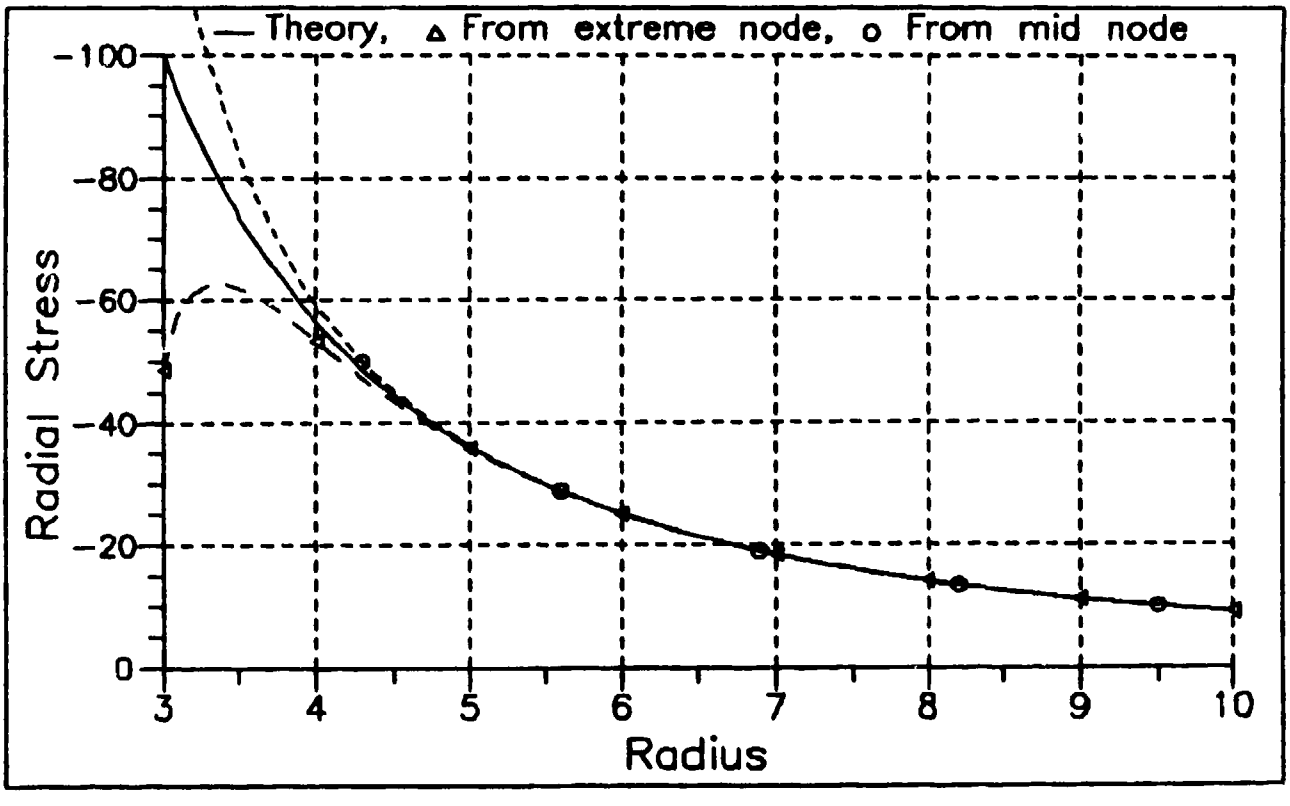

Figure 12b. Model 4: numerical prediction of σ_{rr} versus theory.

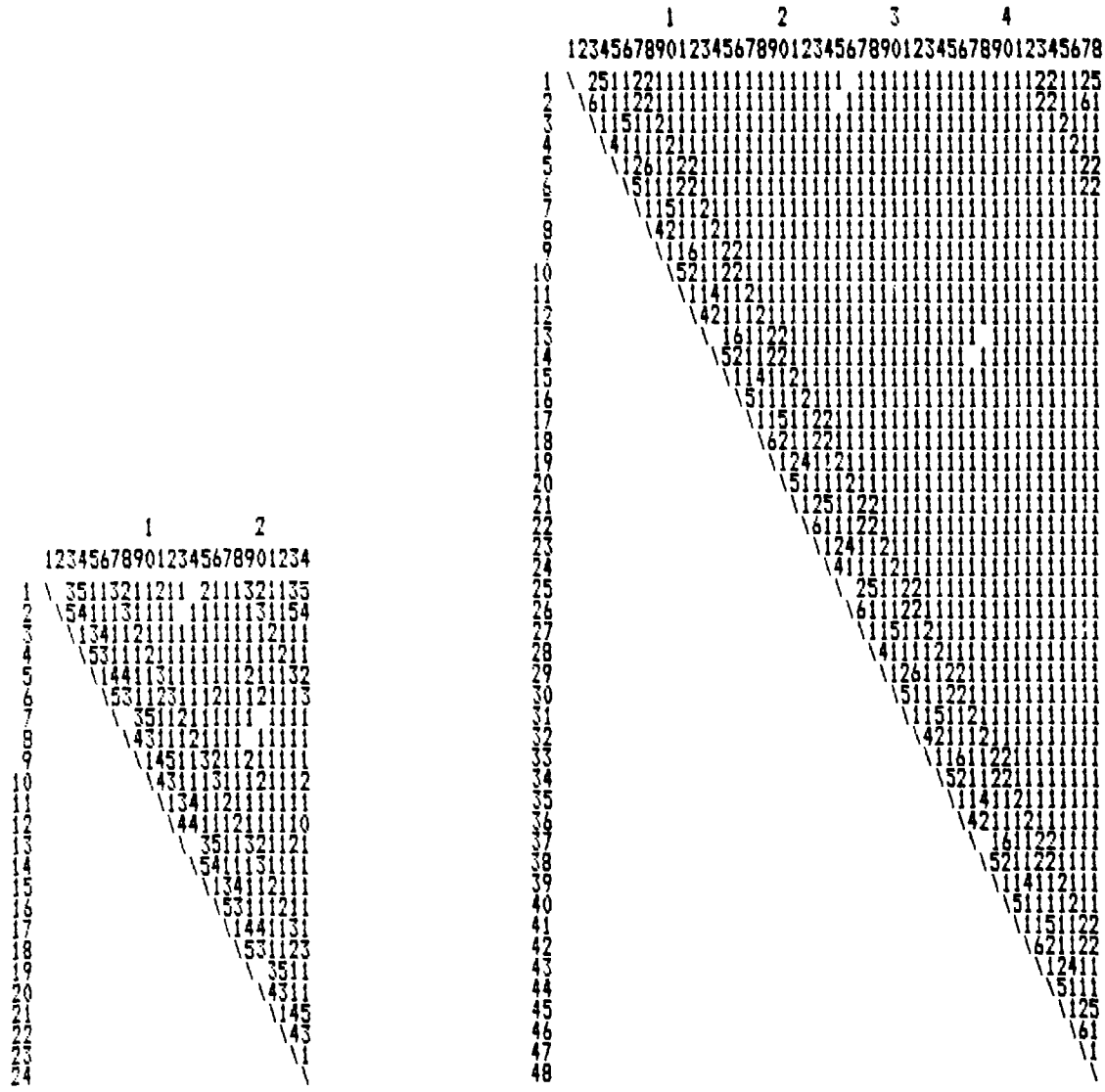

Model 3 Model 4

Figure 13. Asymmetry in the stiffness matrices of circular cavity models 3 and 4.

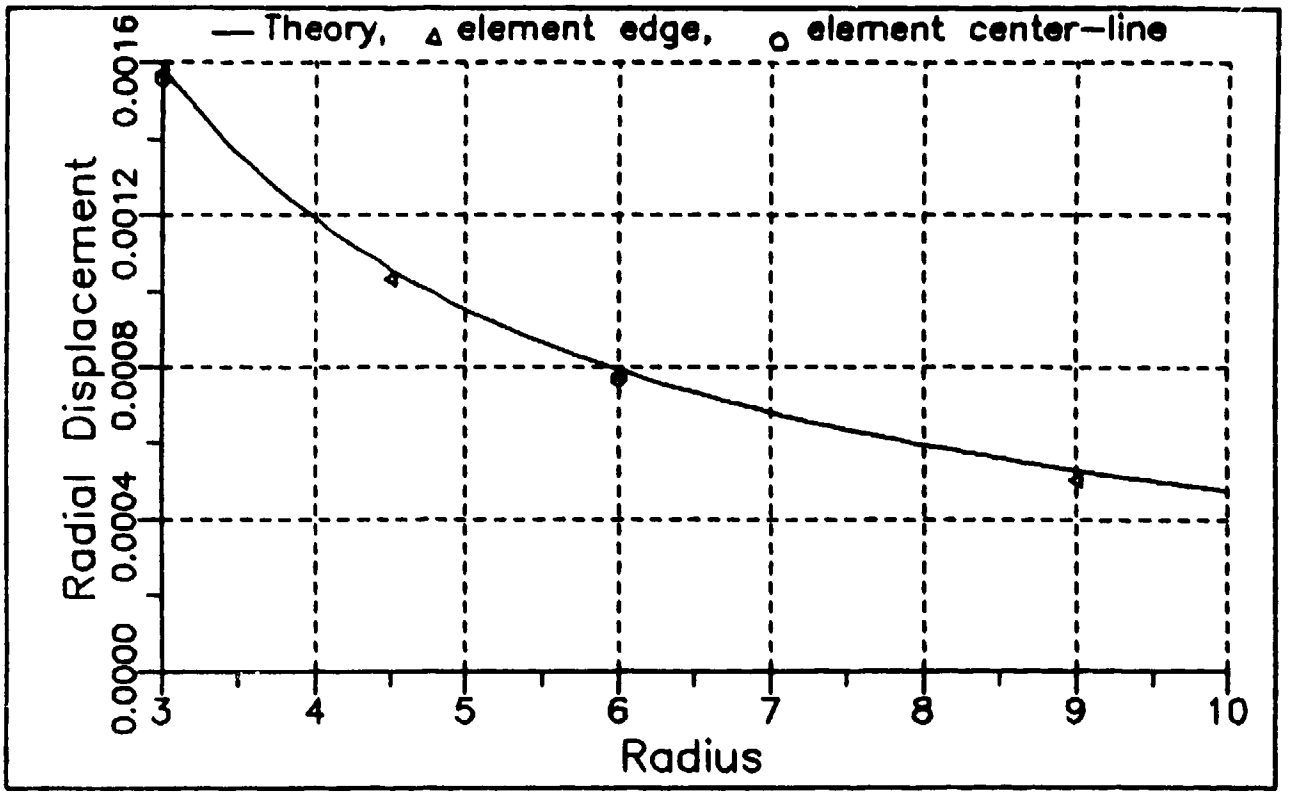

Figure 14a. Model 5: numerical prediction of u_r versus theory.

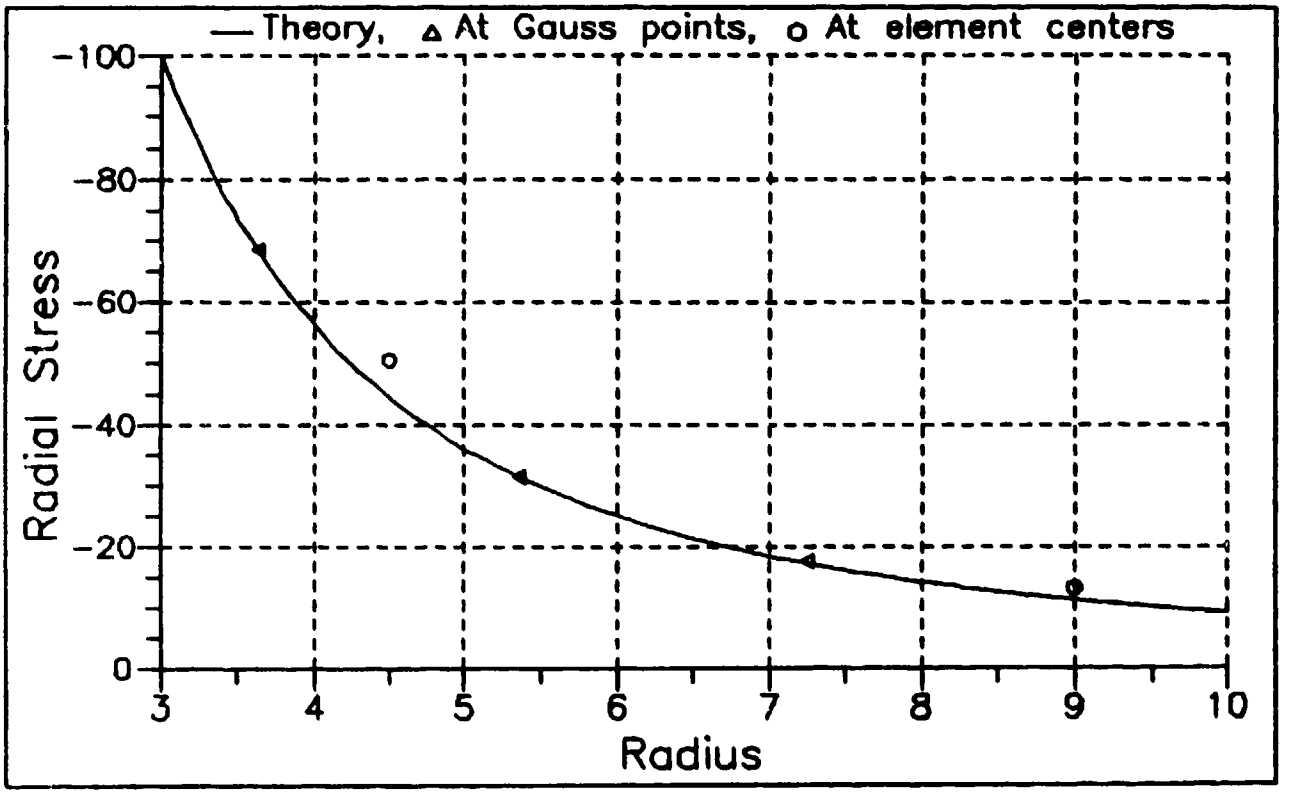

Figure 14b. Model 5: numerical prediction of σ_{rr} versus theory.

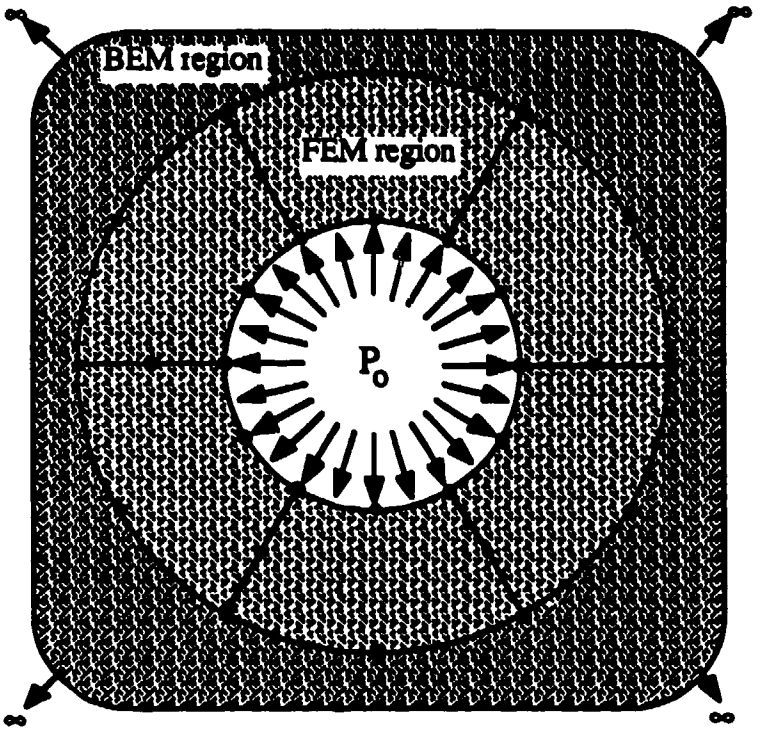

Figure 15a. Model 6: 6 FEs, 6 BEs, and 50 dof.

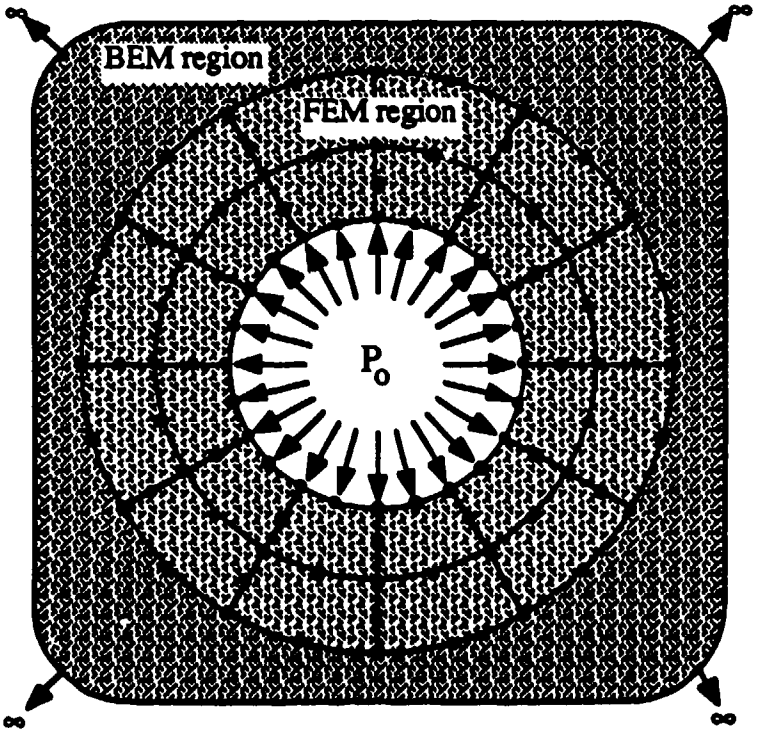

Figure 15b. Model 7: 24 FEs, 12 BEs, and 172 dof.

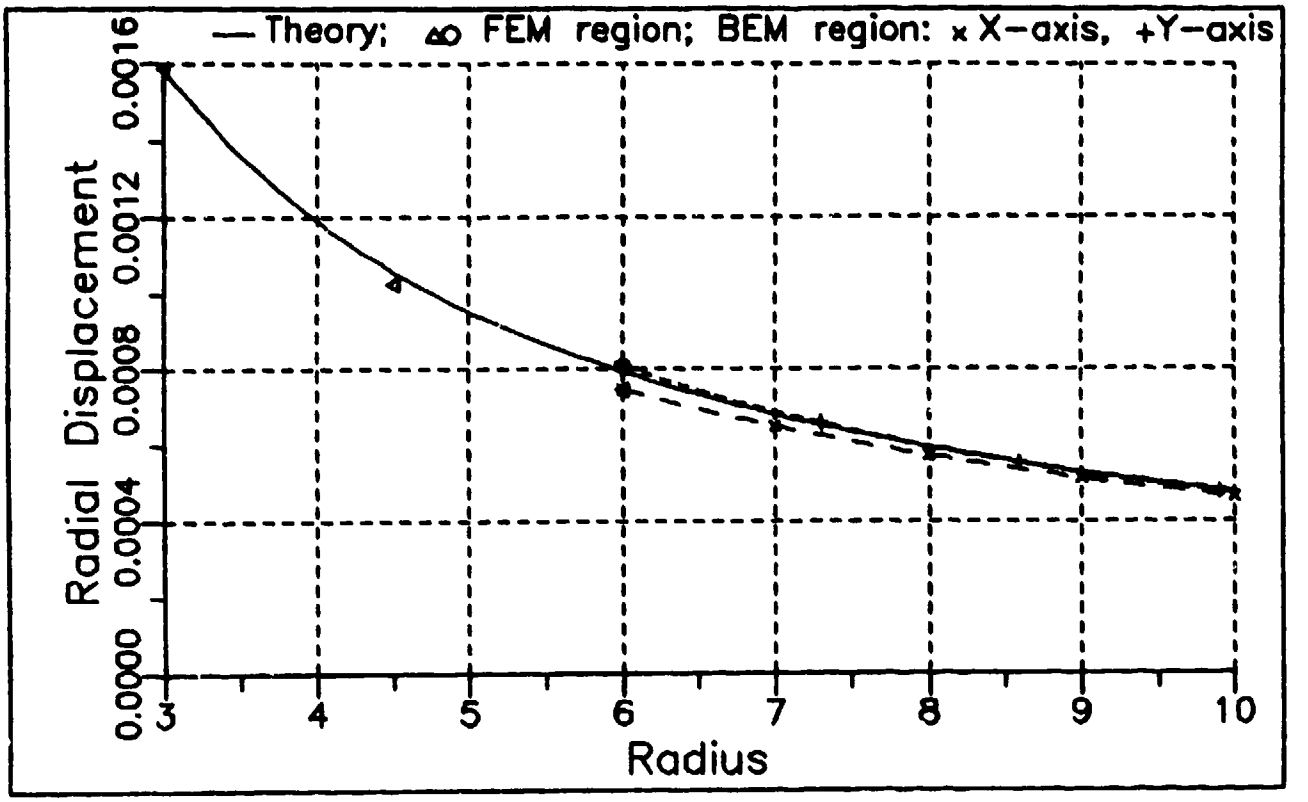

Figure 16a. Model 6: numerical prediction of u_r versus theory.

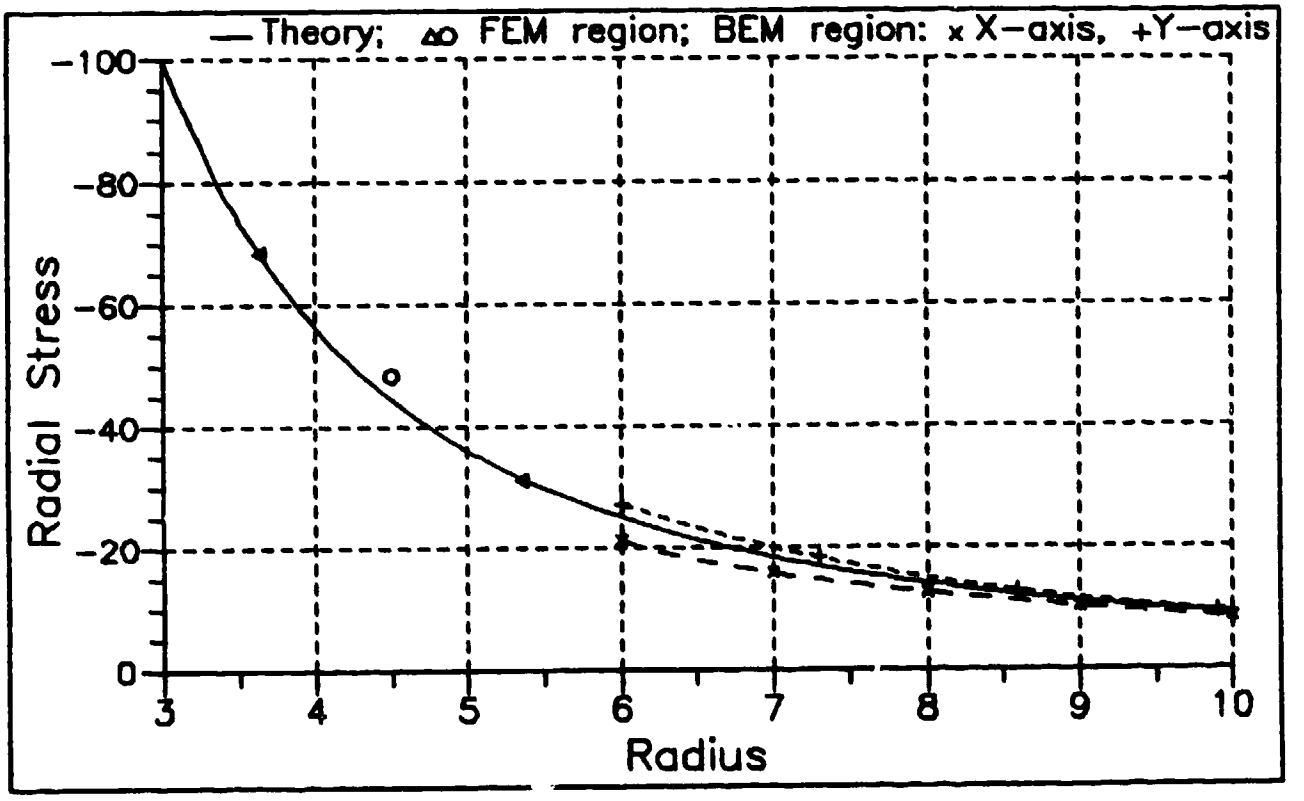

Figure 16b. Model 6: numerical prediction of σ_{rr} versus theory.

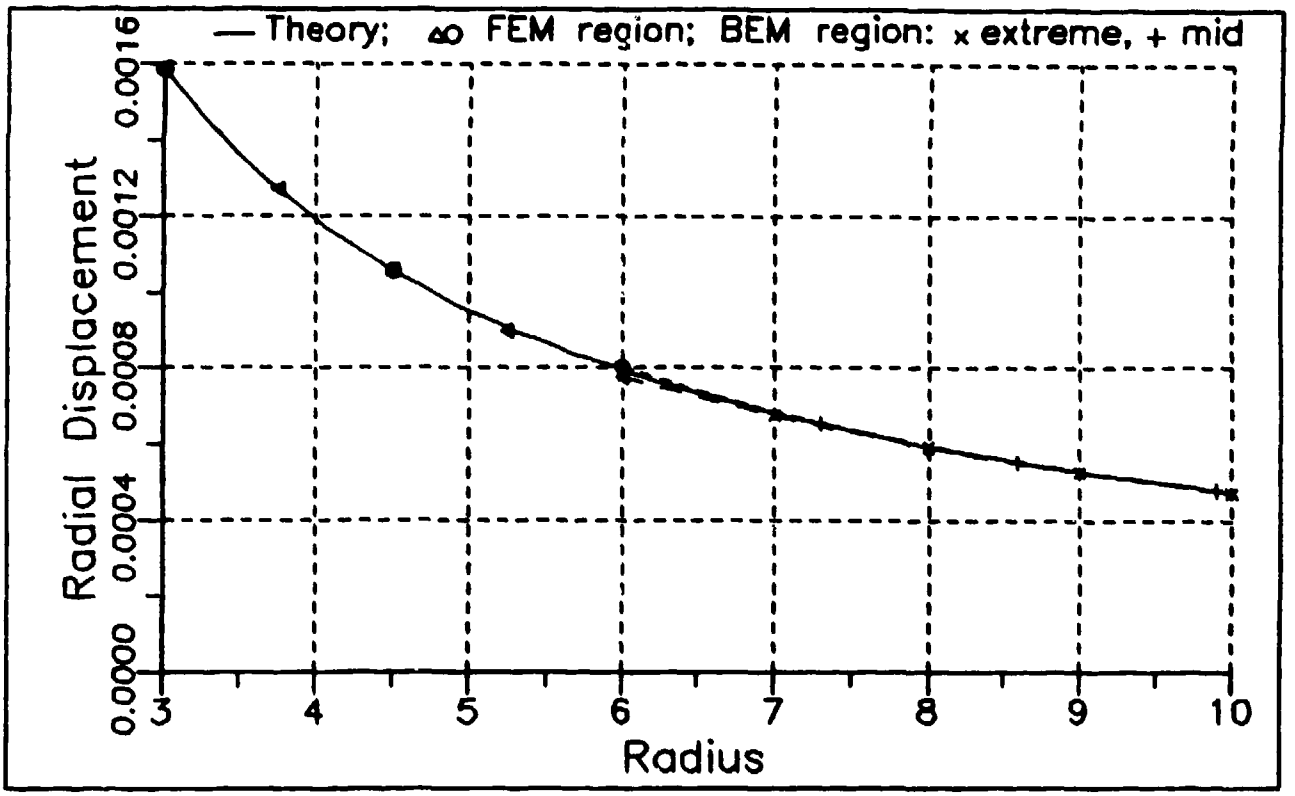

Figure 17a. Model 7: numerical prediction of u_r versus theory.

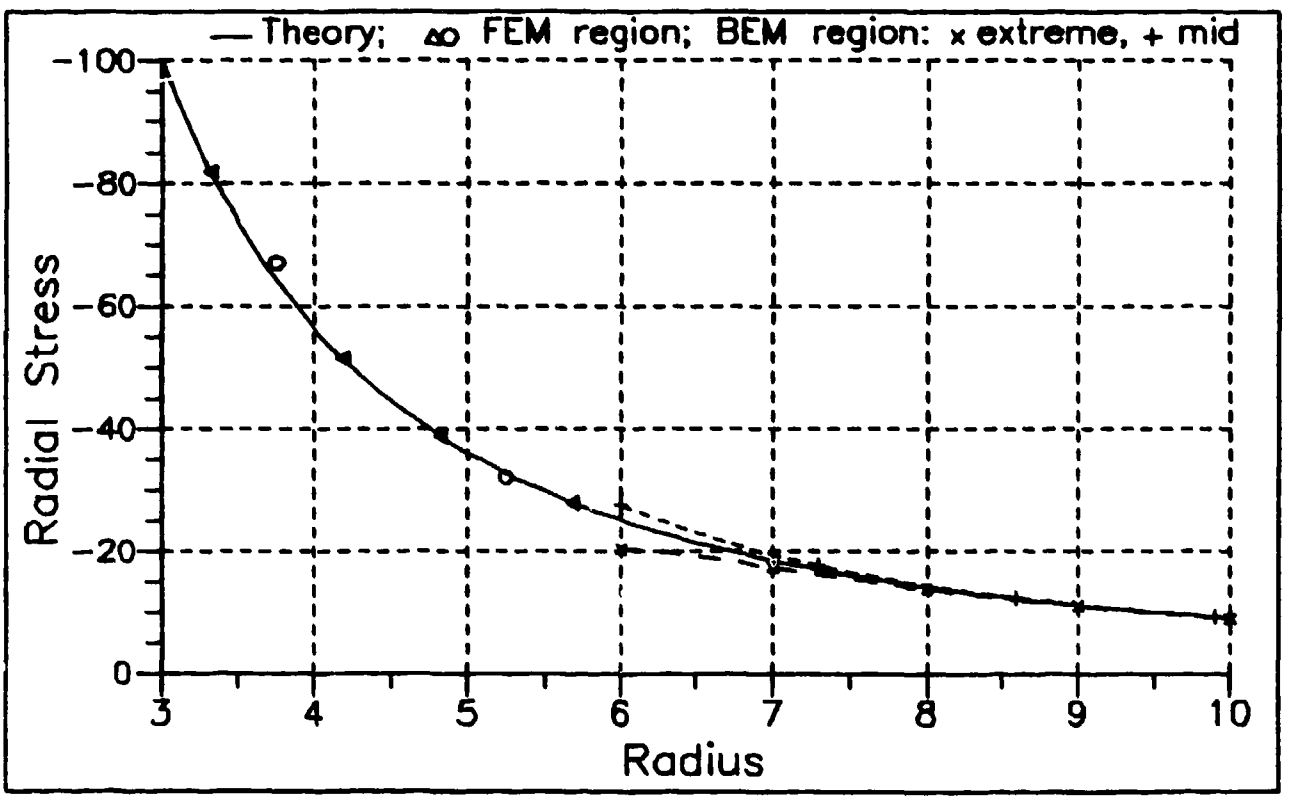

Figure 17b. Model 7: numerical prediction of σ_{rr} versus theory.

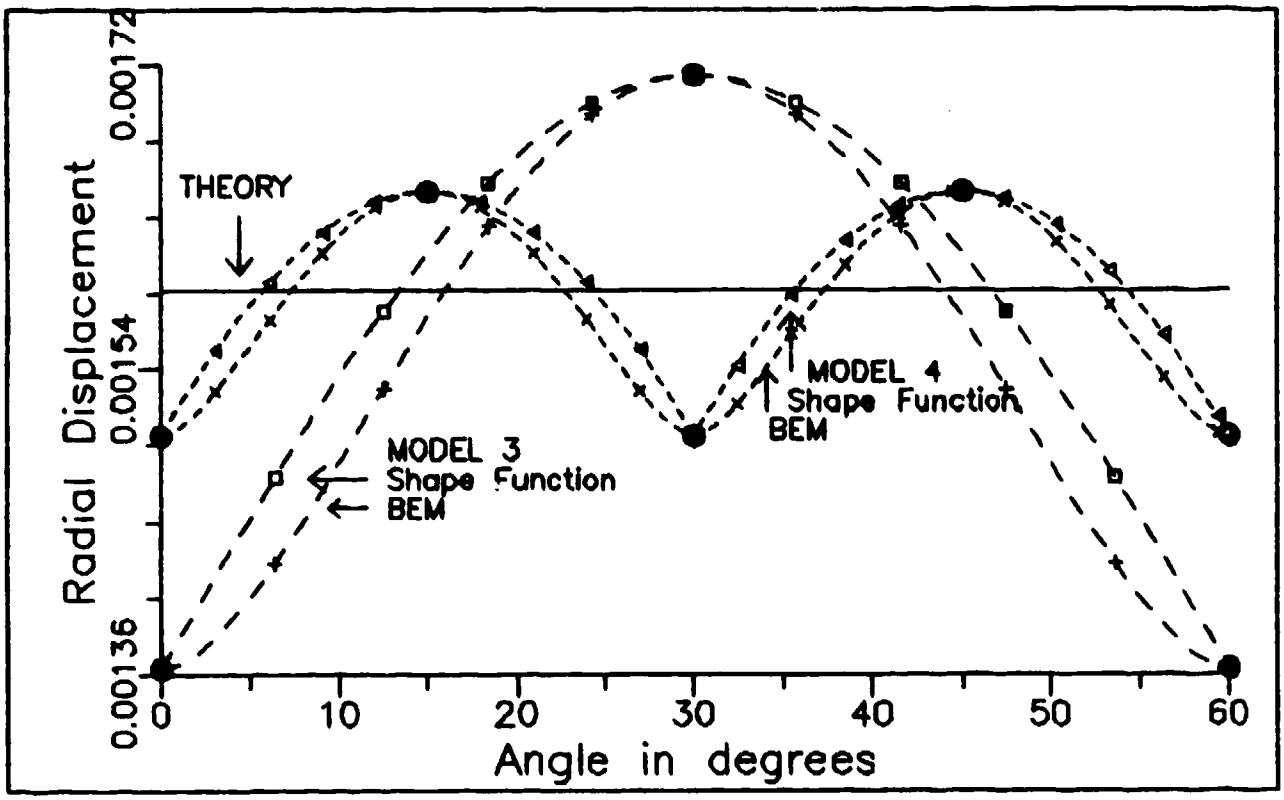

Figure 18. u_r for IBEM stiffness formulation (models 3 and 4) along Γ.

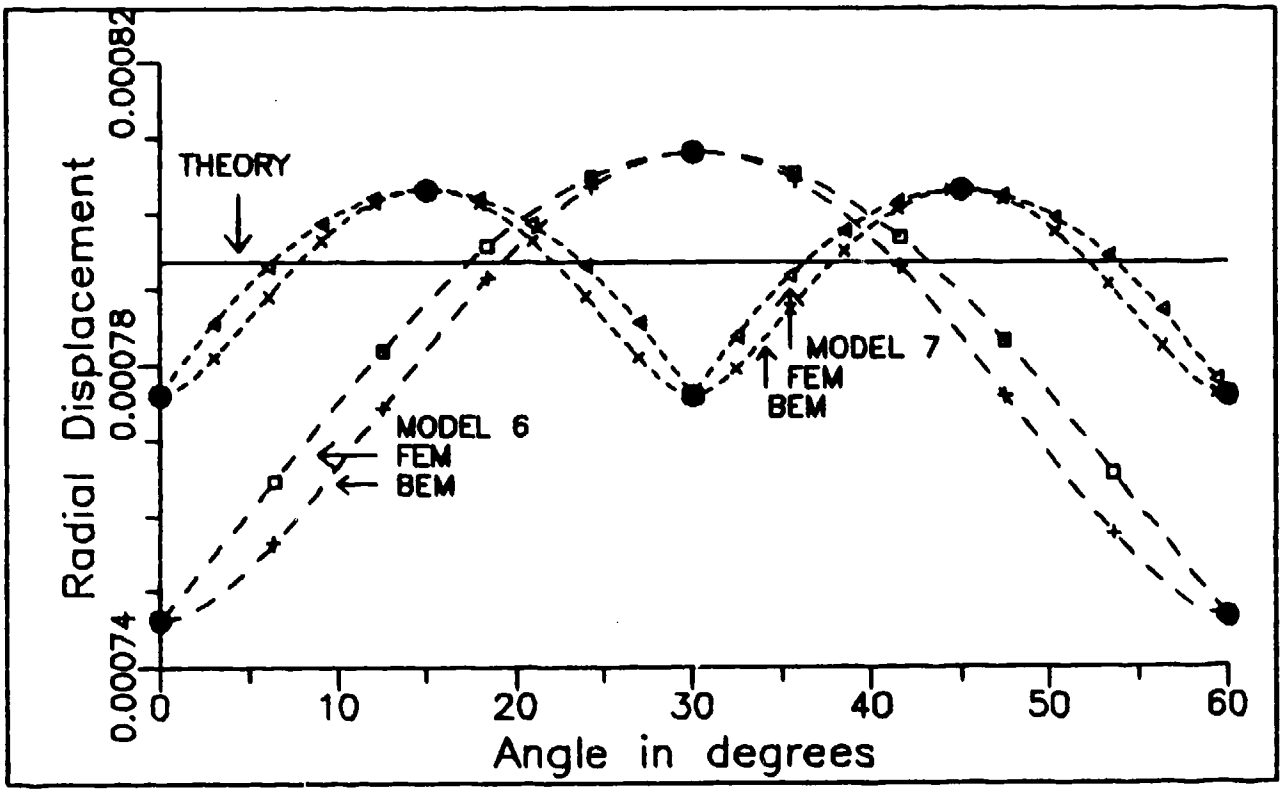

Figure 19. u_r for coupled solution (models 6 and 7) along Γ_I.

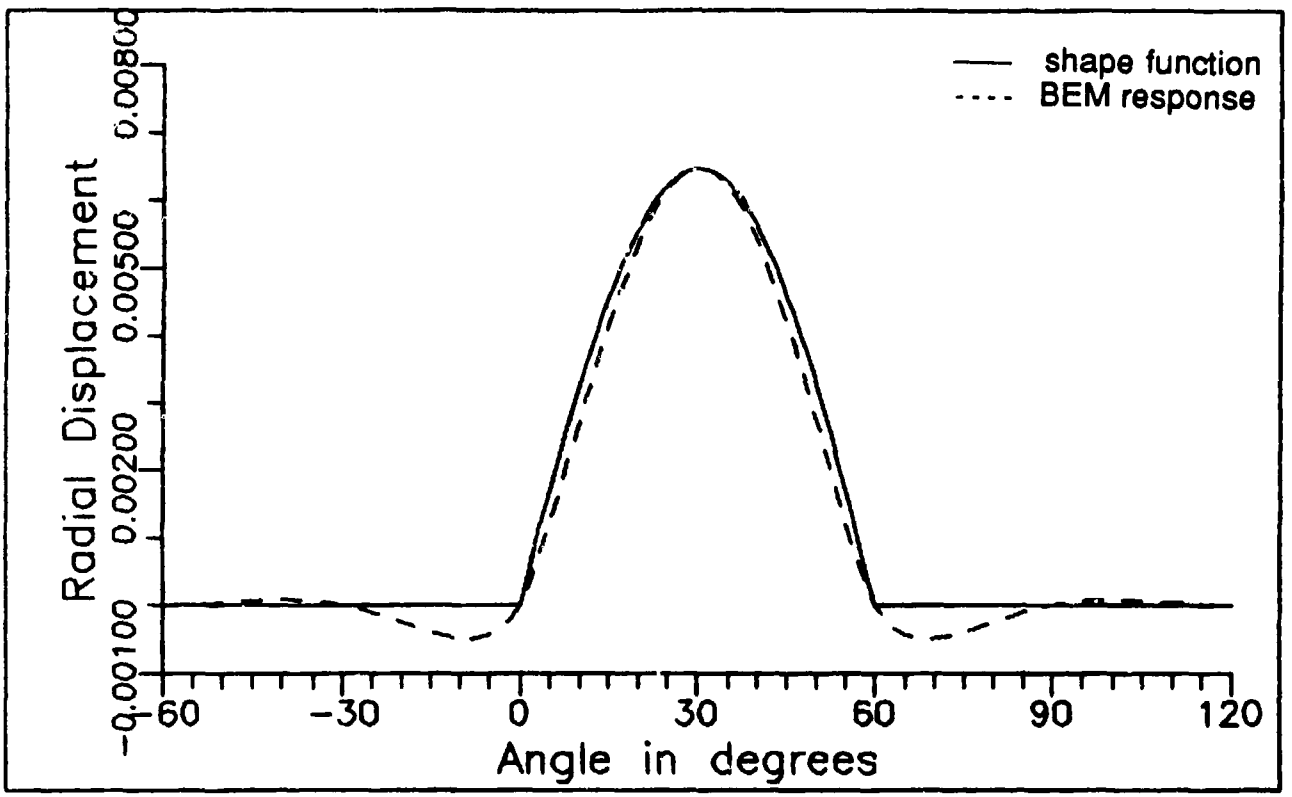

Figure 20. "Model 3": u_r along Γ due to a radial load of 1000 applied at a mid-side node.

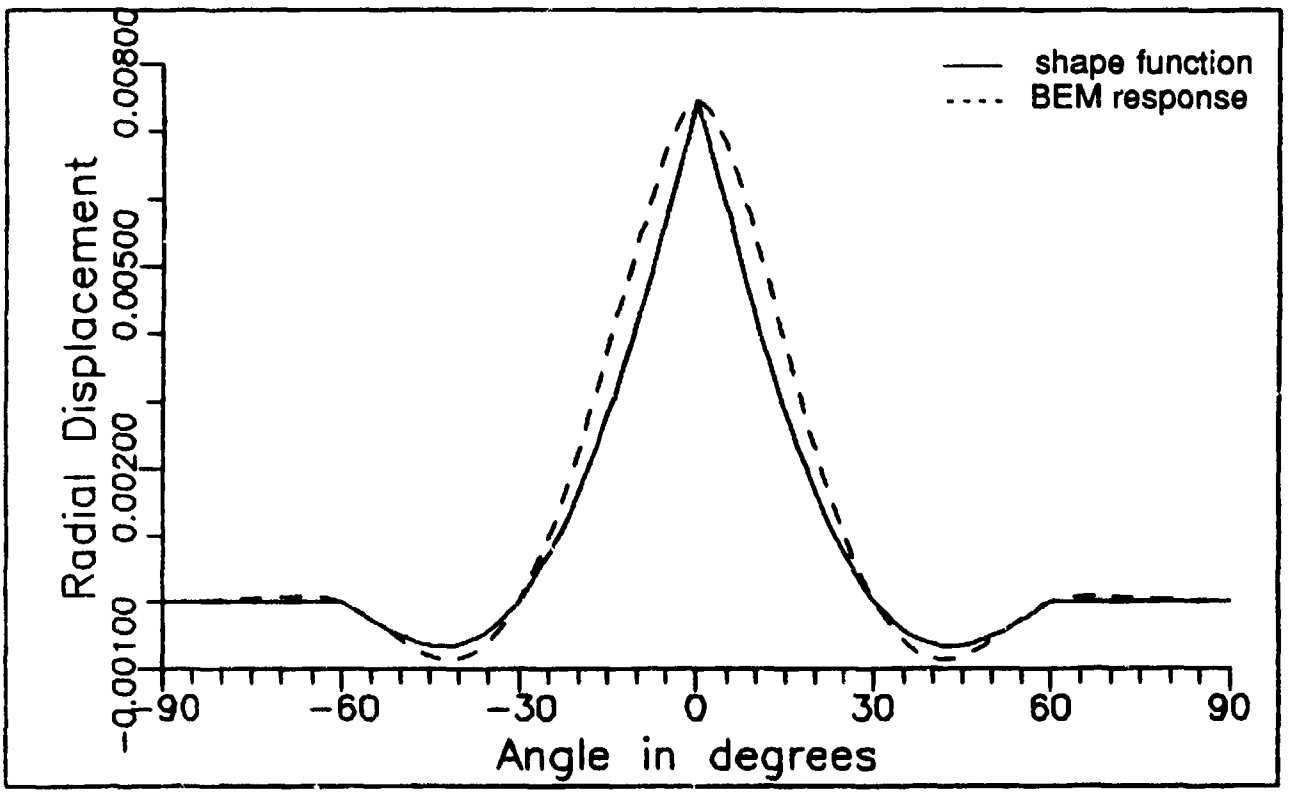

Figure 21. "Model 3": u_r along Γ due to a radial load of 1000 applied at a extreme node.

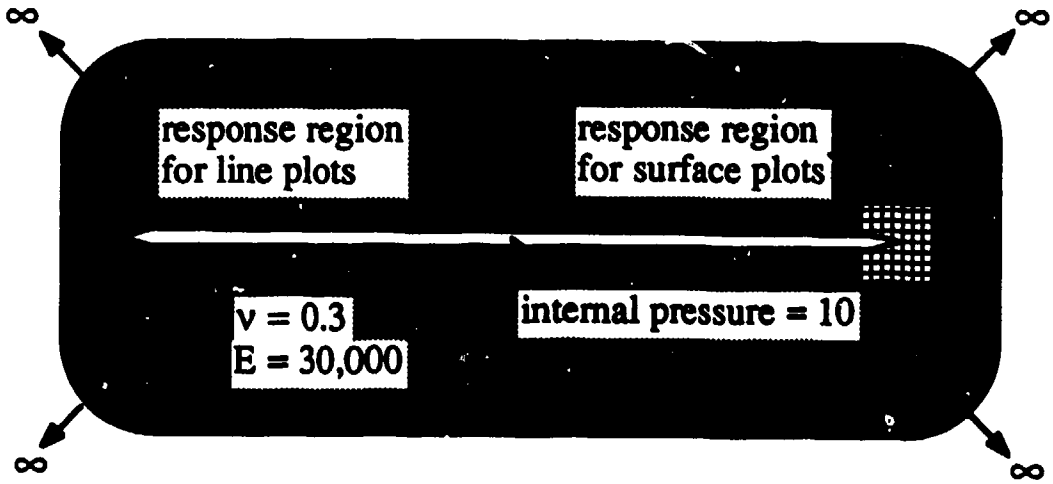

Figure 22. Pressurized crack problem.

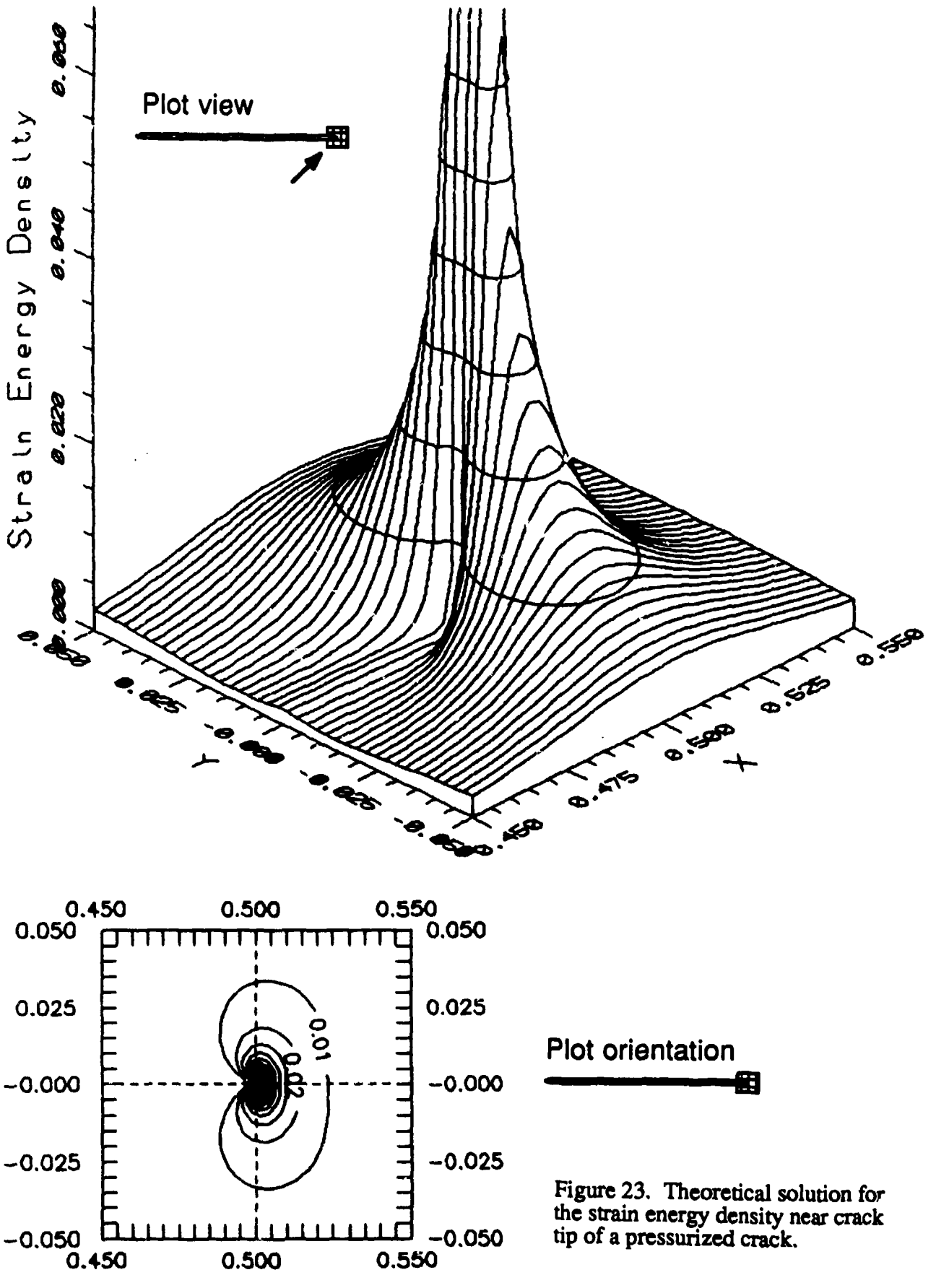

Figure 23. Theoretical solution for the strain energy density near crack tip of a pressurized crack.

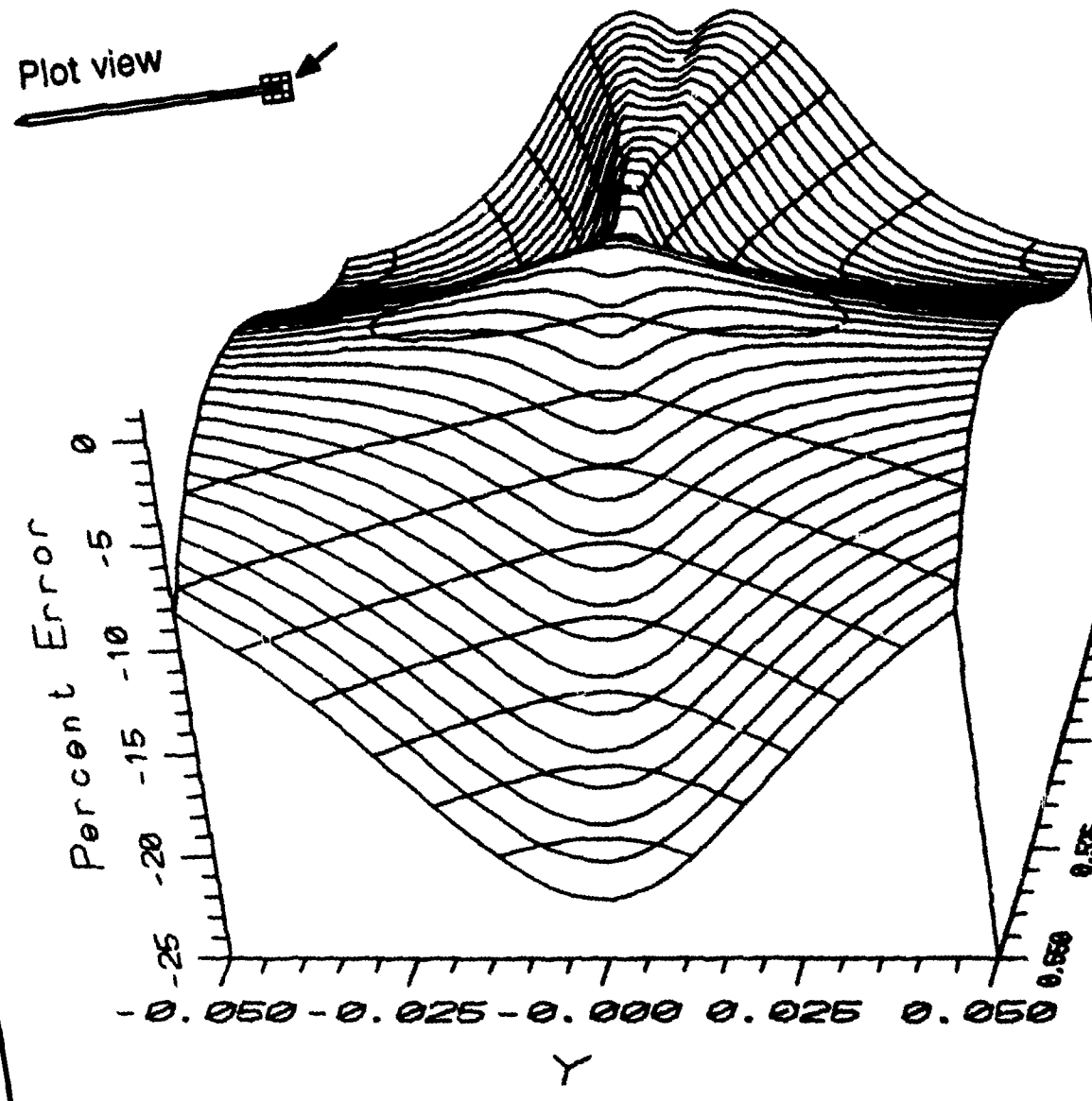

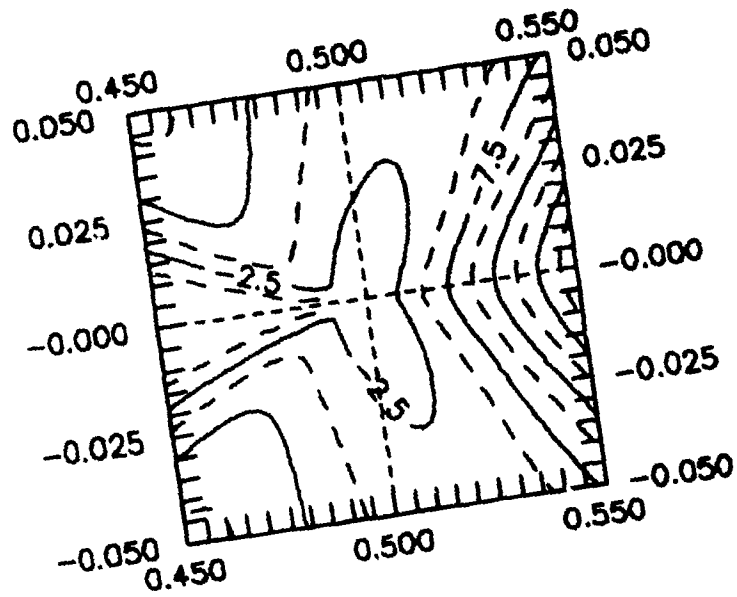

Figure 24. Difference between the strain energy density for the complete solution and the singular term.

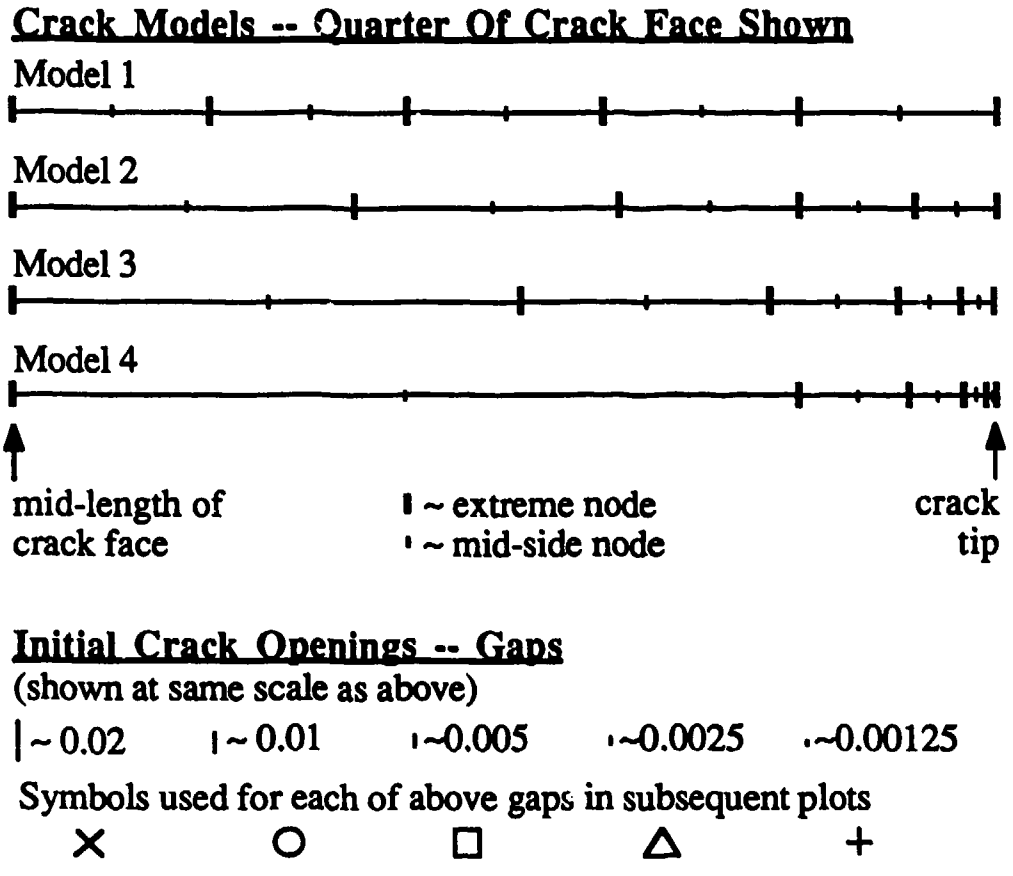

Figure 25. IBEM crack models.

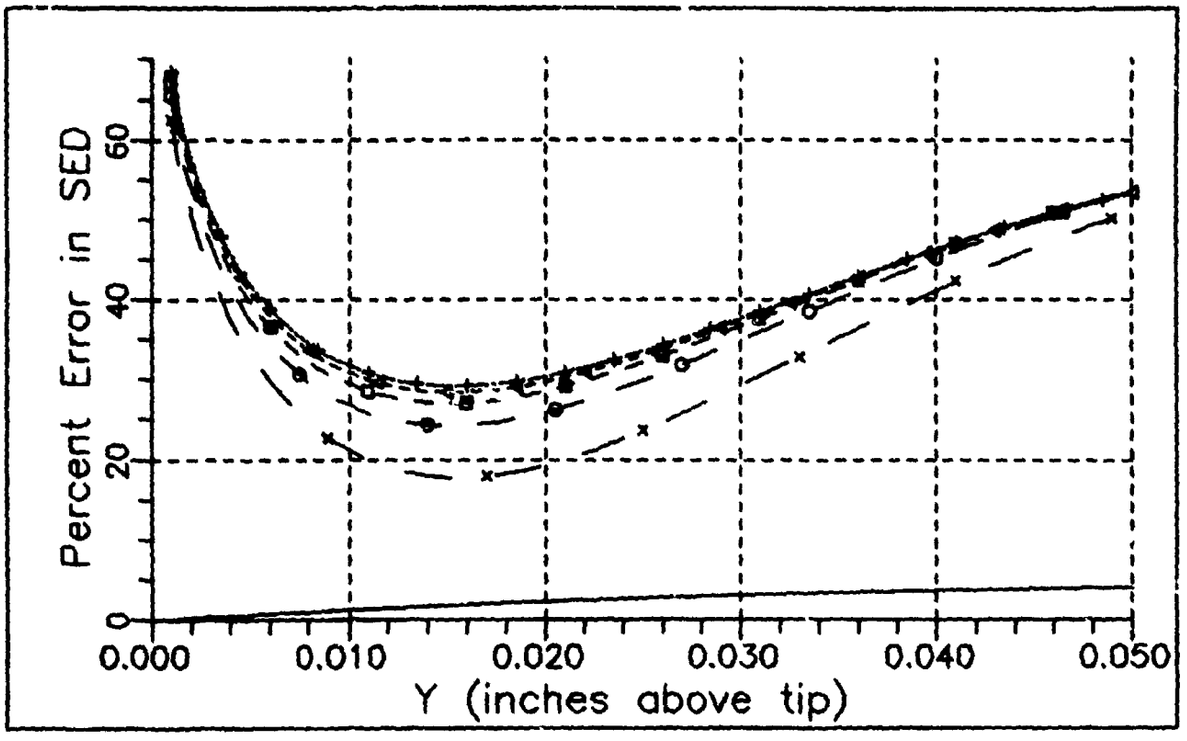

Figure 26. Model 1: error in strain energy density for various gaps.

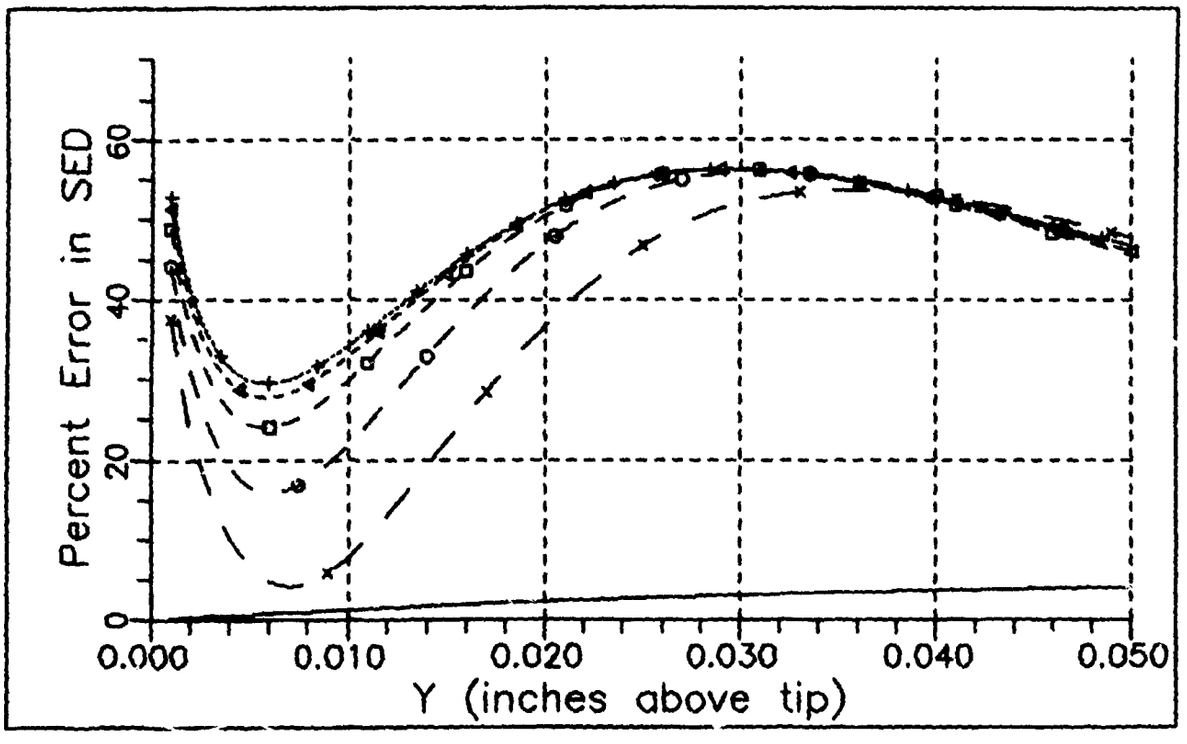

Figure 27. Model 2: error in strain energy density for various gaps.

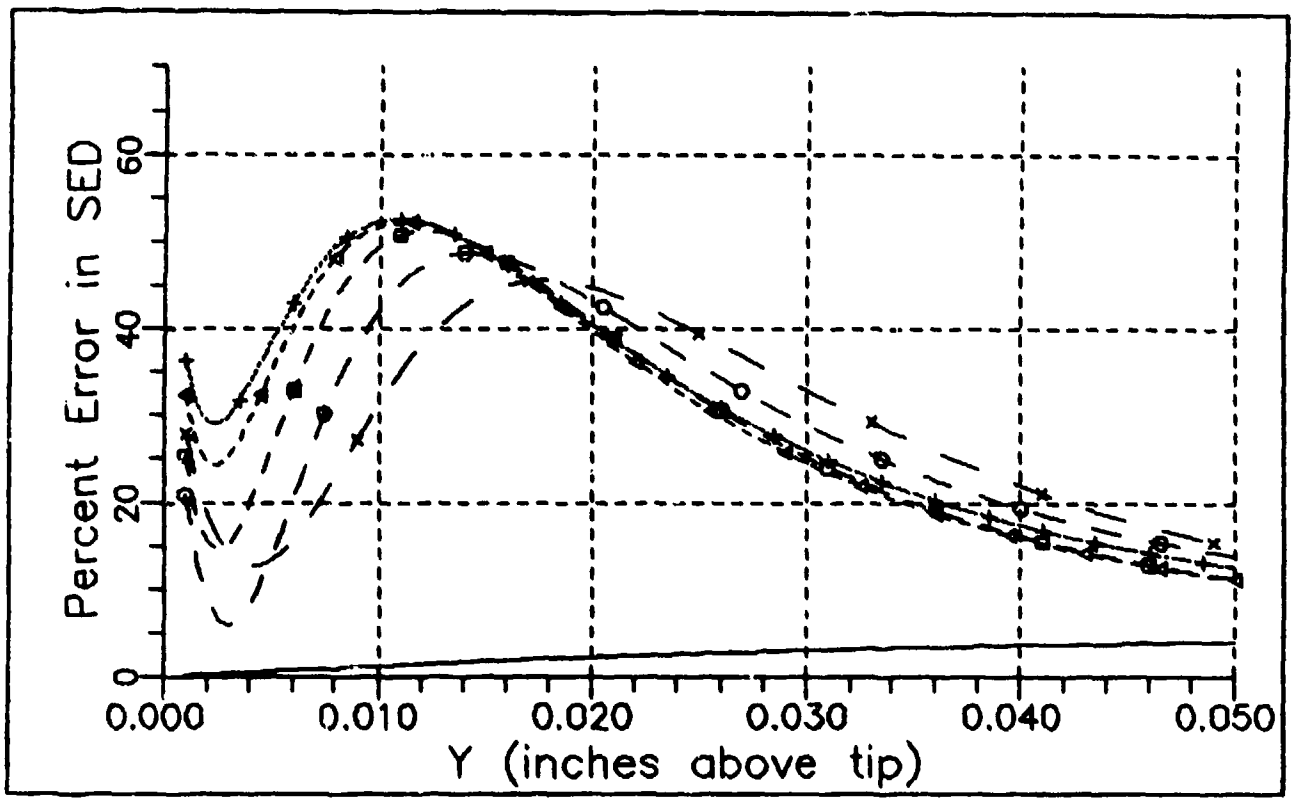

Figure 28. Model 3: error in strain energy density for various gaps.

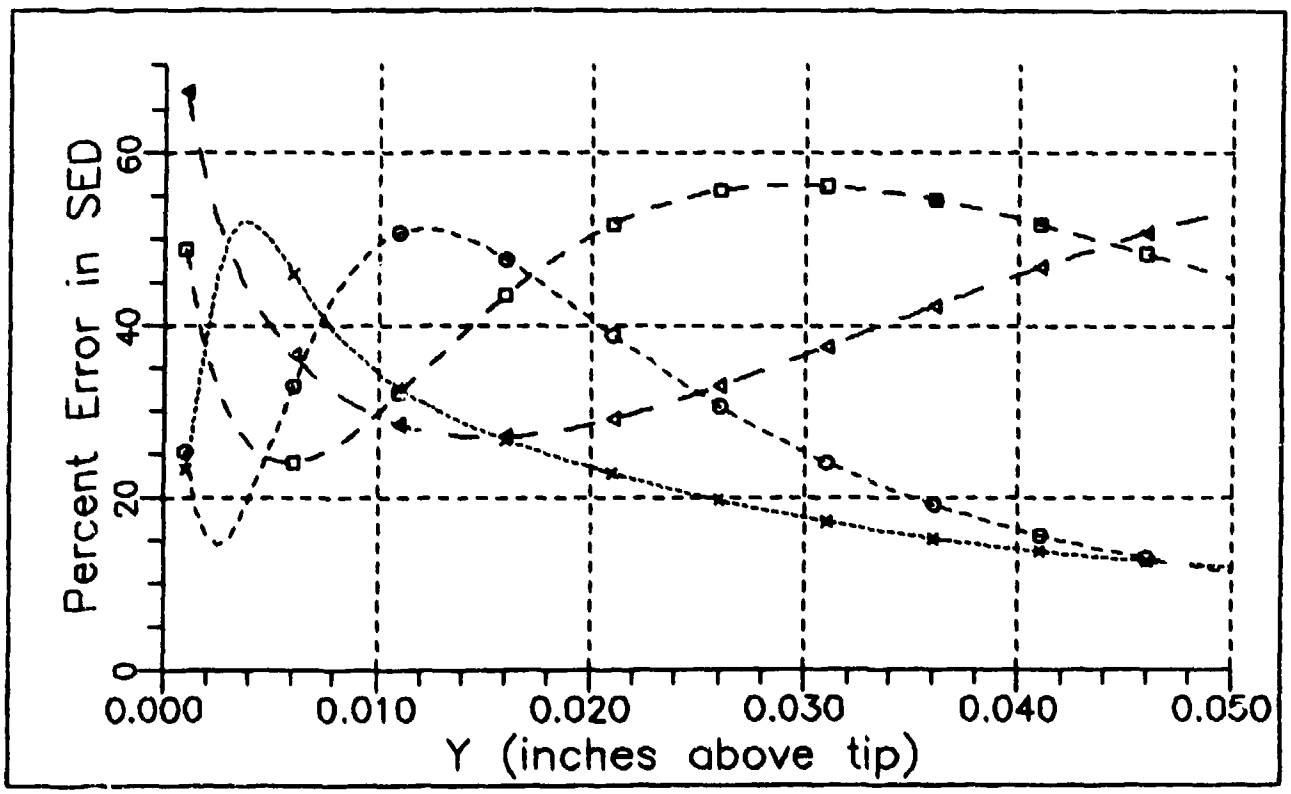

Figure 29. Error in strain energy density for various models with a gap of 0.005 (Δ ~ model 1, □ ~ model 2, O ~ model 3, × ~ model 4).

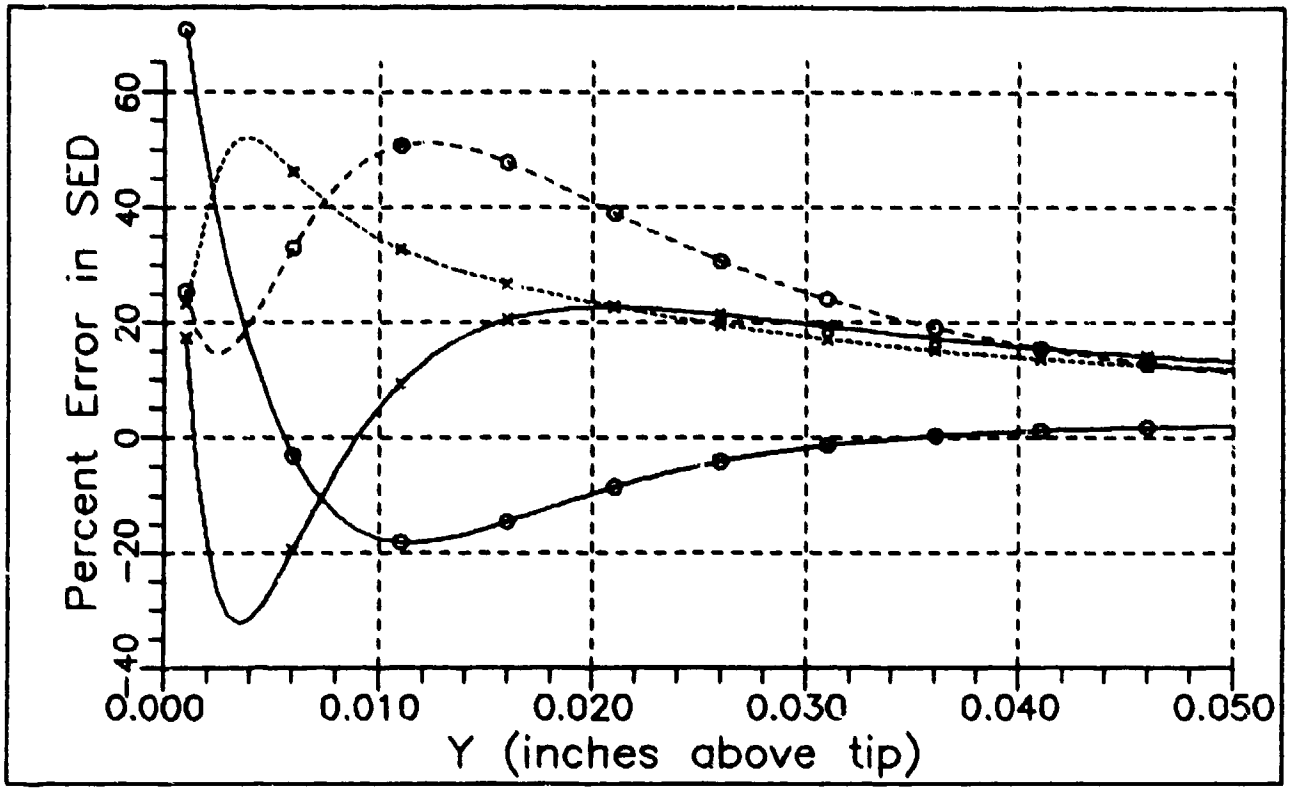

Figure 30. Error in strain energy density: internal collocation (- - -) versus nodal collocation (—) at the crack tip (O ~ model 3, × ~ model 4).

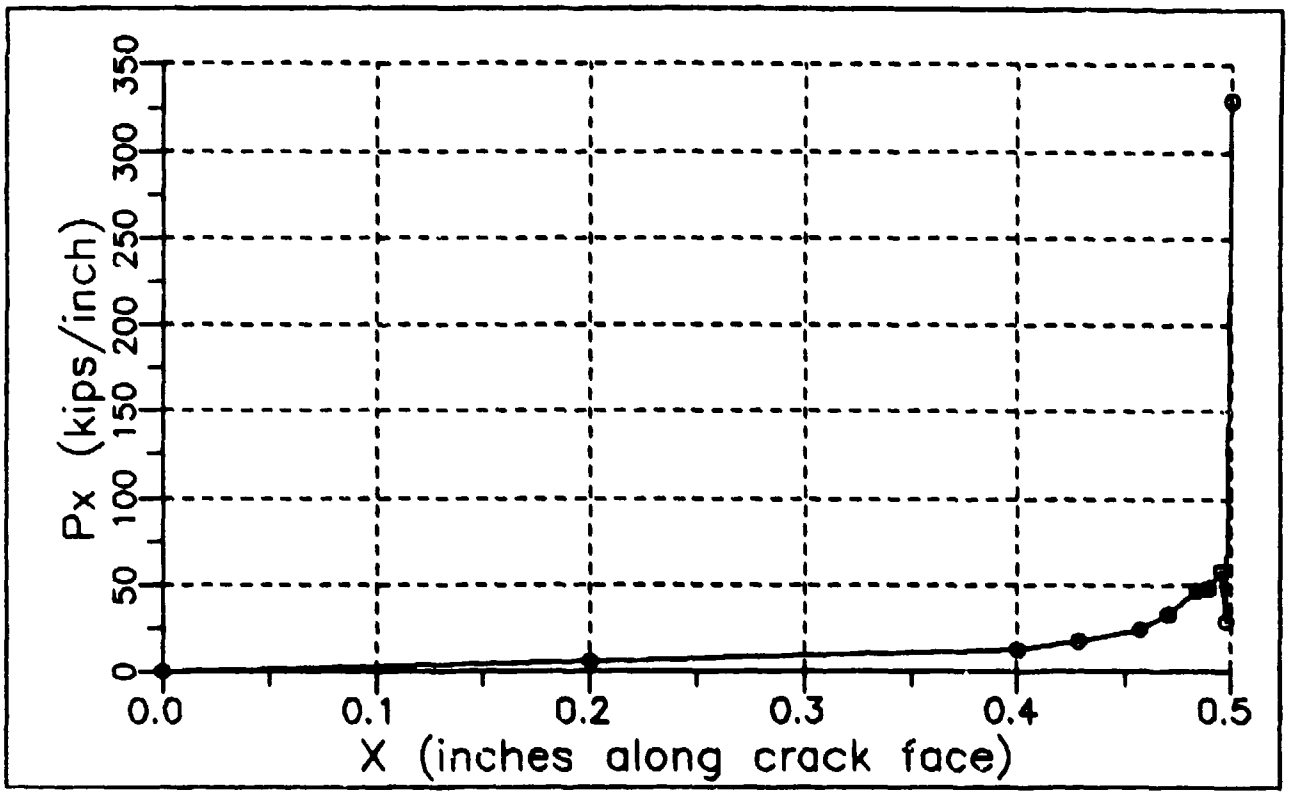

Figure 31a. Horizontal component of the artificial traction vector along top right face of model 4.

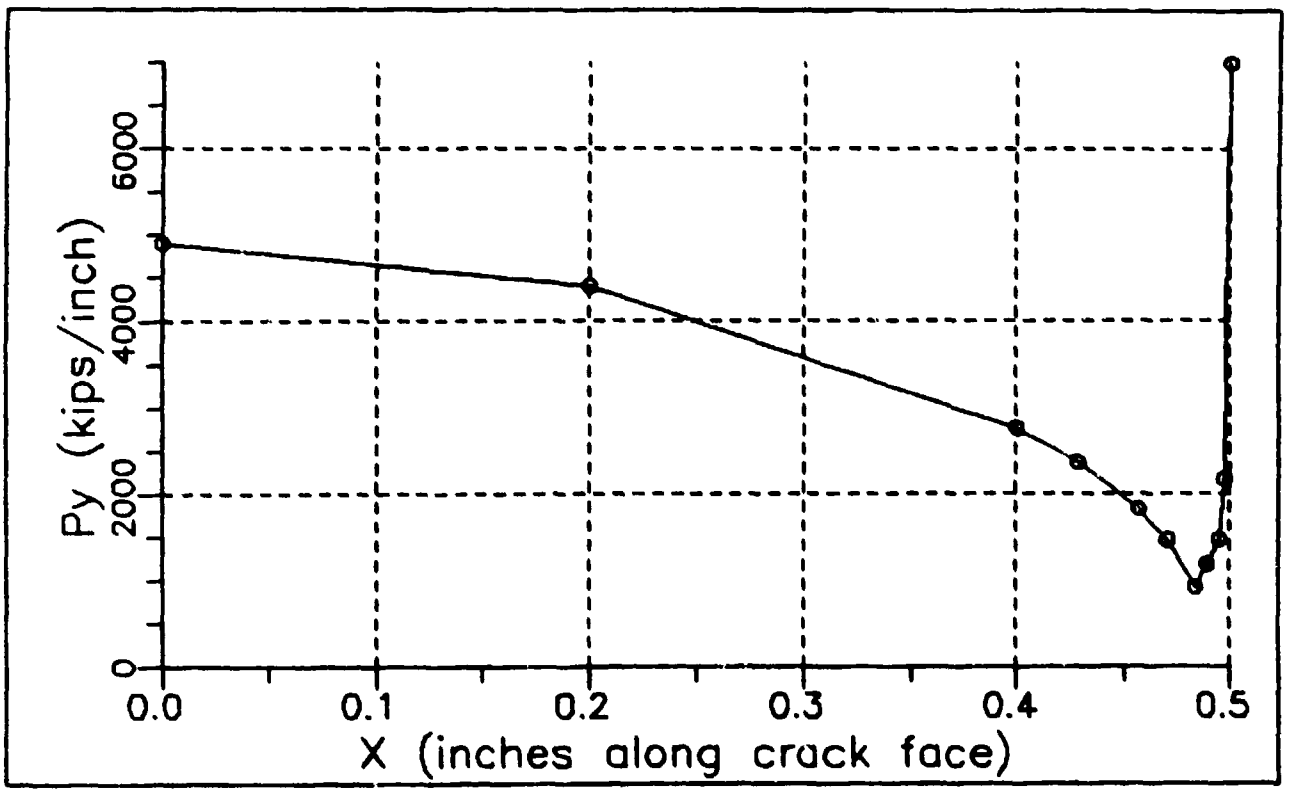

Figure 31b. Vertical component of the artificial traction vector along top right face of model 4.

U.S. GOVERNMENT PRINTING OFFICE: 1989 679-795/

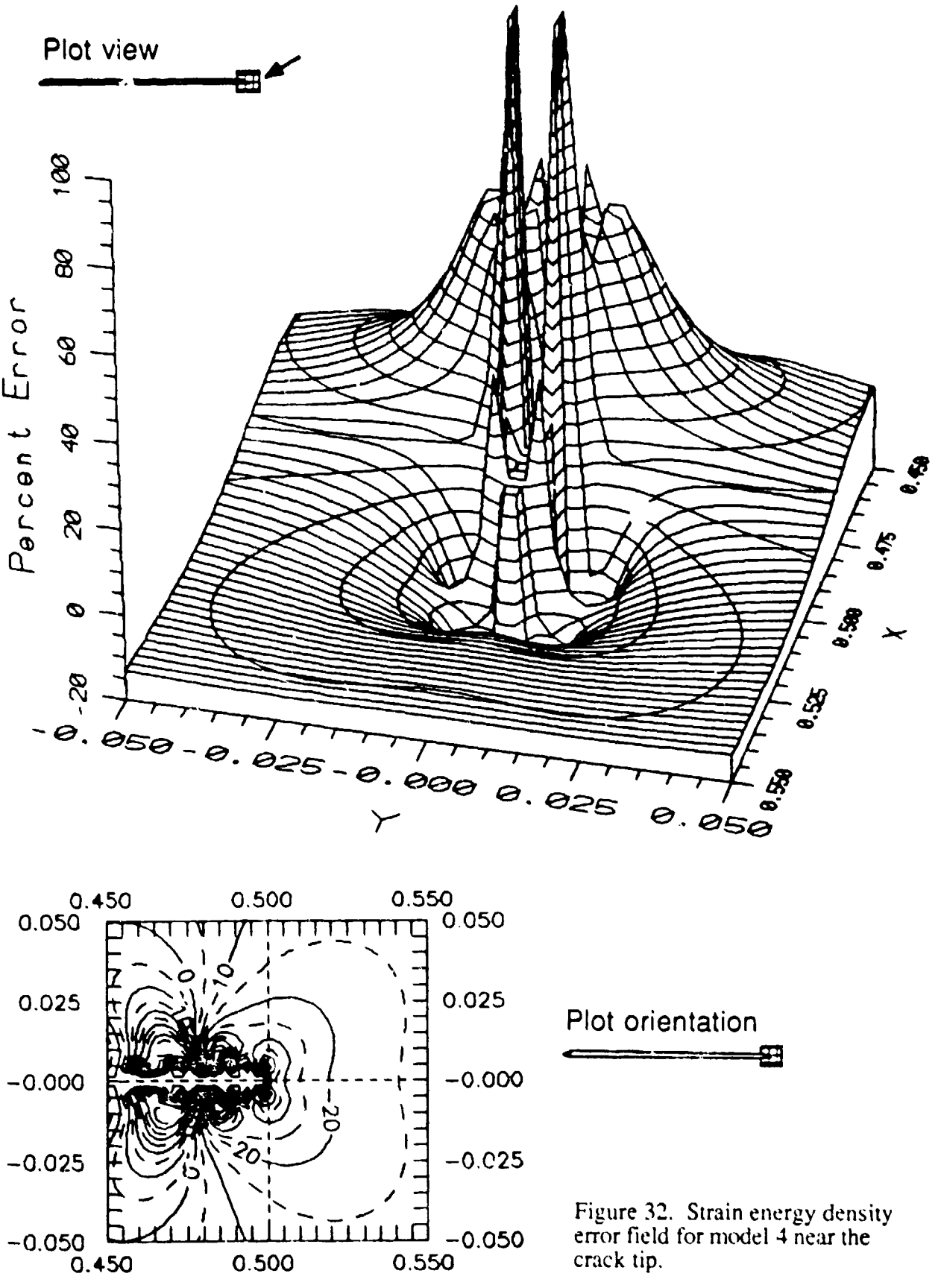

Figure 32. Strain energy density error field for model 4 near the crack tip.

DISTRIBUTION LIST

AF 1004 SSG DE, Sunnyvale, CA; 323 CES DEEE (Tjoa), Mather AFB, CA; AFIT DET (Hudson), Wright-Patterson AFB, OH; AFIT DET, Wright-Patterson AFB, OH; CAPT Holland, Saudia Arabia
AF HQ ESD AVMS, Hanscom AFB, MA; ESD DEE, Hanscom AFB, MA
AFB 82nd ABG DEMC, Williams AFB, AZ; HQ MAC DEET, Scott AFB, IL
AFESC TST (Library), Tyndall AFB, FL
AFOSR NA, Bolling AFB, DC
ARMY 416th ENCOM, Akron Survey Tm, Akron, OH; CECOM R&D Tech Lib, Ft Monmouth, NJ; CEHSC-FU-N (Krajewski), Ft Belvoir, VA; HQ, EEAK, Ch Bldgs & Grnds Div, Yongsan, Korea; HQDA (DAEN-ZCM), Washington, DC; POJED-O, Okinawa, Japan
ARMY BELVOIR R&D CEN STRBE-BLORE, Ft Belvoir, VA
ARMY CERL CECER-EME (Hayes), Champaign, IL; CERL-ZN, Champaign, IL; Library, Champaign, IL
ARMY CORPS OF ENGRS HQ, DAEN-ECE-D (Paavola), Washington, DC
ARMY DEPOT Letterkenny, SDSLE-SF, Chambersburg, PA
ARMY EHA HSHB-EW, Aberdeen Proving Grnd, MD
ARMY ENGR DIST CENPS-ED-SD, Seattle, WA, LMVCO-A Bentley, Vicksburg, MS; Library, Seattle, WA; Phila, Lib, Philadelphia, PA
ARMY ENGR DIV CEHND-ED-CS, Huntsville, AL; ED-SY (Loyd), Huntsville, AL; HNDED-SY, Huntsville, AL
ARMY EWES GP-EC (Webster), Viesburg, MS; Library, Vicksburg MS; WES-SS (Kiger), Vicksburg, MS; WESCV-Z (Whalin), Vicksburg, MS; WESGP-E, Vicksburg, MS; WESIM-C (N. Radhadrishnan), Vicksburg, MS
ARMY LMC Fort Lee, VA
ARMY MISSILE R&D CMD Ch, Docs, Sci Info Ctr, Arsenal, AL
ARMY MMRC DRXMR-SM (Lenoe), Watertown, MA
ADMINSUPU PWO, Bahrain
BUREAU OF RECLAMATION D-1512 (GS DePuy), Denver, CO
CBC Code 10, Davisville, RI; Code 15, Port Hueneme, CA; Code 155, Port Hueneme, CA; Code 430, Gulfport, MS; Library, Davisville, RI, PWO (Code 400), Gulfport, MS; PWO (Code 80), Port Hueneme, CA, Tech Library, Gulfport, MS
CNA Tech Library, Alexandria, VA
COGARD R&DC Library, Groton, CT
COMCBLANT Code S3T, Norfolk, VA
COMDT COGARD Library, Washington, DC
COMFLEACT PWO, Sasebo, Japan
COMNAVSUPPFORANTARCTICA DET, PWO, Christchurch, NZ
COMNAVSURF Code N42A, Norfolk, VA
COMOCEANSYS Lant, Code N9, Norfolk, VA
COMTRA Lant, SCE, Norfolk, VA
DESC OWE, Alexandria, VA
DIA DB-6E1, Washington, DC; DB-6E2, Washington, DC; VP-TPO, Washington, DC
DIRSSP Tech Lib, Washington, DC
DOD DESC-FE, Cameron Station, Alexandria, VA; Explos Safety Brd (Lib), Washington, DC
DOE Wind Ocean Tech Div, Tobacco, MD
DOT Dr. Pin Tong, Cambridge, MA
DTIC Alexandria, VA
DTRCEN Code 172, Bethesda, MD; Code 1720, Bethesda, MD; Code 4111, Bethesda, MD
FAA Code APM-740 (Tomita), Washington, DC
GIDEP OIC, Corona, CA
GSA Ch Engrg Br, PQB, Washington, DC
LIBRARY OF CONGRESS Sci & Tech Div, Washington, DC
MARCORBASE Code 4.01, Camp Pendleton, CA, Code 406, Camp Lejeune, NC; PAC, PWO, Camp Butler, JA; PWO, Camp Lejeune, NC; PWO, Camp Pendleton, CA; Pac, FF, Camp Butler, JA
MARCORPS FIRST FSSG, Engr Supp Offr, Camp Pendleton, CA
MCAS PWO, Yuma, AZ
MCLB PWC (Sachan), Barstow, CA
MCRD PWO, San Diego, CA
MCRDAC M & L Div Quantico, VA, PWO, Quantico, VA
NAF AROICC, Midway Island; Dir, Engrg Div, PWD, Atsugi, Japan
NAS Chase Fld, Code 18300, Beeville, TX, Chase Fld, PWO, Beeville, TX; Code 110, Adak, AK; Code 15, Alameda, CA; Code 1833, Corpus Christi, TX; Code 70, South Weymouth, MA; Code 8, Patuxent River, MD; Code 83, Patuxent River, MD; Miramar, PWO, San Diego, CA; NI, Code 183, San Diego, CA; OL, Alameda, CA; PW Engrg (Branson), Patuxent River, MD; PWO (Code 182) Bermuda; PWO, Cecil Field, FL; PWO, Dallas, TX; PWO, Glenview, IL; PWO, Keflavik, Iceland; PWO, Key West, FL; PWO, Kingsville

TX PWO, New Orleans, LA, PWO, Sigonella, Italy, PWO, South Weymouth, MA, SCF, Parkers Point HI, SCF, Cabo Point, RP, Whiting Fld, PWO, Milton, FL
NAVAIRDEVCEN Code 832, Warminster, PA
NAVAIRENGCEN Code 182, Lakehurst, NJ, PWO, Lakehurst, NJ
NAVAIRTESTCEN PWO, Patuxent River, MD
NAVAUDSVCHQ Director, Falls Church, VA
NAVAVNDEPOT Code 640, Pensacola, FL
NAVCHAPGRU Code 00, Washington, DC
NAVCOASTSYSCEN CO, Panama City, FL, Code 7360, Panama City, FL, Code 740, Panama City, FL, Tech Library, Panama City, FL
NAVCOMMSTA Code 401, Nea Makri, Greece
NAVFLEXCEN DET, OIC, Winter Harbor, ME
NAVFLOPTECHCEN Tech Library, Indian Head, MD
NAVFAC PWO (Code 500), Brawdy Wales, UK, PWO, Oak Harbor, WA
NAVFACENGCOM Code 00, Alexandria, VA, Code 03, Alexandria, VA, Code 03L (Essoglou), Alexandria, VA, Code 04A, Alexandria, VA, Code 04A1, Alexandria, VA, Code 04A1D, Alexandria, VA, Code 04A5, Alexandria, VA, Code 04A30, Alexandria, VA, Code 04B2 (Cecilio), Alexandria, VA, Code 04B1 (Wu), Alexandria, VA, Code 04R, Alexandria, VA, Code 0631, Alexandria, VA, Code 07, Alexandria, VA, Code 07M (Grosse), Alexandria, VA, Code 09M124 (Libr), Alexandria, VA
NAVFACENGCOM CHES DIV, FPO PI, Washington, DC
NAVFACENGCOM EAST DIV, Br Off, Det, Naples, Italy, Code 114, Norfolk, VA, Library, Norfolk, VA
NAVFACENGCOM NORTH DIV, Code 04, Philadelphia, PA, Code 04M, Philadelphia, PA
NAVFACENGCOM PAC DIV, Code 09P, Pearl Harbor, HI, Code 101 (Kerr), Pearl Harbor, HI, Library, Pearl Harbor, HI
NAVFACENGCOM SOUTH DIV, Code 04A3, Charleston, SC, Code 114, Charleston, SC, Code 406, Charleston, SC, Library, Charleston, SC
NAVFACENGCOM WEST DIV, Code 04A2.2 (Libr), San Bruno, CA, Code 04B, San Bruno, CA, Code 408.2 (Deuner), San Bruno, CA, Pac NW Br Ofc, Code C50, Silverdale, WA
NAVFACENGCOM CONTRACTS Code 400, Portsmouth, VA, Code 423, Everett, WA, DROICC, Fremont, CA, Earle, ROICC, Colts Neck, NJ, North Bay, Code 1013, VA, Vallejo, CA, OICC, Guam, OICC ROICC, Norfolk, VA, OICC ROICC, Virginia Beach, VA, ROICC, Corpus Christi, TX, ROICC, Crane, IN, ROICC, Keflavik, Iceland, ROICC, Point Mugu, CA, ROICC, Quantico, VA, SW Pac, OICC, Manila, RP
NAVFLTFE DET, OIC, Yokohama, Japan
NAVHOSP CO, Millington, TN, Hd, Fac Mgmt, Camp Pendleton, CA, SCF, (Knapowski), Great Lakes, IL, SCF, Pensacola, FL
NAVMAG SCF, Subic Bay, RP
NAVMARCORESCEN LTFG Davis, Raleigh, NC
NAVMEDCOM SWREG, Fac Engr, PWD, Oakland, CA, PACREG, Code 22, Barbers Point, HI, SE REG, Hd, Fac Mgmt Dept, Jacksonville, FL, SWREG, Head, Fac Mgmt Dept, San Diego, CA, SWREG, SCF, San Diego, CA
NAVOCEANCOMCEN CO, Guam, Mariana Islands
NAVOCEANO Code 6100 (M Paget), Bay St. Louis, MS
NAVOCEANSYSCEN Code 9642B, San Diego, CA
NAVPGSCOL PWO, Monterey, CA
NAVPHIBASE PWO, Norfolk, VA, SCF, San Diego, CA
NAVSCOLCECOFF Code 33, Port Hueneme, CA
NAVSCSCOL PWO, Athens, GA
NAVSEACENPAC Code 32, San Diego, CA
NAVSEASYSCOM Code PMS299E22 (T Rekasi), Washington, DC
NAVSHIPREPFAC Library, Guam, SCF, Subic Bay, RP; SCF, Yokosuka, Japan
NAVSHIPYD Code 202.4, Long Beach, CA, Code 202.5 (Library), Bremerton, WA, Code 440, Portsmouth, NH, Code 443, Bremerton, WA, Library, Portsmouth, NH, Mare Island, Code 202.13, Vallejo, CA, Mare Island, Code 250, Vallejo, CA, Mare Island, PWO, Vallejo, CA, Norfolk, Code 440, Portsmouth, VA, PWO, Bremerton, WA
NAVSTA CO, Long Beach, CA, CO, Roosevelt Roads, PR, Code N4214, Mayport, FL, Engr Div, PWD, Rodman, Panama Canal, Engrg Div, PWD, Rota, Spain, SCF, San Diego, CA, WC 93, Guantanamo Bay, Cuba
NAVSUPPACT PWO, Naples, Italy
NAVSUPPFAC Contract Admin Tech Library, Diego Garcia
NAVSWC Code E211 (Miller), Dahlgren, VA, DET, White Oak Lab, Code WSO, Silver Spring, MD
NAVWARCOL Code 24, Newport, RI
NAVWPNCEN AROICC, China Lake, CA, PWO (Code 266), China Lake, CA
NAVWPNSTA Code 092B (Hurt), Yorktown, VA, Dir, Maint Control, PWD, Concord, CA, PWO, Charleston, SC, PWO, Seal Beach, CA, PWO, Yorktown, VA
NAVWPNSUPPCEN PWO, Crane, IN
NETC Code 42, Newport, RI, PWO, Newport, RI

NCR 20, CO
NEESA Code 111E (McClaine), Port Hueneme, CA
NMCB 3, Ops Offr; 40, CO; 5, Ops Dept
NOAA Joseph Vadus, Rockville, MD
NORDA Code 360, Bay St. Louis, MS
NRL Code 2511, Washington, DC; Code 4430 (Ramberg), Washington, DC; Code 4670 (B. Faraday), Washington, DC
NSC Code 54.1, Norfolk, VA
NSD SCE, Subic Bay, RP
NUSC DET Code 3232 (Varley), New London, CT; Code 44 (Carlsen), New London, CT; Code 44 (RS Munn), New London, CT; Code TA131, New London, CT; Lib (Code 4533), Newport RI
PACMISRANFAC HI Area, PWO, Kekaha, HI
PHIBCB 1, CO, San Diego, CA; 1, P&E, San Diego, CA; 2, CO, Norfolk, VA
PMTC Code 1018, Point Mugu, CA; Code 5041, Point Mugu, CA
PWC ACE Office, Norfolk, VA; Code 10, Great Lakes, IL; Code 10, Oakland, CA; Code 101 (Library), Oakland, CA; Code 1011, Pearl Harbor, HI; Code 102, Oakland, CA; Code 123-C, San Diego, CA; Code 30, Norfolk, VA; Code 400, Great Lakes, IL; Code 400, Oakland, CA; Code 400, Pearl Harbor, HI; Code 400, San Diego, CA; Code 420, Great Lakes, IL; Code 420, Oakland, CA; Code 420B (Waid), Subic Bay, RP; Code 421 (Kaya), Pearl Harbor, HI; Code 421 (Quin), San Diego, CA; Code 421 (Reynolds), San Diego, CA; Code 422, San Diego, CA; Code 423, San Diego, CA; Code 424, Norfolk, VA; Code 500, Great Lakes, IL; Code 500, Oakland, CA; Library (Code 134), Pearl Harbor, HI; Library, Guam, Mariana Islands; Library, Norfolk, VA; Library, Pensacola, FL; Library, Yokosuka, Japan; Tech Library, Subic Bay, RP
SPCC PWO (Code 08X), Mechanicsburg, PA
SUBASE Bangor, PWO (Code 8323), Bremerton, WA
SUPSHIP Tech Library, Newport News, VA
US DEPT OF INTERIOR Natl Park Sve, RMR-PC, Denver, CO
USDA Ext Serv (T Maher), Washington, DC; For Sve Reg 8, (Bowers), Atlanta, GA; For Sve, Reg Bridge Engr, Aloha, OR; For Sve, Tech Engrs, Washington, DC
USNA Ch, Mech Engrg Dept, Annapolis, MD; Ocean Engrg Dept (McCormick), Annapolis, MD; PWO, Annapolis, MD
CAL POLY STATE UNIVERSITY CE Dept (Penalba), San Luis Obispo, CA
CALIFORNIA STATE UNIVERSITY C.V. Chelapati, Long Beach, CA
CATHOLIC UNIV of Am, CE Dept (Kim), Washington, DC
CITY OF BERKELEY PW, Engr Div (Harrison), Berkeley, CA
CITY OF LIVERMORE Dackins, PE, Livermore, CA
CLARKSON COLL OF TECH CE Dept (Batson), Potsdam, NY
COLORADO STATE UNIVERSITY CE Dept (Criswell), Ft Collins, CO
CORNELL UNIVERSITY Civil & Environ Engrg (Dr. Kulhawy), Ithaca, NY; Library, Ithaca, NY
DAMES & MOORE Library, Los Angeles, CA
FLORIDA ATLANTIC UNIVERSITY Ocean Engrg Dept (Su), Boca Raton, FL
FLORIDA INST OF TECH CE Dept (Kalajian), Melbourne, FL
GEORGIA INSTITUTE OF TECHNOLOGY CE Scol (Kahn), Atlanta, GA; CE Scol (Swanger), Atlanta, GA; CE Scol (Zuruck), Atlanta, GA; Mech Engrg (Fulton), Atlanta, GA
INSTITUTE OF MARINE SCIENCES Library, Port Aransas, TX
JOHNS HOPKINS UNIV CE Dept (Jones), Baltimore, MD
LAWRENCE LIVERMORE NATL LAB FJ Tokarz, Livermore, CA; Plant Engrg Lib (L-654), Livermore, CA
LEHIGH UNIVERSITY Linderman Library, Bethlehem, PA
LONG BEACH PORT Engrg Dir (Allen), Long Beach, CA
MICHIGAN TECH UNIVERSITY CE Dept (Haas), Houghton, MI
MIT Engrg Lib, Cambridge, MA; Lib, Tech Reports, Cambridge, MA; RV Whitman, Cambridge, MA
NATL ACADEMY OF SCIENCES NRC, Naval Studies Bd, Washington, DC
NEW MEXICO SOLAR ENERGY INST Dr. Zwibel, Las Cruces, NM
NEW YORK-NEW JERSEY PORT AUTH R&D Engr (Yontar), Jersey City, NJ
NORTHWESTERN UNIV CE Dept (Belytschko), Evanston, IL
OHIO STATE UNIVERSITY CE Dept (H. Adeli), Columbus, OH; CE Dept (Sierakowski), Columbus, OH
OREGON STATE UNIVERSITY CE Dept (Hicks), Corvallis, OR; CE Dept (Hudspeth), Corvallis, OR; CE Dept (Leonard), Corvallis, OR
PENNSYLVANIA STATE UNIVERSITY Arch Engrg Dept (Geschwindner), University Park, PA; Gotolski, University Park, PA; Rsch Lab (Snyder), State College, PA
PORTLAND STATE UNIVERSITY Engrg Dept (Migliori), Portland, OR
PURDUE UNIVERSITY CE Scol (Leonards), W. Lafayette, IN; Engrg Lib, W. Lafayette, IN
RUTGERS UNIVERSITY CE Dept (Hanaor), Piscataway, JH
SAN DIEGO PORT Port Fac, Proj Engr, San Diego, CA
SAN DIEGO STATE UNIV CE Dept (Krishnamoorthy), San Diego, CA
SEATTLE UNIVERSITY CE Dept (Schwaegler), Seattle, WA

SOUTHERN ILLINOIS UNIVERSITY CE & Mech Dept (Kassimali), Carbondale, IL
SOUTHWEST RSCH INST Energetic Sys Dept (Esparza), San Antonio, TX; King, San Antonio, TX; M. Polcyn, San Antonio, TX; Marchand, San Antonio, TX
STANFORD UNIVERSITY App Mech Div (Hughes), Stanford, CA
STATE UNIVERSITY OF NEW YORK CE Dept (Reinhorn), Buffalo, NY; CE Dept, Buffalo, NY
TEXAS A&I UNIVERSITY Civil & Mech Engr Dept, Kingsville, TX
TEXAS A&M UNIVERSITY CE Dept (Machemehl), College Station, TX; CE Dept (Niedzwecki), College Station, TX; Ocean Engr Proj, College Station, TX
UNIVERSITY OF CALIFORNIA CE Dept (Fenves), Berkeley, CA; CE Dept (Gerwick), Berkeley, CA; CE Dept (Herrmann), Davis, CA; CE Dept (Kutter), Davis, CA; CE Dept (Romstad), Davis, CA; CE Dept (Shen), Davis, CA; CE Dept (Taylor), Berkeley, CA; CE Dept (Taylor), Davis, CA; Engrg (Williamson), Berkeley, CA; Geotech Model Cen (Cheney), Davis, CA; Mech Engrg Dept (Armand), Santa Barbara, CA; Mech Engrg Dept (Bayo), Santa Barbara, CA; Mech Engrg Dept (Bruch), Santa Barbara, CA; Mech Engrg Dept (Goldsmith), Berkeley, CA; Mech Engrg Dept (Mitchell), Santa Barbara, CA; Mech Engrg Dept (Tulin), Santa Barbara, CA; Naval Arch Dept, Berkeley, CA
UNIVERSITY OF COLORADO CE Dept (Hon-Yim Ko), Boulder, CO
UNIVERSITY OF CONNECTICUT CE Dept (Murtha-Smith), Storrs, CT
UNIVERSITY OF FLORIDA CE Dept (Townsend), Gainesville, FL; Engrg Sci Dept (Malvern), Gainesville, FL
UNIVERSITY OF HAWAII CE Dept (Chiu), Honolulu, HI; Manoa, Library, Honolulu, HI; Ocean Engrg Dept (Ertekin), Honolulu, HI
UNIVERSITY OF HOUSTON CE Dept (K.J. Han), Houston, TX
UNIVERSITY OF ILLINOIS CE Lab (Abrams), Urbana, IL; CE Lab (Pecknold), Urbana, IL; Library, Urbana, IL; M.T. Davisson, Urbana, IL; Metz Ref Rm, Urbana, IL
UNIVERSITY OF MARYLAND CE Dept (Goodings), College Park, MD; CE Dept (Wolde-Tinsae), College Park, MD
UNIVERSITY OF MICHIGAN CE Dept (Richart), Ann Arbor, MI
UNIVERSITY OF NEBRASKA Polar Ice Coring Office, Lincoln, NE
UNIVERSITY OF NEW MEXICO HL Schreyer, Albuquerque, NM; NMERI (Bean), Albuquerque, NM; NMERI (Falk), Albuquerque, NM; NMERI (Leigh), Albuquerque, NM
UNIVERSITY OF PENNSYLVANIA Dept of Arch (P. McCleary), Philadelphia, PA
UNIVERSITY OF SOUTH CAROLINA Engrg Coll (Karabalis), Columbia, SC
UNIVERSITY OF TEXAS CE Dept (Stokoe), Austin, TX; CE Dept (Thompson), Austin, TX; Construction Industry Inst, Austin, TX; ECJ 4.8 (Breen), Austin, TX
UNIVERSITY OF WASHINGTON CE Dept (Mattock), Seattle, WA
UNIVERSITY OF WISCONSIN CE Dept (Peyrot), Madison, WI; Great Lakes Studies Cen, Milwaukee, WI
WASHINGTON DHHS, OFE/PHS (Ishihara), Seattle, WA
ARINA ENGRG, INC Walczak, Watertown, MA
ADVANCED COMPOSITE ENGRG Leewood, West Lafayette, IN
ADVANCED TECHNOLOGY, INC Ops Cen Mgr (Bednar), Camarillo, CA
AMERICAN CONCRETE INSTITUTE Library, Detroit, MI
AMETEK OFFSHORE RSCH Santa Barbara, CA
APPLIED RSCH ASSOC, INC Higgins, Albuquerque, NM
ARMSTRONG AERO MED RSCH LAB Ovenshire, Wright-Patterson AFB, OH
ARVID GRANT & ASSOC Olympia, WA
ASSOCIATED SCIENTISTS Dr. McCoy, Woods Hole, MA
ATLANTIC RICHFIELD CO RE Smith, Dallas, TX
BATTELLE D Frink, Columbus, OH
BECHTEL CIVIL, INC Woolston, San Francisco, CA
BETHLEHEM STEEL CO Engrg Dept (Dismuke), Bethlehem, PA
BRITISH EMBASSY Sci & Tech Dept (Wilkins), Washington, DC
BROWN & ROOT Ward, Houston, TX
CANADA Biokinetics & Assoc, LTD, Ottawa, Ontario; Concordia, CE Dept (Marsh), Montreal, Quebec; Viateur De Champlain, D.S.A., Matane, Canada
CHEVRON OIL FLD RSCH CO Strickland, La Habra, CA
CHILDS ENGRG CORP K.M. Childs, Jr, Medfield, MA
CLARENCE R JONES, CONSULTN, LTD Augusta, GA
COLLINS ENGRG, INC M Garlich, Chicago, IL
CONRAD ASSOC Lusoni, Van Nuys, CA
CONSOER TOWNSEND & ASSOC Schramm, Chicago, IL
CONSTRUCTION TECH LABS, INC G. Corley, Skokie, IL
DILLINGHAM CONSTR CORP (HD&C), F McHale, Honolulu, HI
DRAVO CORP Wright, Pittsburg, PA
EVALUATION ASSOC, INC MA Fedele, King of Prussia, PA
GEIGER - KKBNA K.P. Hampton, Bellingham WA
GEN MOTORS RSCH LABS Khalil, Warren, MI

GRUMMAN AEROSPACE CORP Tech Info Ctr, Bethpage, NY
HAYNES & ASSOC H. Haynes, PE, Oakland, CA
HIRSCH & CO I. Hirsch, San Diego, CA
HJ DEGENKOLB ASSOC W Murdough, San Francisco, CA
HUGHES AIRCRAFT CO Tech Doc Cen, El Segundo, CA
HUWALDT ENGRS MH Huwaldt, Denver, CO
IFFLAND KAVANAGH WATERBURY, PC New York, NY
INTL MARITIME, INC D Walsh, San Pedro, CA
IRE-ITTD Input Proc Dir (R. Danford), Eagan, MN
JOHN J MC MULLEN ASSOC Library, New York, NY
LEO A DALY CO Honolulu, HI
LEV ZETLIN ASSOC, INC DA Cuoco, New York, NY
LIN OFFSHORE ENGRG P. Chow, San Francisco CA
LINDA HALL LIBRARY Doc Dept, Kansas City, MO
LOCKHEED Rsch Lab (Nour-Omid), Palo Alto, CA
LOCKWOOD GREENE ENGRS, INC KV Bendapudi, Dallas, TX
MARATHON OIL CO Gamble, Houston, TX
MARC ANALYSIS RSCH CORP Hsu, Palo Alto, CA
MARITECH ENGRG Donoghue, Austin, TX
MC CLELLAND ENGRS, INC Library, Houston, TX
MOBIL R & D CORP Offshore Engrg Lib, Dallas, TX
EDWARD K NODA & ASSOC Honolulu, HI
NEW ZEALAND NZ Concrete Rsch Assoc, Library, Porirua
NUHN & ASSOC A.C. Nuhn, Wayzata, NM
PACIFIC MARINE TECH (M. Wagner) Duvall, WA
PILE BUCK, INC Smoot, Jupiter, FL
PMB SYS ENGRG, INC Bea, San Francisco, CA; S. Nour-Omid, San Francisco, CA
PRESNELL ASSOC, INC DG Presnell, Jr, Louisville, KY
SANDIA LABS Library, Livermore, CA
SARGENT & HERKES, INC JP Pierce, Jr, New Orleans, LA
SAUDI ARABIA King Saud Univ, Rsch Cen, Riyadh
SEATECH CORP Peroni, Miami, FL
SHELL OIL CO E Doyle, Houston, TX
SIMPSON, GUMPERTZ & HEGER, INC E Hill, CE, Arlington, MA
SRI INTL Engrg Mech Dept (Grant), Menlo Park, CA; Engrg Mech Dept (Simons), Menlo Park, CA; J.L. Jones, Chem Engr Lab, Menlo Park, CA
THE FANTOZZI CO, INC W. Fantozzi, Cupertino, CA
TRW INC Crawford, Redondo Beach, CA; Dai, San Bernardino, CA; Engr Library, Cleveland, OH; M Katona, San Bernardino, CA; Rodgers, Redondo Beach CA
TUDOR ENGRG CO Ellegood, Phoenix, AZ
UNITED KINGDOM Univ Coll Swansea (Zienkiewicz), Wales
VSE Ocean Engrg Gp (Murton), Alexandria, VA
WEIDLINGER ASSOC F.S. Wong, Palo Alto, CA
WELLSPRING COMM H Zarecor, Marshall, VA
WESTINGHOUSE ELECTRIC CORP Library, Pittsburg, PA
WISS, JANNEY, ELSTNER, & ASSOC DW Pfeifer, Northbrook, IL
WOODWARD-CLYDE CONSULTANTS R Dominguez, Houston, TX; West Reg, Lib, Oakland, CA
BIRNSTIEL, C Forrest Hills, NY
BROWN, ROBERT University, AL
BULLOCK, TL La Canada, CA
CHAO, JC Houston, TX
CLARK, T. Redding, CA
COX, J Davis, CA
GIORDANO, A.J. Sewell, NJ
HARDY, S.P. San Ramon, CA
HAYNES, B. No. Stonington, CT
HEUZE, F Alamo, CA
MEDWADOWSKI, SJ Consult Struct Engr, San Francisco, CA
NIEDORODA, AW Gainesville, FL
PETERSEN, CAPT N.W. Pleasanton, CA
QUIRK, J Panama City, FL
SPIELVOGEL, L Wyncote, PA
STEVENS, TW Long Beach, MS
ULASZEWSKI, CDR T.J. Honolulu, HI
VAN ALLEN, B Kingston, NY
WEBSTER, R Brigham City, UT

INSTRUCTIONS

The Naval Civil Engineering Laboratory has revised its primary distribution lists. The bottom of the label on the reverse side has several numbers listed. These numbers correspond to numbers assigned to the list of Subject Categories. Numbers on the label corresponding to those on the list indicate the subject category and type of documents you are presently receiving. If you are satisfied, throw this card away (or file it for later reference)

If you want to change what you are presently receiving:

- Delete - mark off number on bottom of label.
- Add - circle number on list.
- Remove my name from all your lists - check box on list.
- Change my address - line out incorrect line and write in correction **(DO NOT REMOVE LABEL).**
- Number of copies should be entered after the title of the subject categories you select.

Fold on line below and drop in the mail.

Note: Numbers on label but not listed on questionnaire are for NCEL use only, please ignore them.

Fold on line and staple.

DEPARTMENT OF THE NAVY

Naval Civil Engineering Laboratory
Port Hueneme, CA 93043-5003

Official Business
Penalty for Private Use, $300

NO POSTAGE
NECESSARY
IF MAILED
IN THE
UNITED STATES

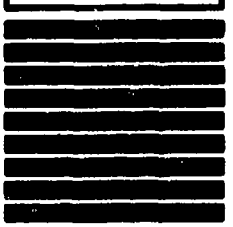

BUSINESS REPLY CARD

FIRST CLASS PERMIT NO. 69

POSTAGE WILL BE PAID BY ADDRESSE

Commanding Officer
Code L34
Naval Civil Engineering Laboratory
Port Hueneme, California 93043-5003

DISTRIBUTION QUESTIONNAIRE

The Naval Civil Engineering Laboratory is revising its Primary distribution lists.

SUBJECT CATEGORIES

1 SHORE FACILITIES
2 Construction methods and materials (including corrosion control, coatings)
3 Waterfront structures (maintenance/deterioration control)
4 Utilities (including power conditioning)
5 Explosives safety
6 Aviation Engineering Test Facilities
7 Fire prevention and control
8 Antenna technology
9 Structural analysis and design (including numerical and computer techniques)
10 Protective construction (including hardened shelters, shock and vibration studies)
11 Soil/rock mechanics
14 Airfields and pavements

15 ADVANCED BASE AND AMPHIBIOUS FACILITIES
16 Base facilities (including shelters, power generation, water supplies)
17 Expedient roads/airfields/bridges
18 Amphibious operations (including breakwaters, wave forces)
19 Over-the-Beach operations (including containerization, materiel transfer, lighterage and cranes)
20 POL storage, transfer and distribution

28 ENERGY/POWER GENERATION
29 Thermal conservation (thermal engineering of buildings, HVAC systems, energy loss measurement, power generation)
30 Controls and electrical conservation (electrical systems, energy monitoring and control systems)
31 Fuel flexibility (liquid fuels, coal utilization, energy from solid waste)
32 Alternate energy source (geothermal power, photovoltaic power systems, solar systems, wind systems, energy storage systems)
33 Site data and systems integration (energy resource data, energy consumption data, integrating energy systems)
34 ENVIRONMENTAL PROTECTION
35 Solid waste management
36 Hazardous/toxic materials management
37 Waste water management and sanitary engineering
38 Oil pollution removal and recovery
39 Air pollution

44 OCEAN ENGINEERING
45 Seafloor soils and foundations
46 Seafloor construction systems and operations (including diver and manipulator tools)
47 Undersea structures and materials
48 Anchors and moorings
49 Undersea power systems, electromechanical cables, and connectors
50 Pressure vessel facilities
51 Physical environment (including site surveying)
52 Ocean-based concrete structures
54 Undersea cable dynamics

TYPES OF DOCUMENTS

85 Techdata Sheets 86 Technical Reports and Technical Notes
83 Table of Contents & Index to TDS
82 NCEL Guides& Abstracts
91 Physical Security

☐ None-remove my name